_____
Unterschrift BetreuerIn

**TECHNISCHE
UNIVERSITÄT
WIEN**
Vienna University of Technology

DIPLOMARBEIT

On the Physics and Ageing of Medium Voltage-Cables in an Austrian Distribution Grid

ausgeführt am Institut für Angewandte Physik
der Technischen Universität Wien

unter der Leitung von
Ao.Univ.Prof. Dipl.-Ing. Dr.techn. Martin Gröschl
betreut von
Dipl.-Ing. David Sturm (Kärnten Netz GmbH)
Ing. Karl Schoaß (Kärnten Netz GmbH)

durch

Georg Rauchenwald BSc BSc

Weidenweg 8, 9322 Micheldorf

9. Februar 2019

_____
Unterschrift StudentIn

Abstract

Medium Voltage power cables are essential components of electricity grids, at the same time many cables have yet been more than 30 years in service and their condition can hardly be evaluated. Repairs and exchange of underground cables on the one hand always lead to high work effort, official procedures and costs. On the other hand, cable failures can lead to power outages and difficulties in security of supply.

In the present thesis, an overview of the physics and ageing of cables and the current state of research to this topic is given. The practical main problem here is the gathering of data about the current cable condition, because relevant cable-parameters can usually not be determined while in operation.

Possibilities for an assessment of the actual cable condition are technical diagnostic techniques. The most widely used ones, measurements of partial discharges and the dissipation factor $tan\delta$ are explained with practical examples of measurements from the grid of Kärnten Netz GmbH. Finally, the current state of research of a promising method for using power line communication (PLC) signals for an online condition monitoring of cable grids is shown, analyzed and compared to the current methods.

Kurzfassung

Mittelspannungskabel stellen einen wesentlichen Bestandteil der Stromnetze dar, gleichzeitig sind viele Kabel bereits seit 30 Jahren oder länger in Betrieb und ihr Zustand ist nur schwer festzustellen. Reparaturen und der Austausch von Erdkabeln sind einerseits mit hohem Arbeitsaufwand, Behördenverfahren und Kosten verbunden. Schäden können andererseits zu Stromausfällen und Beeinträchtigungen der Versorgungssicherheit führen.

In vorliegender Arbeit wird ein Überblick über die physikalischen Vorgänge und Alterung von Erdkabeln und den aktuellen Stand der Wissenschaft zu diesem Thema gegeben. Das praktische Hauptproblem hierbei ist die Beschaffung von Daten über den aktuellen Kabelzustand, da für die Alterung relevante Parameter der Kabel im Betrieb in der Regel nicht ohne Weiteres festgestellt werden können.

Eine Möglichkeit zur Informationsbeschaffung über den tatsächlichen Zustand der Kabel stellen die Verfahren der technischen Diagnostik dar. Die am weitesten verbreiteten Verfahren, Messung von Teilentladungen und des Verlustfaktors $tan\delta$ wurden vorgestellt und anhand von praktischen Messungen bei Kärnten Netz erläutert. Abschließend wurde der aktuelle Forschungsstand zu einer Methode zur Nutzung von Power Line Communication (PLC) Signalen zur Zustandsbewertung in Netzen vorgestellt, analysiert und mit den etablierten Methoden verglichen.

Contents

Welch Schauspiel! aber ach! ein Schauspiel nur!
Wo fass ich dich, unendliche Natur?

Johann Wolfgang von Goethe, Faust I, Vers 454f.

List of Abbreviations

AC - Alternating Current
ADC - Analog-Digital Converter
AWG - Arbitrary Waveform Generator
CIR - Channel Impulse Response
CDPV - Contaminants, Defects, Protrusions or Voids
CTR - Channel Transfer Function
DC - Direct Current
FDR - Frequency Domain Reflectometry
FFT - Fast Fourier Transformation
JTFDR - Joint Time-Frequency Domain Reflectometry
MV - Medium Voltage
OC - Open Circuit
OFDM - Orthogonal Frequency-Division Multiplexing
PD - Partial Discharge
PE - Polyethylene
PVC - Polyvinylchloride
SC - Short Circuit
SVM - Support Vector Machine
TDR - Time Domain Reflectometry
XLPE - Cross Linked Polyethylene

Introduction

This thesis was written in cooperation with the Austrian grid operator Kärnten Netz GmbH between summer 2018 and winter 2018/19. The thesis is dedicated to the subject of ageing and degradation effects within medium voltage (MV) power cables and their effects on the physics and reliability of the grids.
The goals of this thesis shall be:

- To give an overview of the physics of underground power cables and the ageing mechanisms affecting them,

- to analyze currently used diagnostic methods for the condition assessment of the cables, and finally

- to give an outlook on new promising diagnostic methods and their current state of research.

The focus in all this shall lie on the physics and the understanding of the physical problems behind these questions, not on specific technical solutions. Therefore, the thesis is divided into four chapters:

1. An introductional chapter with the fundamentals on the physics and technologies behind cable grids.

2. A chapter in which the different ageing effects and processes on cables are explained in detail.

3. A chapter about measurement tests in the grids to get information about the actual condition of the cables, called *diagnostic tests*. The two most widely used diagnostic techniques nowadays, the measurement of partial discharges and the dissipation factor $tan\delta$, are shown in detail.

4. A last chapter with an outlook on a possible future diagnostic technique using signals from powerline communication in a grid for diagnostic purposes. The current state of research and possible future applications shall be explained.

1 Underground Cables –
Fundamentals and Layout

In this first chapter, a few basic insights into underground cables shall be given. Starting from a short history of the cable-technology to the situation in a distribution grid nowadays, the basic physical properties and the layout of classical modern power cables and the challenges regarding ageing effects in operation shall be explained.

1.1 Underground Power Cables - Introduction

1.1.1 Historic Development of Cables and Motivation

From the beginning of the use of electricity, around 150 years ago, there have been basically two options for the transport of electrical energy over distances: building overhead power lines - hung onto transmission towers or power poles, or digging cables - buried in the ground. This thesis deals with the latter - cable grids used for the distribution of electrical energy.

Cables consist of at least two very basic components: An electrical conductor and an adequate insulation. Speaking in terms of practical experience, problems or outages are hardly caused by the conducting material, but by problems with the insulation.[28, S.11]

Historically, the first known underground cables were used around 1880 in Berlin for the power supply of arc lamps. In many cities of this time, power lines and cables for the newly discovered inventions like electrical lighting, telephone and telegraph wires were just hung over the streets separately, uncoordinated and in a very chaotic way. Underground cables were an approach to bring some kind of order into this vast amount of wires and cables. Nevertheless, the development of capable synthetic insulation materials was only in its very early stages in the 1880s, so Guttapercha, a latex of the Asian Guttapercha-tree was used as insulating material. Unfortunately, the thermal resistance of this material was not sufficient. When the cables heated themselves up, the insulation became soft and squashy

already around 45°C. Hence, it was clear that from the very early days of cable-technolgy on, better suited insulation materials had to be developed.

Around 1900, Siemens already fabricated cables in an industrial scale in Germany and over 500 cable types were available. High reliability played a major role in this technology from the beginning on. With the cables being buried at least a meter underneath the surface, the replacement of damaged cables always leads to high work efforts and costs. [7, S.19] [36, S.59]

Figure 1.1
Cables and wires on the Broadway
on a postcard from 1880. [66]

Figure 1.2
Digging of a cable trench by
Siemens in Germany in 1912. [58]

Nowadays, underground cables are laid all around the world, providing billions of people with electrical energy. Due to this enormous extent, the grids represent major assets and huge investment objects for energy production and grid operating companies. Excavation works, repair and replacement of damaged cables are still a complex matter, but in comparison to 1880 there is an additional major factor nowadays grid operators have to deal with: Security of supply. Damages and disturbances of cables usually lead to power outages in a certain region. Due to just-in-time production, fully automized, connected and computer-controlled working procedures even short outages can lead to enormous costs.

These problems led to more and more sophisticated techniques and an ongoing development. From 1890 on, paper as insulating material was used. Conductors were basically wrapped with several layers of paper and impregnated with oil or a viscous oil-mass. These cables needed an outer coating of lead though, to prevent moisture ingress into the paper. Oil impregnated paper was the most used insulation for decades until the developments in polymer chemistry after World War II led to the use of polymeric insulating materials. Insulating materials made from Polyethylene (PE - 1942) or Cross Linked Polyethylene (XLPE - 1968) were developed, which are still in use in large parts of the grids. [43, S.52f]

1.1.2 Situation in a modern Distribution Grid and Scope

While generally in high voltage grids (110-380kV) overhead power lines are dominantly used, in medium voltage grids (10-30kV) around 85% cables are installed. Due to lack of space especially in cities or densely populated areas, the amount of cables is assumed even to rise in future. [7, S.26]

The situation in the distribution grid of Kärnten Netz is a good practical example and representation of the already mentioned historical development of cable technology.

Kärnten Netz operates an electrical distribution grid in Carinthia, in the south of Austria, with about 217200 customers and about 18100km of electrical grid, with nearly 2900km of underground cables. In figure 1.3 the number (not the length!) of installed MV underground cables is shown depending on the year (from 1945 to 2018) and the cable type. It is clearly visible, that until the mid 1970s oil impgregnated paper-mass cables were the most used cable types, then PE cables and from the 1990s on XLPE cables of the first and second generation were used:
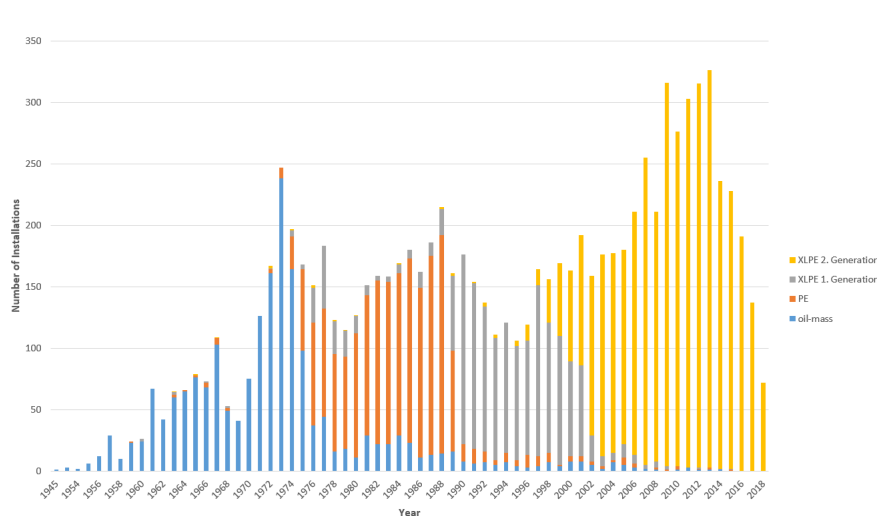
Figure 1.3: Number of installed cables sorted by cable technology and year (picture: Kärnten Netz)

Looking at the total lengths of installed cable, the distribution can be broken down to the following different cable types:
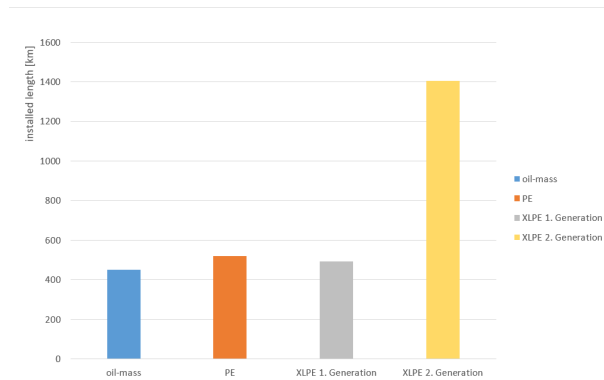
Figure 1.4: Total installed length per cable type in 2018 (picture: Kärnten Netz)

From the total of 2870km of underground cable, around 15,7% consists of old oil-mass cables, around 18% are PE cables, and the rest of around 2/3 of the cable grid consist of XLPE cables from 1st or 2nd generation. In other words, over 80% of the grid consist of cables with a polymer insulation, therefore this type of insulation will primarily be the subject of this thesis. Another interesting diagram is the total installed length of cable depending on the year:
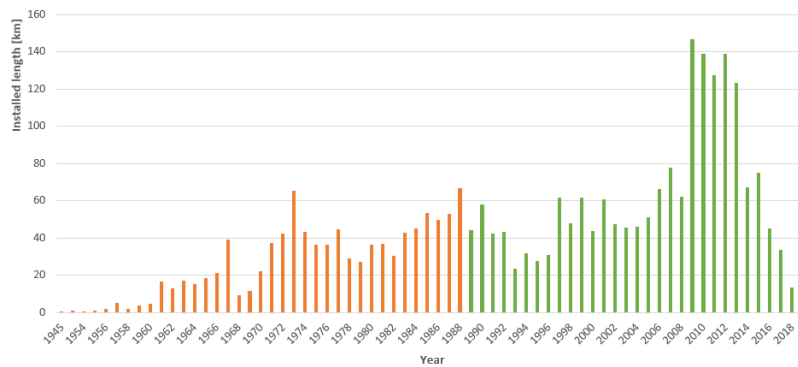
Figure 1.5: Total installed length per cable type in 2018 (picture: Kärnten Netz)

In figure 1.5, all cable installations up to 1988, with being over 30 years in service are marked in red. Out of the total amount of 2870km approximately 980km of cable are older than 30 years, which is 34%. This also shows the necessity of considering ageing effects and mechanisms in cables to gain a better understanding of their residual lifetime.

1.2 Physical Properties of Cables

As already mentioned in section 1.1.1, a cable - at the very minimum - consists of a conducting and an insulating material. To understand the physics of the cable in operation, a few details of the physics of cables need to be discussed first.

Cables are used for a wide variety of purposes and their behaviour regarding electrical, mechanical, thermal and other properties are a large field of research and development. Due to the focus of this thesis on cables for power distribution in the area of 20kV, only the most relevant properties for this application are shortly explained. For further information there is plenty of recommendable literature e.g. [7], [15], [27] or [34].

For the requirements for cables in a 50Hz power grid, cable characteristics, like quality of transmitted signals or behaviour at different frequencies are mostly negligible, the main purpose is the transport of electrical energy. Therefore, different types of losses play a major role and the minimization of losses is a main focus in cable development. Nevertheless, it is still always a compromise between costs, efforts and security of supply.

### 1.2.1 Resistance and Effective Resistance

The most obvious property of a conductor and cause for losses is the ohmic resistance R. From a physics point of view, the ohmic resistance R is depending on length l, cross section A and conductivity σ:

$$R = \frac{l}{\sigma \cdot A} \tag{1.1}$$

This resistance R is, strictly speaking, a DC-property and therefore described by real numbers. As an example, σ for the two most widely used conductors copper and aluminium is 58 and $35 m/(\Omega \cdot mm^2)$. This means the conductivity of aluminium is about 40% lower than the one of copper. So for the same ohmic resistance a circular aluminium conductor needs a 70% bigger cross section, which results in a 29% greater diameter. The aluminium conductor in this case weighs still around 50% less than the copper conductor. [15, S.24]

Resistance is a temperature dependant property, so heating of the cable must be taken into consideration as well. Due to different losses or induction within the cable layers, the temperature of the conductor rises in operation. In the technical

relevant area up to around 150°C the increase of resistance is proportional to the increase of temperature. For the resistance $R(T)$ the following equation is met:

$$R(T) = R_{20} \cdot [1 + \alpha \cdot (T - 20°C)] \tag{1.2}$$

Where R_{20} is the resistance at 20°C, which is the usual reference value. The temperature coefficient α for metals is usually $\approx 0,4\% K^{-1}$. So for a temperature increase of 100K, there is an increase of resistance of 40%. Operational temperatures of cables are around 80-90°C. Maximum tolerable values for the resistance of different conductors are regulated by standards, e.g. IEC 60228. In practical use, the resistance per unit length of the cable is used $R' = R/l$ in $[\Omega/km]$.
[15, S.24] [34, S.88f] [51, S.31f]

For a realistic view on the losses in a AC-cable, additional interactions need to be considered which leads to the *effective resistance* $R' = R' + \Delta R'$. The main effects contributing to $\Delta R'$ are the so-called *skin-effect*, *proximity-effect* and *hysteresis losses* which only occur in DC-operation. Strictly speaking, the skin- and proximity-effect are frequency dependent, whereas this dependency is negligible in our case, because this thesis only deals with the central European grid frequency of 50Hz.

The **skin-effect** is the tendency of currents in AC-operation to increase from the middle of the conductor towards the surface. The current density J therefore is higher near the surface of the conductor, practically the *skin* of the conductor. This distribution is shown in figure 1.6:
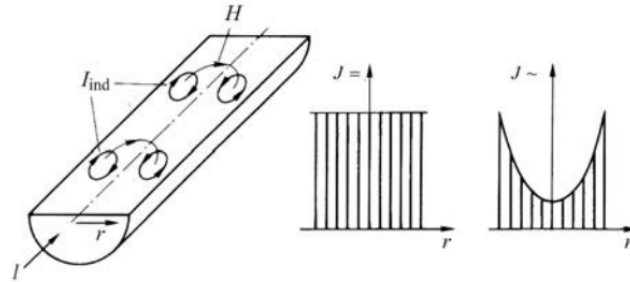

Figure 1.6: skin-effect and distribution of the current density J for DC-(left) and AC-operation (right). [15, S.30]

The oscillating magnetic field H of the cable induces eddy currents I_{ind} within the conductor, overlapping with the AC-current (inductance is explained in de-

9

tail in section 1.2.2). This effect causes an uneven current distribution within the conductor and leads to an apparent reduction of the effective cross section and increase of the resistance, especially for bigger conductor cross sections. The skin-effect can be avoided by segmenting a conductor and insulating the segments from each other (e.g. in a *Milliken-conductor*, see also section 1.3.3. [15, S.30]

The **proximity-effect** is also caused by induced eddy currents due to the AC-voltage, but in this case from adjacent conductors of other cables. The eddy currents again overlap with the AC-current and cause a single-sided current-distribution.
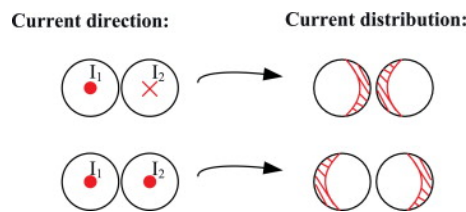
Figure 1.7: Current distribution in two adjacent cables due to proximity-effect in AC-operation. [21]

Figure 1.7 shows the change in current distributions due to the proximity-effect. In operation, the impact of the proximity-effect is low especially compared to the ones caused by skin-effect, and decreases strongly with the distance between the conductors. Because both effects are caused by inductive processes, they depend on the frequency of the AC-voltage. [15, S.31]

Ferromagnetic parts near the conductor, like cable racks or protective layers of the cable, are continuously magnetised and remagnetised. The energy needed for this effect is an additional loss for the cable, called **hysteretic loss**, and increases R'. For the calculation of R', with all this components described, empiric formulas exist (e.g. in IEC standard 287) but the matter is rather complex and the formulas complicated. Experience shows, that hysteretic losses heavily depend on the design of the cable and especially the outer layers which contribute the largest part to the occurring external electrical field. For the exact determination of R' measurements are necessary. [15, S.35f][34, S.88f]

1.2.2 Inductance

Michael Faraday was the first to realize, that in a conductor in a time-variable magnetic field a voltage can be measured, which he called *Induction Voltage*. For

a coil with cross section A and a magnetic field $\vec{B}$ this results in **Faraday's law of induction**:

$$U_{ind} = -\frac{d}{dt} \int \vec{B} \cdot d\vec{A} = \frac{d\Phi_m}{dt} \qquad (1.3)$$

Φ_m in this case is the magnetic flux.

In an AC-system the magnetic flux changes with every sine oscillation of the voltage. For an electric current that flows through a coil, a voltage in the coil itself is induced, which is contrary to the voltage applied after Lenz's law. The magnetic field of the coil is proportional to the current I which gives the following equation for the magnetic flux:

$$\Phi_m = \int \vec{B} \cdot d\vec{F} = L \cdot I \qquad (1.4)$$

The proportionality-constant L is called *coefficient of self induction* and has the physical dimension $[L] = \frac{1V \cdot s}{A} = 1 Henry = 1H$. Therefore, an inductivity of $1H$ means, that 1 Volt of voltage is induced in the conductor, when there is a change in current of $1A/s$.

For electrical grids, a good approximation model of the inductance is built by two parallel conductors with radius r_0 and distance d, through which a current I with opposed direction flows (see figure 1.8). In this model the current density is assumed to be constant inside the conductors and there are no ferromagnetic materials within the range of the magnetic field.
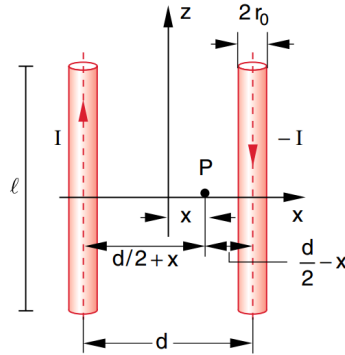

Figure 1.8: Model of two parallel conductors with distance d and opposing currents I [10, S.136]

The coefficient of self induction for this model now is (derivation can be found in literature, e.g. in [10]):

$$L = \frac{\mu_0 \cdot l}{\pi} \cdot [\frac{1}{2} + ln\frac{d - r_0}{r_0}] \qquad (1.5)$$

where:
$\mu_0 = $ vacuum permeability $[\mu_0 = [H/m]]$
$r_0 = $ radius of the conductor

Equation 1.5 shows, that self induction increases logarithmically with distance d, and decreases with conductor radius r_0. Therefore, the conductors need to be placed as closely together as possible to minimize induction. Inductance gets minimal at $L(d = 2r_0) = \frac{\mu_0 \cdot l}{2\pi}$.[10, S.127ff]

Again, in practical use, also the inductance is mostly considered per unit length, as $L' = \frac{L}{l}$. Inductance depends heavily on the distances between conductors, shielding and outer layers of the cables or ferromagnetic material within the field. All of these factors are excluded in equation 1.5 and are usually not considered in the catalogues of cable producers as well. [15, S.40]

Quite vividly, the inductivity can be described as an energy storage within the cable, where energy from the grid is transferred into the magnetic field. The applied voltage U causes a current I, which builds up the magnetic field. In AC-grids with frequency f or angular frequency $\omega = 2\pi f$, this energy has to be provided with every change of phase, which causes a delay in the phase of the current in comparison to voltage. This resulting phase shift between voltage and current can be visualized in a complex vector diagram and is therefore is described by an imaginary number, which increases with frequency. This frequency dependent, inductive property is called *inductive reactance X_L*:

$$X_L = j \cdot \omega \cdot L \qquad (1.6)$$

[10, S.155f] [62, S.961ff]

1.2.3 Capacitance

Similar to the phenomenon of inductivity, also the *capacitance* is a property which stores energy taken from the grid, but in this case to build up an electrical field. At a given voltage, the capacitance is a characteristic value of the charge a material can hold. The SI unit for the capacitance is Coulomb per Volt and called *Farad* $1F = 1C \cdot V^{-1}$. [62, S.762]

The simplest practical model to illustrate the parameter capacitance in a cable is a plate capacitor with two conducting plates with area A (e.g. the conductor and conductive sheathing in the cable), distance d and a dielectric with relative permittivity ϵ_r in between (the cable insulation).
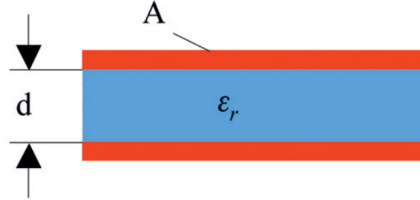
Figure 1.9: plate capacitor

[27, S.238]

The capacitance of this plate capacitor is:

$$C = \epsilon_0 \cdot \epsilon_r \cdot \frac{A}{d} \tag{1.7}$$

where:
$C =$ Capacitance of the plate capacitor
$\epsilon_0 =$ Vacuum permittivity, a constant

This very simple model of the plate capacitor already provides information about a few central characteristics of the capacitance in electrical cables:

- The capacitance increases with the area A - cable cross sections are usually constant over length, and therefore the capacitance of a cable is proportional to the length.

- A higher distance between the conductors decreases the capacitance.

- A higher relative permittivity ϵ_r increases the capacitance.

Because of the small distance between conductors and the outer sheath (which is at ground potential) of cables and the high ϵ_r of the cable insulation, the capacitance of cables is by orders of magnitude higher than of overhead power lines.

The model of the plate capacitor is very simple compared to the complex real properties of cables. In real life, capacitances occur both between a conductor and earth potential and between the conductors within. Therefore the calculation of real capacitances of cables is rather complex and measurements have to be used to

13

determine the actual values. In practical use, the capacitance of cables is mostly considered per unit length $C' = \frac{L}{l}$.[27, S.237f]

In AC-operation, this capacitance is charged and discharged with every change of phase in current and an oscillating electrical field results. Because of the continuous charging and discharging of the capacitance, an apparent current is flowing. Due to the development of the field, the electrical voltage follows the current with a delay, a phase shift.

Similar to the inductive one described in the last section, the capacitive phase shift can be described by an imaginary number, which in this case decreases with frequency. This capacitive property is called *capacitive reactance* X_C:[10, S.156] [62, S.961ff]

$$X_C = \frac{1}{j \cdot \omega \cdot C} \tag{1.8}$$

The physical properties of X_L and X_C are shown in figure 1.10 in a vector diagram. In the vector diagram, an ohmic resistance has no imaginary part but only a real part on the real axis $Re(Z)$, and therefore causes no phase shift ϕ. An ideal inductance causes a phase shift of $\phi_L = +90°$ and would therefore have no real but only an imaginary part, being situated on the positive y-axis. An ideal capacitance causes a phase shift of $\phi_C = -90°$ and is situated on the direct opposite part of the negative y-axis.
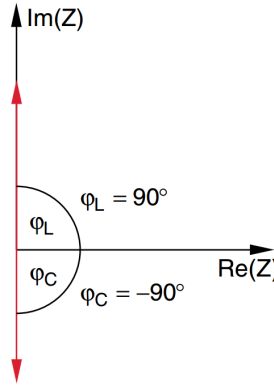
Figure 1.10: Phase shift of f $\phi = \pm 90°$ for ϕ_L and ϕ_C [10, S.156]

In AC-operation, the *charging current* I_C and *charging power* P_C for the given capacitance is highly important. It can be calculated via

$$I_C = U \cdot \omega \cdot C \tag{1.9}$$

$$P_C = U \cdot I_c = U^2 \cdot \omega \cdot C \tag{1.10}$$

and describes the constant flowing currents and power, responsible for charge and discharge of the capacitance in the cable.

As shown in the model of the plate capacitor in equation 1.7, I_C increases proportionally to the length of the cable, and the charging current adds itself to the transmitted current I. The resulting total current is limited to the maximum permissible current value of the given cable (called *ampacity*, which must not be exceeded because otherwise the cable would overheat). Therefore, for long cables, the necessary P_C in the cable for the capacitance limits the transmissible power. These limits are shown in figure 1.11 for a voltage of 110kV. Due to their high ϵ_r, for oil- and gas-insulated cables at already around 70km, I_C equals the maximum permissible current. The cable then only transports charging power and there is no power transmission. The maximum length for XLPE-cables is better, because their ϵ_r is around 1.5-times smaller. [15, S.42ff]
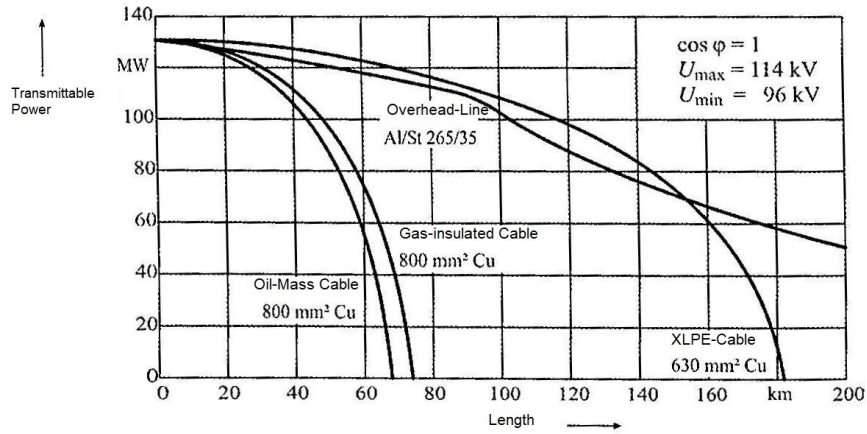
Figure 1.11: Transmissible power of cables and overhead power lines for 110kV as a function of the length. [15, S.46]

1.2.4 Dielectric Losses and Dissipation Factor

As already mentioned regarding the plate capacitor in section 1.2.3, the dielectric plays a major role in the capacitive behaviour of the cable. The central parameter in the dielectric is the *relative permittivity* ϵ_r. If a dielectric is placed in an electric field, the atoms of the dielectric act as dipoles and align with the electric field.

15

This leads to a polarization in the dielectric and an additional field, opposed to the initial one. This polarization field therefore weakens the strength of the original field. The better the dielectric, the higher the decrease of the resulting voltage in the capacitor, and therefore the increase of C. Based on equation 1.7, in analogy to the magnetic flux density $B = \mu H$ an electric flux density in the dielectric can be defined:

$$D = \epsilon E = \epsilon_0 \epsilon_r E \qquad (1.11)$$

ϵ_r therefore is the decivice property of the dielectric. ϵ_r for air and other gases is around 1, for most insulating materials in cables $2 \leq \epsilon_r \leq 8$. Water though, which can occur in traces in nearly every insulating material, has an substantially higher ϵ_r of ≈ 80. Within a dielectric, impurities or cavities lead to large differences of ϵ_r and therefore a locally elevated field strength D, which in the worst case can lead to ionizing of the gas in the cavities and partial discharges. In case of water within the dielectric, a change of ε_r for the factor of 10-40 occurs, which makes even small amounts of water within an insulating material a serious problem.[54, S.347ff] [10, S.24f]

In AC-operation, due to the constant change of voltage and therefore polarization of the dipoles, losses occur called *polarization losses*. Also, small amounts of AC-current flow through the dielectric and ionizing losses due to partial discharges between the conducting layers can occur. These cause not only an ideal capacitive current I_C to flow through the capacitor, but also a resistive part I_R, which would be 0 for an ideal capacitor. This can be visualized in a complex vector diagram:
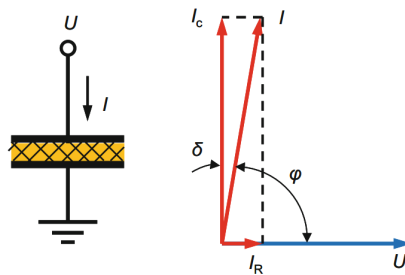

Figure 1.12: A real, lossy capacitor and its vector diagram. [54, S.349]

Figure 1.12 shows, that the ratio of this ideal capacative current I_C and the (usually much smaller) resistive part I_R is the tangens of the loss angle $tan\delta$.

$$tan\delta = \frac{I_R}{I_C} \qquad (1.12)$$

Also, I_R is in phase with the voltage U, so that for the phase shift between voltage U and the resulting current I the following equation applies:

$$\phi = -90° + \delta \qquad (1.13)$$

ϕ therefore is called *loss angle* and *tanδ dissipation factor.* [54, S.347ff] [10, S.24f] [15, S.51ff]

The values for the dissipation factor of dielectrics are often not constant and very temperature-dependent. For insulation materials the dissipation factor *tanδ* is usually in the order of magnitude of 1/1000:

Material	tanδ[10^{-3}]
Oil/Paper	3-9
PVC	<80
PE	<0,4
XLPE	<0,4

Table 1.1: Usual dissipation factors for different insulating material [15, S.43]

1.2.5 Ampacity and Heating

In section 1.2.3, it is already shown that the maximum permissible ampacity is responsible for the limited possible length of power cables. So the limitations of current within a cable and the physics behind it shall be considered as well.

The ampacitiy of a cable depends on different conditions like the given voltage drop or the prevention of power losses, but the main factor is heating to prevent damages on the insulation. Responsible for the heating of a cable are the different losses occuring within the different constructional parts of the cables:

- Losses within the conductor have already been explained in section 1.2.1 like the skin-effect or proximity losses.

- Also dielectric losses within the insulation have already been discussed in the previous section 1.2.4. Talking about modern insulation material, dielectric losses only play a role in the area of extra high voltage.

- Inductive losses and eddy currents within conducting parts of the sheathing as described in section 1.2.2.

All of these losses create heat flows $\dot{Q}_i$ flowing towards cooler areas within the cable. The resulting temperature increase $\delta\vartheta$ is proportional to $\dot{Q}$ and in analogy to Ohm's law, the proportionality factor is called *thermal resistance R_{th}*:

$$\delta\vartheta = \dot{Q} \cdot R_{th} \qquad (1.14)$$

In practical use, thermal resistance is usually considered per unit length of a cable R'_{th} and has the dimension $\frac{K \cdot m}{W}$.

Within a cable, the thermal resistance of the conductor is negligible (according to the Wiedemann-Franz law they are good thermal conductors as well). So only the sheathing, insulation and environment of the cable play a role in the consideration of thermal resistance.[34, S.86ff]

Thus, in practical use, the total thermal resistance consists of several partial resistances R_{thi} which have to be added. Especially when dealing with more complex geometries of conductors e.g. in three-core cables, computation or modelling of the total thermal resistance is rather complicated. Additionally, the thermal resistance of the soil surrounding the cable plays a big role as well, because all the heat is eventually emitted into it. The heat resistance R_{th} of the soil around the cable is difficult to evaluate, because it depends on a variety of parameters. On the one hand the nature of the ground (clay, mud, sand, loose or compressed) has very different properties, on the other hand moisture of course plays a big role. For sand, R_{th} is 0,4-3,0 $\frac{K \cdot m}{W}$, depending on on the humidity. To avoid this differences, cables can be laid into a concrete bedding with a thermal resistance of 0,7-1,0 $\frac{K \cdot m}{W}$, which can increase the transmission capacity over 10-20%.

Heat sources near the cables like other cables or pipes have an influence on the heat flow in the soil also. The same applies to cables, which are installed in cable ducts, where a layer of air is between the cable and the ducts. This can actually increase the ampacity in comparison to cables in soil. Calculations for these different circumstances - regarding the cable temperature - can be done as an approximation and are shown e.g. in DIN VDE 0276, but are rather complex. [15, S.81ff]

In case of a short circuit, different and higher ampacities are allowed. In this case, because of the short duration of the short circuit current (up to a maximum of a few seconds), the whole resulting heat due to the short circuit is stored within the conductor and not in the insulation. This is called an *adiabatic heating*.

For normal operation, the ampacity of a grid is usually calculated after mean patterns of daily load. Due to renewable energies and them feeding into the grids

at unusual times of day, loads within many grids increased over the last years. On different spots in distribution grids, thss loads may exceed the values used in the original grid planning. This may not always cause immediate problems, but as explained the main factor regarding ampacity is not the conductor, but the thermal ageing of the insulation, which is explained in detail in chapter 2. [7, S.36ff]

1.2.6 Complex Resistance and Impedance

As already mentioned in sections 1.2.2 and 1.2.3, inductances L and capacitances C in the cable grid cause phase shifts between U and I in AC-operation. The basic mechanism in this case can be derivated considering a model of a grid with an AC-voltage $U = U_0 \cdot e^{j\omega t}$ applied on a cable circuit with ohmic resistance R, inductance L and capacitance C.
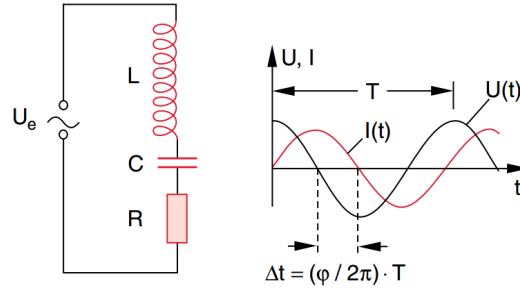
Figure 1.13: An AC-circuit with inductance L, capacitance C and ohmic resistance R in series. [10, S.156]

Due to Kirchhoff's laws, the sum of the voltage $U(t)$ and the inductive voltage $U_{ind} = -L \cdot \frac{dI}{dt}$ must be equal to the voltage drop on R and C: $U_{R+C} = R \cdot I + \frac{Q}{C}$:

$$U = L \cdot \frac{dI}{dt} + \frac{Q}{C} + R \cdot I \tag{1.15}$$

Differentiating this equation (where $\frac{dQ}{dt}$ becomes I) and inserting the complex terms for U and I leads to the following connection between U and I:

$$j\omega U = (-L\omega^2 + j\omega R + \frac{1}{C})I \tag{1.16}$$

In analogy to Ohm's law and ohmic resistance R, now the *complex resistance* $Z = \frac{U}{I}$ can be applied:

$$Z = \frac{U}{I} = R + j\sqrt{\omega L - \frac{1}{\omega C}} \qquad (1.17)$$

So it can be easily seen, that this complex resistance Z, which plays a similar role in AC-operation as the ohmic resistance R in DC-operation, consists of a real resistance part R and an imaginary reactance part X. The reactance consists of the inductive resistance X_L from equation 1.6 and the capacitive resistance X_C from equation 1.8.

The amount of this vector in a complex vector diagram is the *impedance* of the cable:

$$|Z| = \sqrt{R^2 + (\omega L - \frac{1}{\omega C})^2} \qquad (1.18)$$

The total phase shift between voltage and current therefore be calculated as the ratio between the complex and real part of the impedance:

$$tan\phi = \frac{Im(Z)}{Re(Z)} = \frac{\omega L - \frac{1}{\omega C}}{R} \qquad (1.19)$$

This can be vividly illustrated in a vector diagram, where the vector product of inductance, capacitance and resistance adds up to the total complex resistance. Also, when $\omega L = \frac{1}{\omega C}$ the phase shift ϕ becomes 0. [10, S.156f] [12, S.327f]
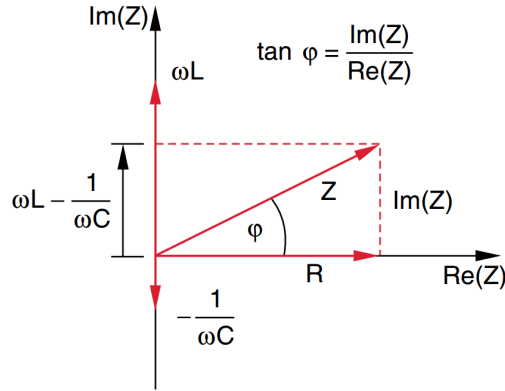
Figure 1.14: Vector diagram of a resulting impedance Z with inductive, capacitive and resistive part.[10, S.157]

1.2.7 Wave Impedance

Another property of interest in cables is the so-called *wave impedance*. To understand this parameter, a power cable with the idealized model of a *coaxial cable* is

explained. This cable consists of a thin conductor with radius a on the inside, and a coaxial conductor with radius b around the conductor, as shown in 1.15. The outer conductor in this case is on ground potential. This causes the field lines to be radial, which is very similar to real medium voltage cables. The magnetic field lines are circular around the inner conductor.
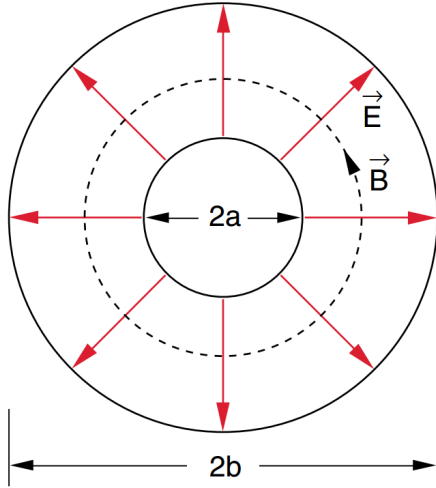
Figure 1.15
Layout of a coaxial cable with radial electrical and circular magnetic field lines [10, S.216]
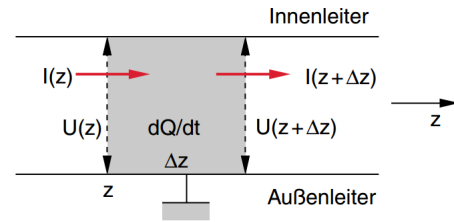
Figure 1.16
Voltage along the z-axis. [10, S.216]

When the conductors run along the z-axis, and an electromagnetic wave propagates along them in z-axis (as illustrated in figure 1.16, the voltage U between the inner and outer conductor becomes a function dependent on z. By applying equation 1.4 and equation 1.4 can be stated:

$$\Delta U = U(z + \Delta z) - U(z) = -L'\Delta z \frac{dI}{dt} \tag{1.20}$$

for $z \rightarrow 0$ follows:

$$\frac{\partial U}{\partial z} = -L' \frac{\partial I}{\partial z} \tag{1.21}$$

In similar manner, the current I is a function of z:

$$\Delta U = U(z + \Delta z) - U(z) \tag{1.22}$$

Within the length Δz the charge Q is:

$$Q = C' \cdot U \cdot \Delta z \tag{1.23}$$

which gives in combination and for $z \to 0$:

$$\frac{\partial I}{\partial z} = -C' \frac{\partial U}{\partial z} \tag{1.24}$$

Via deriving equation 1.21 and equation 1.24 with respect to z and t and mutual inserting of the mixed term $\frac{\partial}{\partial z \partial t}$, two wave equations result:

$$\frac{\partial^2 U}{\partial z^2} = L'C' \frac{\partial^2 U}{\partial t^2} \tag{1.25}$$

$$\frac{\partial^2 I}{\partial z^2} = L'C' \frac{\partial^2 I}{\partial t^2} \tag{1.26}$$

These are the wave equations for the current I and voltage U. From the general form we know that $L'C' = \frac{1}{v_{ph}^2}$ and therefore for the phase velocity of the waves in the cable v_{ph} is:

$$v_{ph} = \frac{1}{\sqrt{L'C'}} \tag{1.27}$$

and consequently only depend on the capacitance per unit length C' and inductivity per unit length L'.

After this equations, at every place z of the cable, the sinusoidal voltage $U(z)$ is proportional to the also sinusoidal current $I(z)$. The cable in this case behaves like an ohmic resistance for the wave, even though it only has capacitive and inductive properties and a negligible resistance R.

This proportionalty factor is called *wave impedance* Z_w and can be calculated by solving the wave equations 1.25 and 1.25:

$$U = \sqrt{\frac{L'}{C'}} \cdot I \tag{1.28}$$

Therefore the wave impedance as proportionality factor Z_w is:

$$Z_w = \sqrt{\frac{L'}{C'}} \tag{1.29}$$

[15, S.68ff][10, S.216f] [12, S.335]

These derivations and equation 1.29 show, that the wave impedance only depends on the inductance L and capacitance C of the cable, which especially depend

22

on the geometry of the cable, type of dielectric etc. (under the assumption of negligible ohmic losses). Also, equation 1.29 is only valid for cable layouts with no electrical field outside the room between the inner and outer conductor (this is also applicable for medium voltage cables, as shown in section 1.3).

An important feature of the wave impedance Z_w is, that when a wave travelling along the cable reaches a spot where a change in Z_w occurs, the ratio of voltage U and current I has to change as well. The maximum change in Z_w occurs at the end of a cable, where $Z_w \to \infty$. The transported energy of the incident wave can not be converted so the wave is completely reflected. The reflected wave afterwards propagates in the opposite direction of the cable. Due to Kirchhoff's laws, the current and voltage of the incident and reflected waves give the voltage and the current at the termination. So the voltage is doubled at the end of the cable, as shown in figure 1.17.
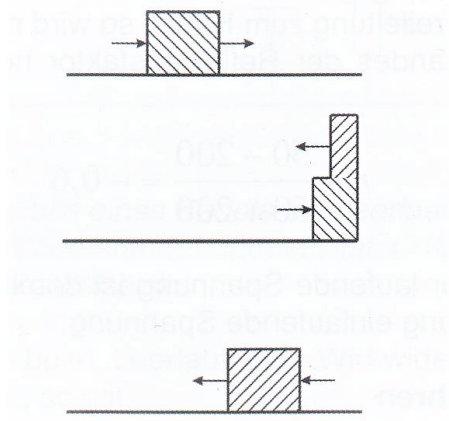
Figure 1.17: Reflection of a square pulse at the end of a cable with $Z_w = \infty$ - in the middle part the increase of the voltage to its doubled value is shown.[15, S.77]

These increases of voltage do not only occur at the end of cables, but also at transition points to a high ohmic resistance and can be a possible danger for the cable. The same goes for any changes of Z_w along the cable with a Z_{w2} higher than the previous Z_{w1}, e.g. at sleeves or overhead power lines, which have a much higher wave impedance than the cable (but not ∞ !). In this case the resulting voltage U_1 at the transition point is $U_1 = U \cdot (1 + r)$ with the *reflection coefficient* r:

$$r = \frac{Z_{w2} - Z_{w1}}{Z_{w2} + Z_{w1}} \tag{1.30}$$

The derivation of equation 1.30 can be done using Kirchhoff's laws and is shown e.g. in [30]. The equation shows, that at a transition from a cable with $Z_{w1} = 50\Omega$ to an overhead power line with $Z_{w2} = 200\Omega$ the reflection coefficient $r = 0,6$. This means that at the transition point, the voltage increases over 60%. If the constellation is the other way round, and the overhead power line leads into the cable, r becomes negative ($r = -0,6$). In this case the voltage in the cable is 60% smaller than before, but the current I in this case increases over 60%. [15, S.74ff][30, S.129ff]

1.2.8 The Physics of Polymer Dielectrics

As already shown in the practical data from the Kärnten Netz grid, in the area of MV cables, polymers are nowadays the most widely used insulation material. Because the insulation is the main subject at considering ageing processes, a few basic principles of polymer physics shall be explained shortly.

In general, properties of different polymers and polymer physics is an enormous wide and complex scientific field. The wide use of polymers in diverse applications, and the replacement of *classical* materials like metals, wood or paper with specifically tailored polymers makes them a huge subject of research. The microscopic processes responsible for the macroscopic physical properties are often very complex, difficult to understand and different for each polymer. In this thesis only a few relevant characteristics and principles for the use on MV cables can be shown, for deeper insights literature like [55] or [63] are recommended.

Basically, polymers consist of large, long-chained macromolecules, made from repeating *monomers*, which are the smallest units of the polymers. The name of the polymer is derived from the according monomer with the prefix *poly*:
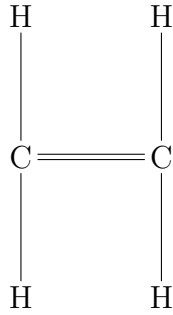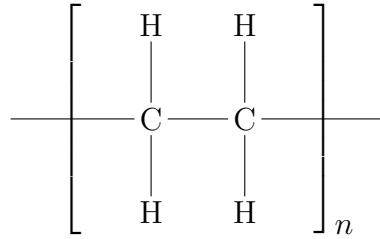
Figure 1.18: Ethylene

Figure 1.19: Polyethylene

n in this case is called *degree of polymerization and usually lays in the range of* $10^3 - 10^5$. [31, S.3ff]

For different uses and applications, different polymers regarding macroscopic properties like density, stiffness, melting point and many more can be constructed. These different characteristics and properties are achieved via variation and structure of the monomers used, the use of additional additives, filles or processes, in which the polymer-chains are connected for increased stability or durability (for the use in cables this process is called *cross-linking* and is explained in more detail in section 1.3.4.2). Because of this variety of possibilities to create tailored materials for different applications, an enormous number of polymers are in use, also for different applications in electrical engineering.

An important process of polymers is the so called *glass transition*, which has effects on nearly every property of the polymer. Above a certain temperature T_G, which is termed the *glass transition temperature*, the polymer-chains moves in segmental motions and can be deformed because it is possible to rotate the C-C bonds. Amorphous, non-crosslinked polymers above T_G therefore practically behave like viscous liquids. Within the liquid, the polymer-chains form disordered clusters, but have no structure.

When the temperature drops towards T_G, the motions of the chains decrease severely. This is, because the return-time to equilibrium within the polymer increases heavily with decreasing temperature. Below T_G, the movements are practically frozen, the non-equilibrium state becomes metastable. Like the freezing of water to ice, the cooling towards T_G in polymers always goes along with crystallization. Because of the long chains and their complex geometry, these processes in polymers are much more complicated than in water. For a full crystallization, the disordered chain-clusters would have to be completely unraveled. Therefore, cooling polymers tend to form a *glas*, which means they freeze while keeping their disordered structure. In this state, the molecules are crossbonded by the van der

25

Waals' attractions between them, which at higher temperatures with higher movement of the chains are too weak for bonding. Consequently Polymers usually only crystallize to a certain degree, even the simple structured polyethylene only crystallizes for about two thirds when cooled down from the molten state. One third of it stays amorphous, and builds a *glass*.

In many practical cases, polymers are processed via cooling of the melt, also in the production of cables, where the insulation is usually extruded around the conductor. The crystallized parts of the polymers often build so-called *lamellae*, where a stack of polymer chains are folded in periodic layers, which are typically about 100nm thick. The lamellae have different chains that hang loose or re-enter the lamellae in some distance. The transition of the loose chains to the partly-crystallized lamellae is shown in figure 1.20:
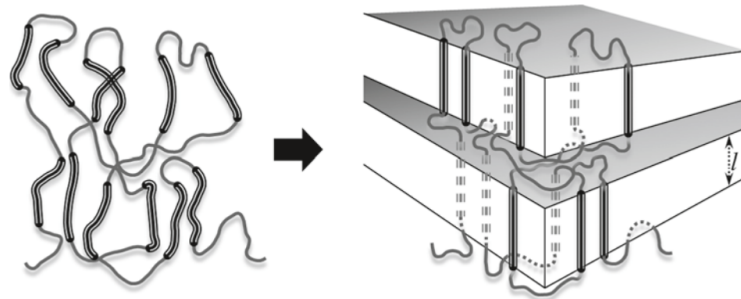
Figure 1.20: Illustration of the transition from loose polymer-chains (left) to partly crystallized lamellae. Because of the loose ends on the surface of the lamellae this model is also called *switchboard model of polymer-crystallization* [55, S.118]

The exact building processes and interactions of the lamellae are very complex and not completely understood nowadays and several models exist - the illustration is very good to understand the characteristics of polymers. Due to the partly crystallized lamellae-structure of the polymer, in the area above T_G and below the melting temperature T_M, a liquid and solid phase coexist in the polymer. The crystallized lamellae are surrounded by liquid. E.g. in case of mechanical compressive stress, it can be absorbed by the liquid phase, and the crystal-structure does not break. This expains the characteristic tough behaviour of polymers between T_G and T_M.[55, S.117f]

Polymers with glass transition temperatures T_G above room temperature are called *thermoplastic*. When T_G is (sufficiently) below room temperature, they are

called *elastomer*. T_G however is not completely clearly defined, and a bit arbitrary, and depends on different factors like the cooling rate or pressure. Furthermore, glass transition has severe impacts on non-mechanical properties like specific volume, entropy or specific heat also.[63, S.114ff] [31, S49]

These transitions from almost liquid to semicrystalline state with amorphous, glass-regions are important to consider, when talking about polymers as electrical insulation materials. When temperature increases and decreases towards T_M occur, the material structures are possibly changed or modified. The morphology of the polymer though, is essential for the mechanical, thermical and dielectric properties of the insulation.[55, S.98] By rule of thumb, polymers can crystallize in a temperature area at least 30°C over T_G and at least 10°C below T_M. If the temperature is too low, the motion of the segmental motion of the polymer-chains is too low to cristallize, at too high temperatures the thermal motion is too strong. [55, S.111]

1.3 Layout of Cable and Layers

After the explanation of the basic physics of power cables and the main processes occurring in them in operation, the design and function of modern underground cables shall be shown. Therefore, after a short explanation of the basic cable classification, from a practical example of an MV-cable the different layers, their function and their characteristics shall be explained.

1.3.1 Classification of Cables according to Voltage

According to Austrian and European standards, cables are designed for the use in a three-phase electric power grid with a nominal Voltage of $U_N = \sqrt{3} \cdot U_0$.

U_N in this formula is the voltage difference between two phases, U_0 the voltage difference between an individual phase and neutral. The cables may be used in grids in which the star point is either earthed with a low impedance, insulated or with earth fault compensation. In grids with earth fault compensation, a single earth fault should not be longer than 8 hours, and the sum of all earth faults in a year should not exceed 125 hours. [36, S.21ff]

According to CENELEC (European Committee for Electrotechnical Standardization) cables in European power grids can be divided into four main categories according to the different nominal voltages in each category:
1. **Low Voltage** $U_0 \leq 1kV$
2. **Medium Voltage** $U_0 \leq 35kV$
3. **High Voltage** $U_0 \geq 35kV$
4. **Extra High Voltage** $U_0 \geq 230kV$[5]

As already mentioned, the focus of this thesis lays on Medium Voltage cables in the area of 20kV.

1.3.2 Layout and Components of a Medium Voltage-Cable

> "...waterproof for 100 years, flexible and extensible, so volt-resisting that the thinnest film suffices, with a specific capacity almost as low as that of air..." (Mervyn O'Gorman, IEE Journal 30, 1900 [15, S.4]

It is easy to see, that the desired properties for cables have been very clear for the last 120 years. To optimize cable design in terms of resilience and reliability, different additional layers of sheaths to the basic conducting and insulating

material were invented over the time. The physics and engineering behind these design-questions are not trivial: even though air is a good insulating material, a 20kV overhead power line needs 180mm of insulation distance while a cable only has 6mm of insulating coating. This shows the high requirements on the material and its processing. [7, S.29]

Every modern cable is characterized by a code of different abbreviations, providing information about these layers and the cable-design. To give a basic insight how the different components and layers may look like, figure 2.9 shows the cross section of a modern cable as an example and the abbreviations for the different layers.
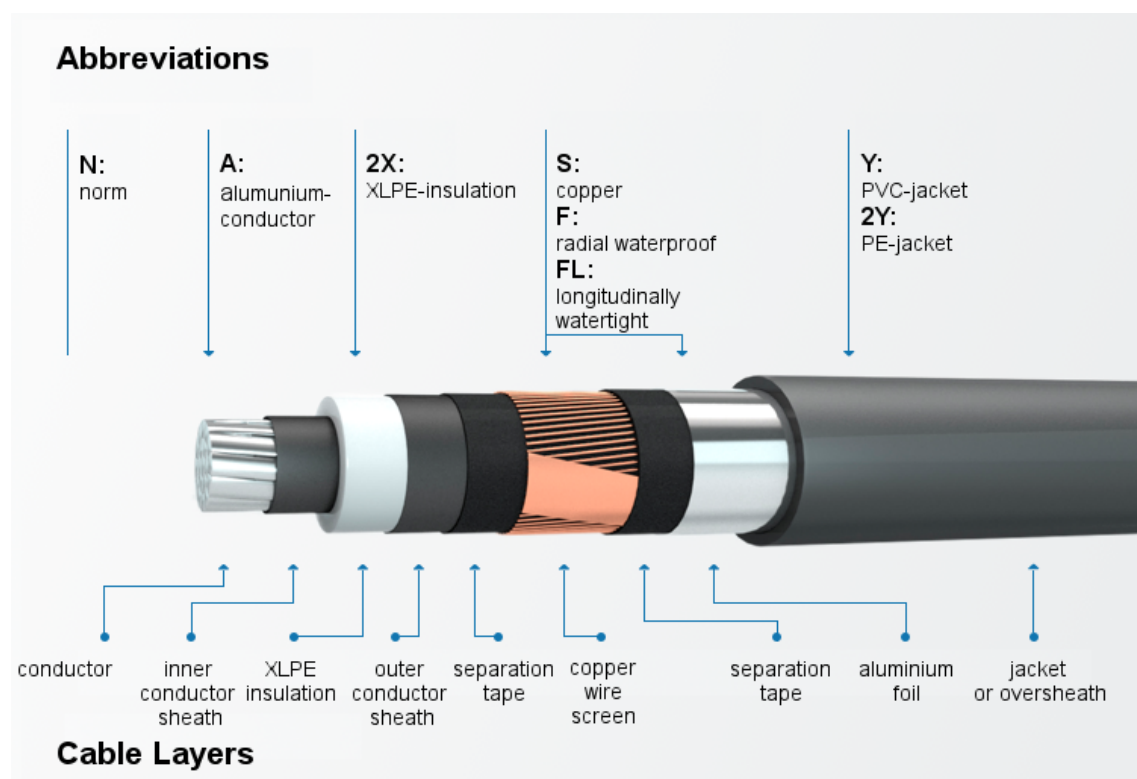

Figure 1.21: Example for cable-layers, adapted figure from the cable-producing company nkt. [41]

The cable shown in figure 2.9 consequently has the abbreviation **NA2XS(F)2Y 12/20KV**.

- **Fundamental Type** - N stands for "according to a national standard"

- **Type of Conductor** - A for aluminium conductor.

- **Type of Insulation** - XLPE-insulation (2X) and helically wounded copper wire screen (S)

- **Water Resistance** - F indicates a radially waterproof screen.

- **Oversheath** - oversheath made from polyethylene (2Y).

Each of these layers is explained in more detail in the following sections. [41]

1.3.3 Conductors

Requirements for conductors in cables are determined in EN IEC 60228 - they can differ regarding material, shape, design and cross section. The main goal of the conductor is to transport the electrical energy with as little loss as possible. Residual currents in case of faults must not lead to overheating over the maximum allowable temperature, so reserves need to be considered in the dimensioning. The necessary conductivity and performance limits are determined by the material and cross section.

The most widely used materials for conductors in cables are either copper or aluminium. Copper is an excellent conducting material (only silver has a better conductivity) and is very easy to forge. Due to this qualities copper has been in use for different electrical applications from the very first days of electrical engineering on. Aluminium was first used as a substitute, especially in Europe, due to shortage of raw materials in World War I. Nowadays in low voltage or medium voltage grids aluminium is the standard material. As already shown in section 1.2.1 even though the conductivity of aluminium is only around 2/3 to copper, the density is so much lower that a conductor of the same conductivity, made of aluminium, has only half the weight. [36, S.31] [34, S.1ff]

The shape of the conductor can differ over a variety of possible forms, depending on the operational purpose and type of the cable. The most fundamental difference is between single-wired conductors or conductors made of several strands. Aluminium conductors can be produced single-wired up to cross sections of $1000mm^2$ and for special purposes up to $2500mm^2$. To ensure a sufficient bendability, for single-wired aluminium conductors a softer aluminium alloy is used for larger cross sections. For mechanical protection purposes, conductors with smaller cross sections are generally made out of a harder material, conductors with large cross sections are made out of a softer material. [7, S.52]
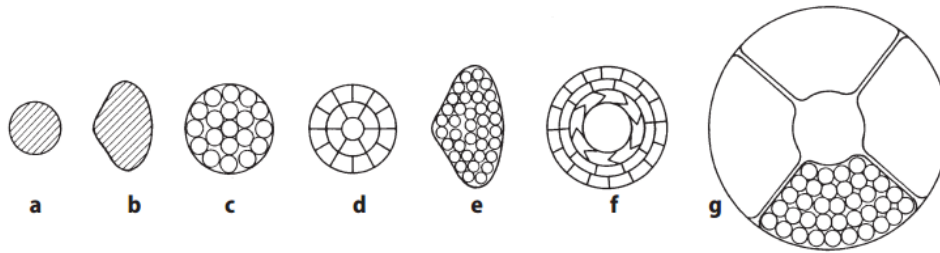
Figure 1.22: Practical examples for different conductor-shapes in MV-cables. a)solid round, b)solid sectional, c)stranded round, d) stranded round and compressed, e)stranded sectional, f) stranded round and compressed with hollow center, g) stranded hollow for large cross sections [13, S.326]

Conductors made out of several strands generally have a higher bendability. The strands can also be insulated against each other as Milliken-Conductors via oxidation or varnish. This is done to reduce the already in section 1.2.1 explained skin effect. [7, S.52]

Cross sections of conductors are always stated in $[mm^2]$. The values do not represent the geometric cross section but the *electrically effective cross section*, which can only be determined by measurements.

1.3.4 Insulation

As already explained, insulation is a crucial component in every cable, and a few properties of insulating dielectrics were already explained and discussed in section 1.2.

Basically, the insulation must ensure:

- sufficient insulation of the phases among each other and against neutral at nominal voltage, and

- sufficient insulation in the case of short time overvoltages (switch voltage, earth fault...).

Dielectric strength of the insulation is measured in Dielectric Withstanding Voltage Tests (DWV). The insulation has to withstand a voltage test, which usually applies a multiple of the nominal voltage for a certain time on the cable. Also withstanding surge voltage is tested. These tests are described in more detail in literature, e.g. [7] or [49].

The insulation of a cable is not only responsible for electric properties but mechanical qualities as well. Examples for mechanical properties can be tensile strength, elongation at break, thermal expansion or form stability.
[36, S.34ff][7, S.54f]

1.3.4.1 Paper Insulated Cables

The use of paper as an insulating material for cables goes back to the year 1888, when Sebastian Ziani de Ferranti, a British electrical engineer, got a patent on a machine to insulate cables with helically wrapped paper. Later, he impregnated the paper with a mixture of oil and resin which turned out to be an effective insulation as well as a low-cost solution.[34, S.8ff]

Paper insulated cables are nowadays considered to be outdated equipment in medium voltage cables. But as already shown in figure 1.4, due to their wide use in the 20th century and long service life, many of these cables are still in use. The already described main principle of the production always stayed the same: specially suited paper is wrapped helically around the conductor and afterwards dried and impregnated in large boilers. The paper needs to be dried carefully, because it originally has a moisture content of about 6%, after the drying it contains around 0,1% water. Half of the volume of the dryed paper consists of cellulose fibers, the other half of air. Because of the significant difference of the dielectric constants of these two materials, using the dryed paper as an insulation would lead to a very uneven electrical field if a voltage is applied. To avoid this, the paper is impregnated afterwards with an oil to fill up cavities and ensure an even field distribution. Always crucial within the oil-paper-insulation is the moisture content, because of the high ε_r of water, as already described in section 1.2.4. To avoid moisture ingress, the cables need a waterproof sheathing, which in former times was usually made out of lead.

Depending on the nominal voltage and the use of the cables, the thickness of the paper and type of insulation oil can be varied. In medium voltage-applications less viscous oils are used (also called *impregnation mass* - therefore mass impregnated (MI) cables). The advantage of this low viscous mass is to be liquid during impregnation in the boiler at the temperature of about 120°C. During normal operational temperatures the mass stays viscous though. High and extra high voltage cables are filled with oil with a very low viscosity, which are also called Self Contained Fluid Filled (SCFF) cables. [7, S.56ff] [29, S4]

1.3.4.2 Polymer Insulation

Nowadays, in MV-cables, polymers are the dominant type of insulation. Until around 1940, oil impregnated paper insulation had a dominant role as insulating material in cables around the world. The rapid evolution of research and use of polymers soon led to their use in cable technology in the 1940s as well. As an interesting aspect, especially in Germany during wartime in the 1940s, research in polymer insulation was done to find substitutional materials for natural rubber, which was a scarce good due to naval blockades. [34, S.26]

Researchers quickly realized, that polymer cables actually have a lot of advantages in comparison to paper-oil-cables: If produced without defects, polymer insulation is completely homogenous, light weighted, very robust, resistant against moisture and chemicals, cheap in production, easy in installation, maintenance-free and also to mention: the insulation properties are very good.

In the production process, the compressed polymer-insulation is pressed through a special die around the conductor, a procedure called *extrusion*, consequently this kind of insulation is called extruded insulation. [7, S.58] [43, S.55]

The main polymers used in cables nowadays are Polyvinyl Chloride *(PVC)*, Polyethylene *(PE)* and cross linked Polyethylene *(XLPE)*. The main properties of each of them shall be described shortly:

Normally, **PVC** is an amorph thermoplastic and at room temperature a hard and brittle fabric. For the use as cable insulation, different additives like plasticizers (approximately 15-50%), fillers and stabilizers are added. The resulting plasticized PVC is an elastic, rubber-like thermoplastic. [55, S.413]

The basic structural formula of PVC is as follows:

$$\left[\begin{array}{cc} H & Cl \\ | & | \\ -C & -C- \\ | & | \\ H & H \end{array}\right]_n$$
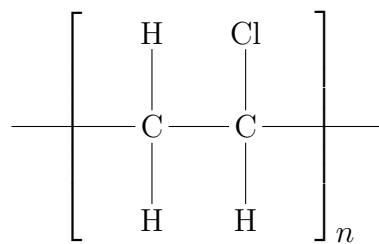
As already discussed in section 1.2.4, oscillating dipoles within a dielectric cause dielectric losses and therefore play a major role in AC-operation. If one is looking at the structural formula of PVC, it is easy to see, that the large chloride-atoms form strong dipoles within the chain. This leads to high dielectric losses in PVC-insulation at higher voltages. Also, the material can become brittle at

low temperatures. These properties and disadvantages limit the use of PVC as a cable insulation. In medium voltage they can be neglected and are only used up to maximum voltages of 10kV. [7, S.61ff] [34, S.25ff]

Nowadays, in the area of 20kV cables **PE** and **XLPE** are the most widely used insulation materials. Polyethylene is a semicrystalline thermoplastic and the structural formula of PE has already been discussed in section 1.2.8, and is as follows:

$$
\left[\begin{array}{ccc}
& \overset{\displaystyle H}{|} & \overset{\displaystyle H}{|} \\
-\!\!\!\!\!\!- & C & \!\!\!\!\!-\!\!\!- C -\!\!\!\!\!\!- \\
& \underset{\displaystyle H}{|} & \underset{\displaystyle H}{|}
\end{array}\right]_n
$$
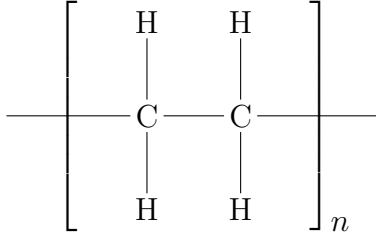
In comparison to the structure of PVC, from an insulation point of view, many advantages are clear:

- PE has no polar groups in its structure, therefore ε_r is low, which leads to small dielectric losses even at higher temperatures.

- There are no large atoms within the structure (like in PVC), which leads to a very tight packing of the molecule structure and consequently small water vapour permeability.

- Also the mechanical properties of PE are very convenient for the use in cables, tensile and pressure strength is high and the material has a good bendability.

The polymer Polyethylene was first discovered in the 1930s and especially the Anglo-Saxon countries were the first to experiment with it as an insulation material for submarine communications cables, due to its high water resistance. After the war, PE soon became the number one insulation material for energy cables as well, even though originally the maximum operating temperature was only at 75°C, which is lower than the operating temperature of paper-oil-cables, which is around 80-90°C.

These properties were dramatically improved with the invention of cross-linked polyethylene *XLPE* in the 1960s. As already shortly mentioned in section 1.2.8, the term *cross-linking* describes a chemical process, which uses a cross-linking agent to create bonds from one polymer chain to another. A cross-linked polymer molecule therefore is basically not a chain anymore, but a giant net-like molecule.

Examples for these cross-linking agents are peroxides (most frequently used) or silanes (for low voltage applications). At higher temperatures, the peroxides decompose into alkoxy-radicals. These radicals then separate hydrogen-atoms from the polymer-chains, which then are able to connect with carbon-carbon-bonds as shown in figure 1.23:
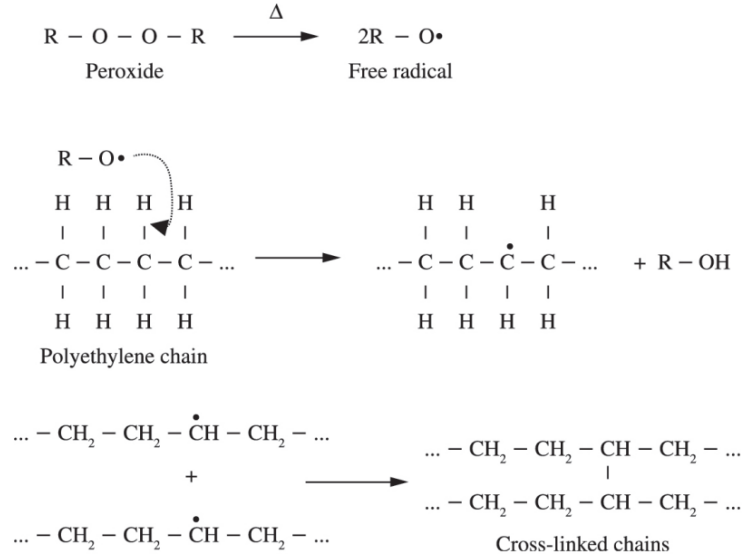

Figure 1.23: Scheme of the mechanism of peroxide cross linking. [38]

The cross-linking improves the properties of PE as an insulation especially regarding their behaviour at higher temperatures. As explained in section 1.2.8, all the explained polymers in use in MV-cables are in operation in a temperature range between the glass-transition temperature T_G and the melting temperature T_M. Normal PVC has a T_G of approximately 85°C [24] which when used as cable insulation is lowered significantly by additives and plasticizers as already explained. Regarding PE, the value of T_G varies depending on the source. In [25] T_G is stated as -78°C, in [53] the difficulties in an exact measurement of this value are explained, and the range from -25°C to -120°C for T_G is stated from different scientific sources and publications. Nevertheless, T_G of polymers used as cable insulation is far below normal operational temperatures. As explained in section 1.2.8, the polymers are therefore operated in the semicrystallized range, where solid and liquid states coexist.

Normal PE has a melting point of approximately 100°C[25], which leads to irreversible changes in the polymer-structure at temperatures in the range of 100-

110°C. Thus, PE gets instable regarding insulation and shape. Due to its improved structure, XLPE is a so-called *thermoelastic* material, able to withstand higher temperatures without changes in shape or structure. This allows maximum allowable operational temperatures of around 90°C and emergency ratings up to 140°C. The cross-linking process, however, increases the production costs of the cables significantly. [34, S.32ff] [43, S.55f] [29, S6ff].

1.3.5 Semiconducting Layers

As shown in section 1.3.2, the cable does not consist only of a conducting material and an insulation layer, but of different additional layers in between. In figure 2.9 on the inner and outer side of the XLPE-insulation, two conducting sheaths can be seen. These are used to ensure a homogenic electric field within the insulation, which will be later explained in detail regarding electrical ageing. The inner conducting sheath seals the interior space between conductor and insulation. Usually paper or textile tapes with a low conductivity (therefore called *semiconducting layers*, even though no actual *semiconductors* are used) are used for these layers, which are extruded with the insulation in one working process. The outer conducting sheath is connected to the wire screen.[7, S.64ff]

In the early years of using this type of layout, too little attention was paid to the properties of these conducting layers around the cables. Due to impurities, ions within the semiconductors could contaminate the insulation and furthermore lead to accelerated ageing and damages - these problems and processes are explained in detail in chapter 2. [29, S6.].

1.3.6 Additional Layers

After the insulation and conductor sheath, figure 2.9 shows additional layers, which represent the outersheathing.

After the outer conductor layer, a **wire screen**, in this case helically wounded and made out of copper covers the cable. The screen is closely meshed and the cross section of it is dimensioned, that it can withstand an earth fault current. If there is a mechanical damage on the cable, the conductor therefore cannot be exposed without causing an earth fault.

Modern cables are usually radially and longitudinally waterproof, which means in case of a mechanical damage on the outer jacket, further ingress and distribution

of water can be prevented. To ensure this, tape layers are placed around the screen, which swell up and seal the cable this way. Additionally, often an aluminium foil is placed just after the outer jacket, which works as a diffusion barrier, because the polymer-oversheaths are not completely vapour-proof.

Modern jackets or oversheaths of PE- and XLPE-cables are usually made from black dyed, UV-resistant PE.[7, S.66ff]

1.3.7 Transition Joints and Closings

Cable joints and closings are used in grids for the connection or termination of cables. The demands on joints and closings are similar as on the cables, because they must not create weak spots within the cable grids. The installation therefore has to be done carefully and by qualified staff, because other than the production of the cables, which is basically done in clean room conditions, the transition joints and closings have to be installed on the construction site.

A basic differentiation of cable joints (Muffen) and closings (Endverschlüsse) can be:

- **Stop joints (Endmuffen)** are closing cable ends voltage-proof without connection to other parts.

- **Connection joints (Verbindungsmuffen)** connect cables of the same type.

- **Transition joints (Übergangsmuffen)** connect cables or different types.

- **Junction joints (Abzweigmuffen)** allow junctions of cables with the same of different type.

- **Closings (Endverschlüsse)** are closing cable ends with a connection to e.g. an overhead power line or a switchboard. [7, S.117f]

2 Ageing of Cables

In the previous section the main characteristics and physics of underground cables were explained. In terms of practical use, the following key-challenges for grid operating companies can be summarized:

- Underground cables are an essential part of modern infrastructure for electrical supply. Many distribution grids depend strongly on cables for the power supply of their customers.

- Within the grid, even small damages and outages may potentially have serious consequences. Power outages can lead to severe impacts on public life or production losses for companies.

- Cable grids represent huge assets and major investment properties for grid operating companies, accompanied with high demands in terms of operational reliability and security of supply.

- The underground installation of the cables involves a great deal of technical efforts and sometimes complex legal processes with public authorities and landowners. Legal procedures may take years, so changes within the grid or the routing of the cables are impossible to execute in short term.

- In operation, power cables are subject to complex processes and high stresses due to voltage, heat development or external influences. These stresses may potentially lead to a deterioration of the cable properties and lead to a higher probability of outages.

This creeping degradation of the cables due to operational stresses is called *ageing*. The high dependencies on the grids in conjunction with the requirements on their availability lead to a strong interest in understanding how ageing processes occur and what impacts they might have on the cables. The state of research regarding these ageing processes shall be explained in detail in this chapter.

2.1 Ageing Processes in General

2.1.1 Ageing of Insulation - Definition and Types of Ageing

The IEC-standard 60505 - Evaluation and Qualification of Electrical Insulation Systems - defines the term *ageing* as follows:

> *"Ageing: Irreversible changes of the properties of an EIS (electrical insulation system) due to action by one or more stresses. (...) Ageing leads to degradation of the EIS."* [44, S.11]

Ageing by this definition means the sum of irreversible changes in the physical properties of insulation materials. By not being reversible, these changes add up and therefore the state worsens over time. This leads to a time dependent ageing-state of the insulation. Ageing includes chemical and physical processes and can be divided into *intrinsic* and *extrinsic* ageing.[28, S.15] [11, S.14]

- **Intrinsic ageing:** processes in the insulation material caused by ageing factors.

- **Extrinsic ageing:** at points, already damaged by contaminants, defects, protrusions or voids (called *CDPVs*)

CDPVs are already brought into the insulation during the production processes and are therefore not in the sphere of influence of the grid operator. Nevertheless, they can be avoided with an accurate quality management and product testing.

2.1.2 Diagnostic Properties and Ageing Factors

For practical application, measurable properties p within the EIS have to be identified, which have time trends correlating to the ageing state and are therefore called *diagnostic properties*. The development of p can then be plotted against the time at a given value of stress S_i. Theoretically, for the threshold p_L, the time-to-maintenance or time-to-failure t_L can then be identified. [44, S.34f]
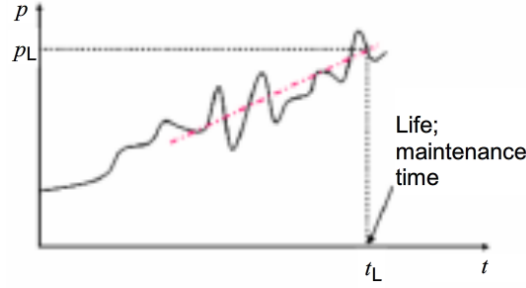
Figure 2.1: Schematic figure of property versus time behaviour in an EIS, detection of threshold p_L and time t_L. [44, S.35]

Apart from CDPVs, four main **ageing factors** for EIS have been identified, which can act individually or synergistically on the insulation system:

1. **Electrical Stress** (voltage, frequency, current...)
2. **Thermal Stress** (temperature cycling, maximum temperature...)
3. **Mechanical Stress** (bending, tension, vibration...)
4. **Environmental Stress** (gases, water/humindity, radiation...)

These basic interdependencies can be shown in the following figure, taken from IEC 60505:
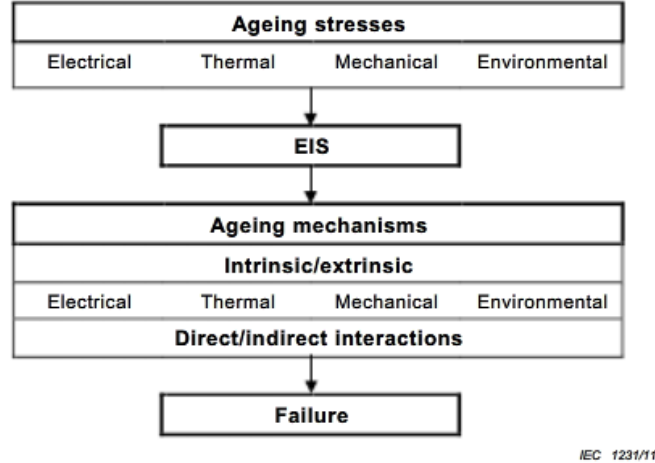

Figure 2.2: Schematic figure of ageing of an EIS [44, S.13]

According to figure 2.2, ageing factors can be classified either into electric or non electric (thermal, mechanical, environmental) origin. In the following sections, beginning with the non electric factors, they shall be analyzed in detail.

2.2 Non Electric Ageing

Non electric ageing involves all kinds of ageing besides the continuous operation with DC- or AC-voltage, or where it is only the cause of secondary effects like heating. These ageing factors shall be examined in detail in the following section, on the one hand because they can lead to a breakdown themselves, but on the other hand because there are cross connections to the electrical ageing mechanisms explained in the next section. Because the focus of this thesis lies on cables with polymeric insulation material, the general chemical and physical ageing processes within them shall be explained first. Then the effects of the previously mentioned thermal, mechanical and environmental stresses are explained.

2.2.1 Physical and Chemical Ageing in Polymer Insulation

Some basics in polymer-physics and -chemistry have already been discussed in section 1.2.8 and the most popular types of polymers as insulation material have been described shortly in section 1.3.4.2.

2.2.1.1 Physical Ageing

Physical ageing effects in polymers have become a subject of interest for research quickly after the wide distribution of polymer-materials in the second half of the 20th century. For many polymer-products, not especially cables, it was soon discovered that especially when stored at elevated temperatures, many of the original properties changed, and the materials in general became stronger and stiffer. [56]

A milestone paper in this issue was published by the Dutch researcher L.C.E. Struik in 1977, where the process of *physical ageing* was well defined for the first time. [61] Based on the known fact, that amorphous materials (like polymers) below their glass-transition temperature T_G are not in a thermodynamic equilibrium, he defined the slow and gradual approach of the material towards this equilibrium as what we know as *physical ageing*. At a molecular level, this is attributable to a higher spacing between the polymer chains after processing, than it would be at thermodynamical equilibrium state.

A *free volume* v_f, which is the packing difference between the material and that of the close-packed molecular form at equilibrium state within the material exists. In amorphous polymers, this is due to the long chains and the bundles they form, which prevent the material from completely close-packing. Because of the attraction of the molecules towards each other, these molecular-level holes of the free

volume increase the internal energy Δu proportional to v_f.[61, S.166]

The free volume has to be clearly distinguished from microscopic voids within the polymer. Voids are caused by impurities during the production process like trapped gas bubbles or excess additive agents and are much larger, approximately 0.1μm.[31, S.53]

Within the polymer, the ageing processes towards thermodynamic equilibrium cause the molecules to move together more closely. Due to this effect, the inter-molecular attraction forces become stronger and the molecules lose more and more freedom of movement. This leads to macroscopic effects of the material becoming stronger, stiffer and losing ductility. These effects, nevertheless only occur in a temperature region below T_G and above the temperature of the so-called highest secondary transition in the polymer T_β. This so-called *ageing range* covers a wide range of temperature, e.g. for non plasticized PVC from -50°C to +70°C. [61, S.165] The specific volume of such a polymer is plotted against temperature in figure 2.3:

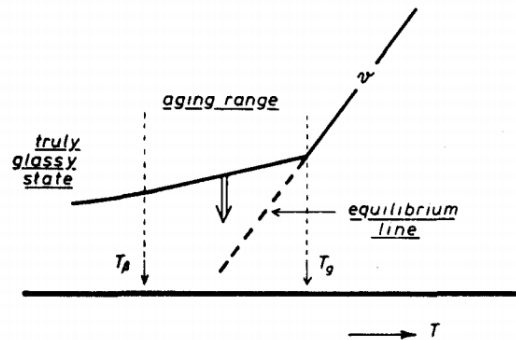**Figure 2.3:** Plot of the specific volume v against temperature T in an ageing polymer as described. Between T_β and T_G the physical ageing occures as described. [61, S.165]

The effect of ageing is clearly visible in this plot, as a creeping approach of the equilibrium line within the ageing range. Above T_G no physical ageing in the described sense occurs, since above T_G liquid phases within the polymer like described in section 1.2.8 are responsible for liquid or rubber-like behaviour. Therefore, it can be assumed, that a polymer above T_G reaches thermodynamical equilibrium. A temperature increase above T_G makes the material *forget* any previous ageing, therefore ageing in this theory is a *thermoreversible* process. [61, S.167]

However, as explained by Struik in [60] experimental data shows, that also semicrystalline polymers and filled rubbers above their T_G show physical ageing effects, and they have a strong affection on the material properties as well. It is suggested, that the reason lies within different T_Gs, whether an amorphous part lies within an *undisturbed* region sufficiently away far enough from the crystalline lamella, or a *disturbed* region adjacent to those. Therefore, the glass-transition is not completely shifted, but broadened to a higher temperature due to the *disturbed* regions. [60, S.51ff] This model is illustrated in figure 2.4:
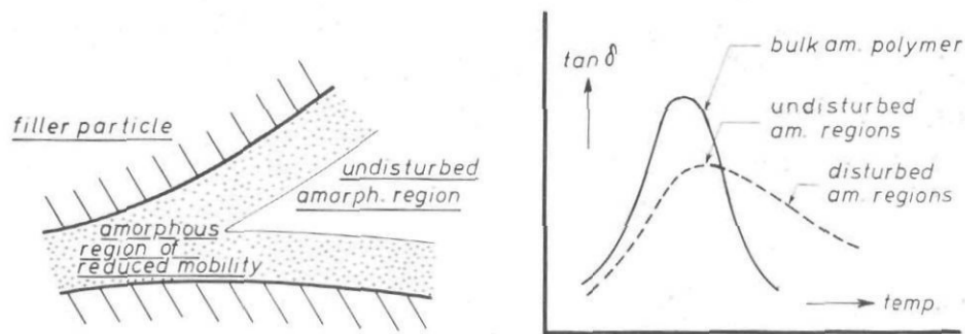

Figure 2.4: Illustration of the model of broadened area of glass-transition of semicrystalline or filled rubber materials. $tan\delta$ on the vertical axis in the right diagram means the damping constant as a quantity of energy absorption and therefore an indicator of glass-transition, not the dielectric dissipation factor. [60, S.55]

For practical use, this means that the described effects of physical ageing can also be applied to MV-cable insulations of semicrystalline polymers, operated above T_G.

2.2.1.2 Chemical Ageing

Chemical ageing is usually caused by free radicals $\dot{R}$ formed within the polymer. Free radicals are highly unstable and reactive molecules with a free electron, which tend to oxidize other molecules and therefore lead to oxidation within the insulation. Within the polymer, the free radicals can lead to chain scissions or cross-linkings via chain reactions. Regarding PE for example, the bond breaking is usually random in space, and the free radical transfer happens between the chains.

The formation of $\dot{R}$ usually follows an initiation step X, which can be thermal, oxidative, mechanical or caused by radiation.

$$X + R_{a+b} \rightarrow \dot{R}_a + \dot{R}_b \tag{2.1}$$

- Thermal initiation occurs via thermal breaking of the chain molecules. Due to Joule-heating the thermal initiation can be indirectly driven electrically.

- Oxidative initiation may occur due to by-products of the polymer-processing, and can be catalysed by metal ions.

- Mechanical initiation can occur through mechanical force during processing.

- Radiation initiation requires the presence either of UV-radiation which can be easily screened or ionizing radiation like x-rays and γ-rays. Ionising radiation photons have a high energy which usually leads to rapid degradation to low weight fragments of the polymer chains. [31, S.55ff]

2.2.2 Thermal Stress

2.2.2.1 Definition and Effects

According to the ISO 60505-standard, thermal ageing effects on cables involve:

1. Thermally induced and accelerated physical and chemical changes in the insulation material e.g. degradation reactions, polymerization, depolymerization, diffusion etc.

2. Thermomechanical effects due to thermal expansion and/or contraction [44, S.18]

The latter category will be considered in the following section 2.2.3, because only the initial cause of the ageing effect is thermal, the actual ageing processes are mechanical.

Regarding the first category, physical and chemical reactions within the insulation, the operating temperature of cables has already been an issue in different sections like 1.2.8, 1.3.4.2 or the previous section 2.2.1. Regarding the durability of the polymeric insulation withstanding ampacity and heating, it was already discussed, that heat generation in the cables is the main limiting factor for maximum loads in a cable grid.

Heat and elevated temperatures have different effects on the insulating material, which can be looked at from three points of view:

- Firstly, as already discussed in previous sections, an increase in temperature changes temperature-dependent properties relevant for the operation of the insulation like resistance, dielectric permittivity ε_r or the dissipation factor $tan\delta$ (see section 1.2.4). Most of these effects are reversible and can be illustrated with a temperature-dependent function or a temperature coefficient.

  In the worst case, an increase over the maximum permissible temperature within the area of T_M can result in failure of the dielectric, called *thermal breakdown*. Breakdown can either occur, when the insulation is so far physically changed (e.g. melted), that its breakdown strength is lowered below the applied voltage. The other possibility is, that because of the higher temperature, the electrical power dissipation is increased so dramatically that it causes an ongoing further increase in temperature on its own until the melting point, a so-called *thermal runaway*. [31, S.243]

- Secondly, at sufficiently high temperatures, the dielectric can ignite or carbonate. There are different classifications of fire resistance for insulating materials, based on the maximum temperatures at which the materials ignite or suffer damages, that impair their use.

- The third and most complex category are the complex creeping chemical and physical changes occuring within the dielectric. Within the insulation, a variety of different chemical reactions are initiated or accelerated at elevated temperatures. The most obvious is softening, which leads to higher fragility, especially when mechanical stress is applied to the cable while heating.

Other temperature-induced reactions (the list is not complete) may be:

- oxidation and the production of oxygenated products with low molecular weight as already discussed in combination with free radicals;

- shrinking due to sublimation;

- loss of plasticizers and therefore hardening, shrinking and formation of cracks;

- variation in cristallinity and polymer structure, and therefore the melting point [42, S.44f] [64]

Generally speaking, for PE exposed to air, oxidation effects are the primary thermally activated chemical reaction. The oxidation rate is limited by the diffusion rate of the oxygen through the polymer sheathing as well as the semiconductor layers.[50, S.562]

Regarding the change of polymer structure, in operation the service temperatures around 90°C of PE and XLPE cables small and imperfect crystalline lamella in the semicrystalline structure can already melt. When these spots cool down, a variety of processes can occur, e.g. a different crystallization of the lamella, which leads to spots of increased volume and therefore tensions or strain within the dielectric. As long as the temperature does not get too high (<90°C), existing microvoids or microcracks can be accelerated or expanded by these stresses. [31, S.55]

2.2.2.2 Current Experimental Research

The practical impact of thermal ageing effects on insulation material can be examined by artificial thermal stressing in laboratory experiments, as shown e.g. in [64]. In these experiments, square plates of 30x30cm made from 2mm thick XLPE were thermally aged at 90°C, 135°C and 150°C for 1350hours in an oven. The tested type of XLPE is originally used as an insulation material in 18/30kV MV-cables. During the artificial ageing, different parameters were tested on the material, like volume resistivity, dissipation factor, dielectric strength or tensile strength. The results showed, that the properties were slightly affected at the normal operation temperature of 90°C, significant degradation was shown at the test-temperatures of 135°C and 150°C. Especially the dissipation factor and dielectric strength showed remarkable degradation at the higher test-temperatures:
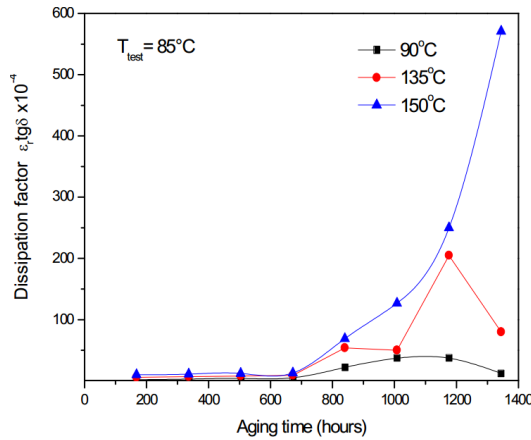

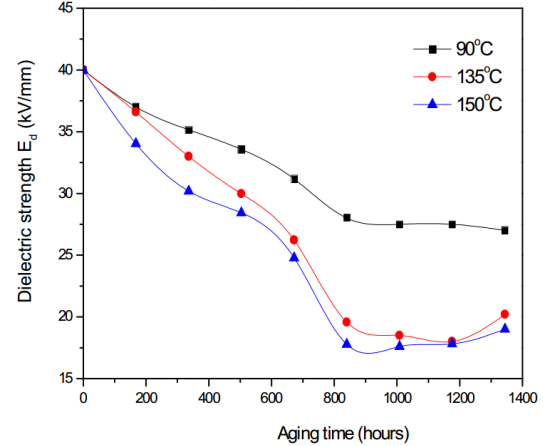**Figure 2.5:** Dissipation factor versus ageing time. [64]

Figure 2.6: Dielectric strength versus ageing time.[64]

Figure 2.5 shows a plot of $\varepsilon_r tan\delta$ against ageing time. The results show clearly that $\varepsilon_r tan\delta$ at all temperatures is practically unaffected until around 680 hours of artifical ageing. After that, only at normal operating temperature of 90°C the properties stay within reasonable values, for elevated temperatures they increase

strongly. These effects are due to the explained chemical and physical degradation mechanisms like oxidation or chain scissoring. In 2.6, the development of the breakdown field E_d against ageing time is shown (destructive test). In this figure the differences between operating at normal or elevated temperatures are clearly visible as well.[64, S.3f]

2.2.2.3 Arrhenius and Eyring Model for Thermal Ageing

Finding a generally applicable connection between heating in a cable, ageing of the insulation, and describing these in an equation for the lifetime-expectancy has been an issue of research since the beginning of the 20th century. In 1948, Thomas Dakin, an electrical engineer working at Westinghouse, published a paper in which he described these ageing processes using the chemical reaction rate theory. This approach uses the *Arrhenius equation* for describing the temperature dependence of the temperature dependence of reaction rates, and is still regarded as a standard work for thermal ageing: [9],[18],[44],[50]

$$L = A \cdot exp(-E/kT) \tag{2.2}$$

where:
L is the life expectancy;
A is a constant representing life at temperature T_0;
E is the activation energy;
k is the Boltzmann constant;
T is the thermodynamic temperature or the thermal stress.

This model can be applied in a so-called *Arrhenius Plot*, where the life expectancy at a particular temperature is illustrated by plotting the logarithm of L against $\frac{1}{T}$ or T. This plot then shows a linear relationship which can be easily extrapolated to the operating temperature from test data. It is important to note, that equation 2.2 is only valid for first order chemical relations and therefore only thermal stresses applied. The model must be adapted when taking other stresses into consideration as well. Also, this linear relation can become non-linear, when polymer insulation is heated above phase transition and partial melting of the insulation occurs. [50, S.561] By rule of thumb, for the majority of EIS, life expectancy can be considered halved when the temperature exceeds operating temperature for 8-15K. [44, S.18]

Sometimes, instead of the Arrhenius-Model, the similar *Eyring-Model* is used:

$$L = (\frac{A_L \cdot h}{kT}) \cdot exp(\Delta G/kT) \tag{2.3}$$

where: A_L is an ageing limit;
ΔG is is the free energy of activation;

This Eyring-equation can also be plotted in a linearized way with $log(LT)$ over $1/T$, in the same way as the Arrhenius-plot. An example for this kind of plot is shown in figure 2.7:
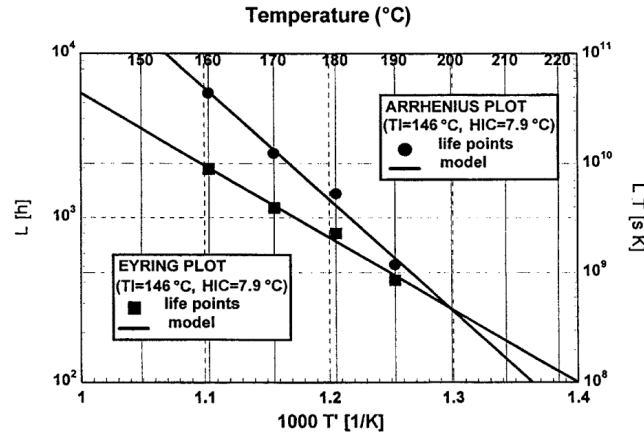

Figure 2.7: Practical example of an Arrhenius-plot and an Eyring-plot in comparison. The lines show the calculated Arrhenius- and Eyring-models, dots and squares show test measurements, the material is 30% glass filled PET. [18, S.1154]

2.2.3 Mechanical Stress

Cables are subject to mechanical stresses in all aspects of their life cycle, beginning with production (thermomechanical stresses have already been mentioned in the previous section), transport, installation and operation. According to ISO 60505 mechanical ageing may involve:

- fatigue failures of insulation components

- thermomechanical effects due to thermal expansion or contraction

- rupture or damage of insulation due to external forces

- abrasion of insulation caused by relative motion between components[44, S.20]

Mechanical stresses on the cable can already occur in the production. Stresses and tensions can arise because after heating processes (like the already in section 1.3.4.2 described cross-linking), and different cooling speeds of the materials while being in use. The insulation can then shrink in the longitudinal direction, causing shrinkback at the cable-ends. Regarding these properties, it must also be considered, that the cables are usually operated at elevated temperatures in comparison to the surrounding. Conductor, sheath and insulation have different thermal expansion coefficients, which can also lead to tensions and stresses within the cable. For example, the thermal expansion of XLPE is approximately 20 times bigger than the one of the conductor. When the insulation gets heated from 20°C to 90°C, it expands approximately over 6%, and another 6% when heated to 115°C. This, of course, causes stresses and tension towards the outer jackets and sheathing. Keeping this *thermomechanical stresses* to a minimum is a demand on the tape and bedding layers in the cable. However, these mechanical stresses within the cables need to be accomplished by constructional measures.

Also, thermomechanical stresses at operating temperature can occur in comparison to soil temperature due to lateral forces. At low temperatures, the compression modulus of XLPE cables is high enough to accommodate bendings or lateral forces by installation. This compression modulus however decreases extremely with temperature, especially above 90°C. This decrease can lead to permanent displacement of the conductor or in worst case radial cracks in shielding or XLPE-insulation..[50, S.566f.]

Storage, transport and installation of the cables are other sources of various mechanical stresses to the cable. Usually, cables are transported coiled on a spool. These spools must have a minimum diameter to avoid the cables from being bended too much. Also damages or e.g. nails on the spools can lead to damages of the cables.

Figure 2.8: Stored MV-cables on wooden spools. [41]

Also, damages during the transport of the spools are possible and must be avoided by cargo securing and proper means of transportation. The installation of the cables must be carried out according to the manufacturers' instructions. Considering this thematic, the instruction and qualification of the personell and sound work is a crucial factor. Experiences show, that the majority of cable damages has mechanical causes. Nevertheless, this includes also a great amount of mechanical damages due to construction and excavation works on cable routes. The damages, mostly caused by the excavator shovel can either lead to earth faults or short circuits immediately, or the damage ist not noticed at first. Water ingress and accelerated ageing of the cables can in this case subsequently lead to severe damages after some time. [7, S. 248ff].

Figure 2.9: Damage on MV-cables in Sylt (Germany) in 2017, which caused a power outage for more than two hours in the surrounding regions.[57]

2.2.4 Environmental Stress, Light and Radiation

2.2.4.1 Definition and Effects

Depending on the type, place and technique of installation, cables may be exposed to a variety of environmental influences and stresses in different intensities. A list of possible variable environmental factors might be:

- moisture

- oxygen

- chemicals

- weathering

- radiation etc.

This wide variety of environmental influences may lead to a wide variety of additional or interacting ageing mechanisms like the already mentioned production of free radicals. Therefore, for environmental ageing factors, no generally applicable formula can be derived, the situation needs to be evaluated differently from case to case. [44, S.21]

Even though XLPE cables are waterproof up to a high grade, the presence of moisture or water can cause degradations. In combination with the electric field, the presence of water leads to a phenomenon called *water treeing*, which is explained in detail in section 2.3.3.

2.2.4.2 Current Experimental Research

Also, laboratory tests of some environmental influences can be done to examine these ageing effects. In [26], samples of LDPE and XLPE were artificially weathered with a weather-Ometer (WOM) and an ultraviolet Weathering Tester (QUV). In the WOM, a Xenon light with 6500W simulates natural radiation in southern latitudes, the QUV uses a flourescent light bulb with a UVB-maximum at 313nm wavelength. Each sample was exposed to the artificial ageing process for 100, 200, 400 or 800h. The differently aged samples were then compared regarding tensile strength in tensile tests, x-ray spectra or scanning electron microscopy (SEM). Especially the SEM-pictures give interesting insights into the ageing effects on the surface of the polymer. As figure 2.10 shows, the formation of microscopic cracks and ruptures in course of artificial ageing is remarkable.

The difference to the new samples is clearly visible. Interestingly, the QUV-aged samples show deeper and more numerous cracks and the cracks have a mosaic-type pattern. The cracks in the WOM samples seem to have preferential directions of propagation.

Also, interestingly the cracks in the LDPE-samples are generally smaller and less developed than in the XLPE-samples. This can be explained, because the additional crosslinking-processes decrease the resistance to weathering because internal stresses are built up (as already described in section 2.2.3, oxidation products are formed or peroxide by-products from the cross-linking agent that can act as degradation catalysts). This again shows the complexity of the various physical and chemical ageing processes within the insulation polymers. [26, S.560f]
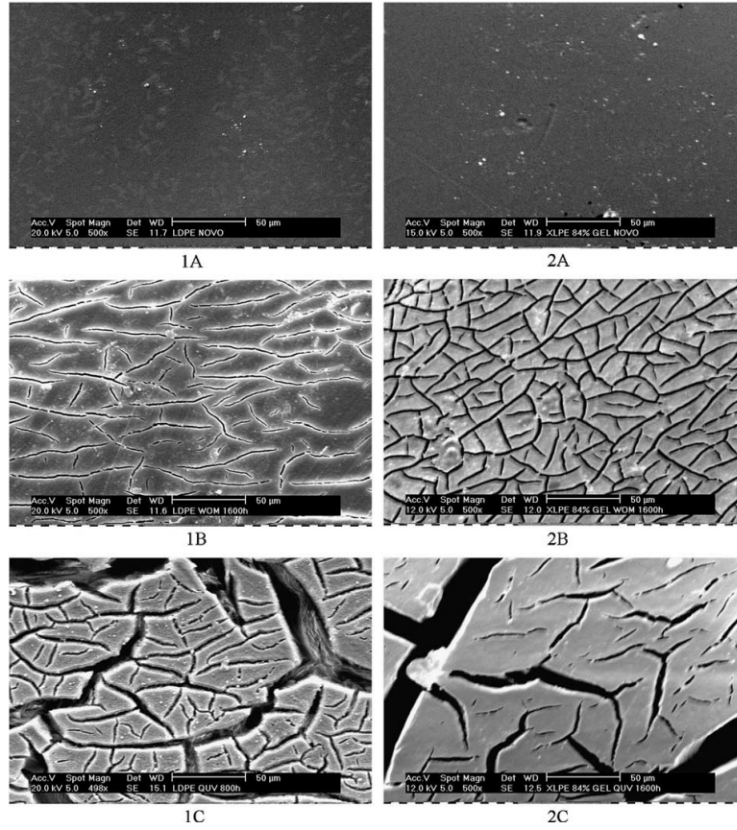
Figure 2.10: SEM-pictures of artificially aged LDPE (1-left) and XLPE (2-right) samples. (A) are the new samples, (B) after 1600h WOM-ageing, (C) after 800h QUV ageing. All pictures have the same scale and are taken at 500x magnification [26, S.560f]

Even though not relevant for the situation of distribution grids in Austria, ionizing radiation as notable environmental factor shall be mentioned briefly. Security relevant cables in nuclear power plants are often exposed to highly elevated ionizing radiation, which makes additional ageing effects of this radiation an issue of interest. Also, when installed in radiologically contaminated areas of the reactor, repair works or changing of damaged cables may be very complicated issues if even possible. Extensive research is carried out e.g. in [**Lee2012**], when the lifetime nuclear power plants is prolonged, and the properties and ageing status of cables must be identified.

2.3 Electric Ageing

The previous sections showed, that many chemical and physical reactions and ageing processes in the insulation of a cable can occur in the absence of an electric field or current. Some non-electric effects are strongly related or effected by electric effects, like increased temperatures due to ohmic or dielectric losses (which also lead to thermal effects within the insulation). When operating temperatures do not exceed the maximum allowed temperatures, electrical stresses though (as explicitely mentioned in IEC 60505 and other standard references like [11]) are the main ageing factor of extruded cable systems.

IEC 60505 gives a general list of mechanisms in electrical insulation systems, which can be attributed to the factor of electric ageing:

1. the effects of tracking;

2. the effects of treeing;

3. the effects of electrolysis; (...)

4. the effects of increased temperatures produced by high dielectric losses;

5. the effect of space charges.

6. the effects of partial discharges when the local field strength exceeds the breakdown strength in the(..)EIS;[44, S.15f]

Practically speaking, electric stress summarizes all the stress mechanisms to the insulation material by the electric field and current of the conductor. The effects of tracking (the development of small, conducting paths on the surface of a dielectric) and electrolysis only play a minor role within extruded cables and can therefore be neglected within this thesis. The effect and behaviour of space charges will be explained in the section of electric trees. The major mechanisms of electric ageing are treeing (electrical and water trees) and partial discharges.[11] [31][37] After a short description of electric fields and the phenomenon of treeing in general, these shall be explained in detail in the following sections.

2.3.1 The Electric Field and Homogenity of Insulation

In the design of cables up to a voltage of approximately 6kV, the insulation thickness and strength is mainly based on mechanical criteria. Up from a voltage of 10kV on, electric criteria are decisive. Some effects and mechanisms have already

been discussed in section 1.2.4, and the electric field, which exists between the conductor and the outer conducting layers, has already been mentioned in section 1.3.5. For the presented coaxial-type design of MV-cables, the electric field strength $E(r)$ at a radius r from the center of the cable can be derived similarly to the field of an infinite wire, and follows the following equation:

$$E(r) = \frac{U_0}{ln\frac{R_1}{R_2}} \cdot \frac{1}{r} \tag{2.4}$$

We can see, that the field strength within the insulation is reciprocally proportional to the distance r from the center, and directly proportional to the voltage U_0. This leads to a hyperbolic decrease between the inner radius R_1 and the outer radius R_2 at the layer interface between the dielectric and conducting layer. R_1 and R_2 are the limits of the field, outside the conducting layer $> R_2$ the field is zero. At the interface of conductor and dielectric lays the maximum of electric field strength, the minimum at the outer interface between dielectric and conducting layer. [15, S.91ff] This field distribution can be seen in figure 2.11: [15, S.91ff]
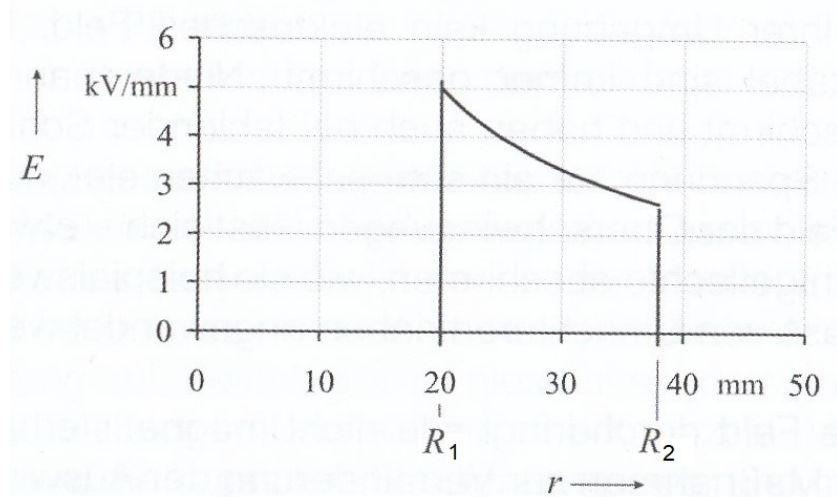

Figure 2.11: Field distribution of $E(r)$ in the insulation of a cable for 64/110kV at $1000mm^2$ cross section. [15, S.92]

For Medium Voltage cables, practical values for E are around 2-4,5 kV/mm. The prevention of inhomogenities in the electric field, as already shortly mentioned in section 1.3.5, is also one major function of the inner conducting sheaths. As known from basic physics, the electrical field strength nearby raised or pointed parts of a surface is significantly higher. Figure 2.12 shows this effect on a conductor with several strands:
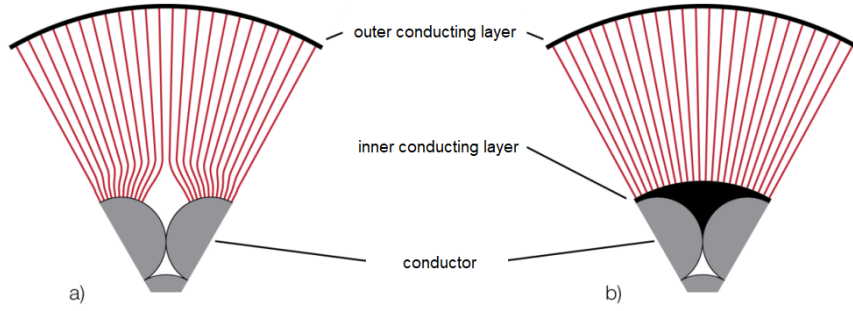
Figure 2.12: Difference in field distribution in comparison between a conducting bundle with and without an inner conducting sheath. [7, S.65]

Due to differences in the relative permittivities ε_r, these peaks in electric field strength also occur locally at CDPVs within the insulation, as already briefly mentioned in section 1.2.4. Absolute purity and absence of CDPVs within a cable insulation are therefore major requirements to prevent locally accelerated ageing spots within the cable insulation. [34, S.79f][15, S.91ff]

Examples for CDPVs within an extruded insulation in a cable can be:

- tips or spinters of the conductor penetrating the dielectric or scratches, asperities or depressions on the interface;

- cavities or regions of free volume within the dielectric with different sizes. These can be due to movement of additives or insufficient pressure during cross-linking;

- impurities like included foreign particles, moisture and spots of imperfect mixing or fillers.[31, S.203]

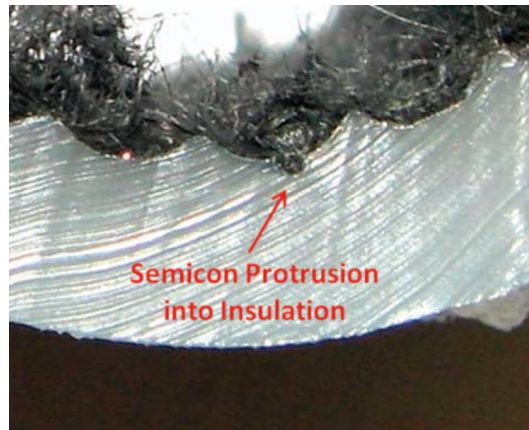An example for such an impurity is shown in figure 2.13:

Figure 2.13: Protrusion of the semiconducting layer into the insulation - the protrusion was caused during the extrusion onto the semiconducting paper tape. [2, S.64]

2.3.2 Lichtenberg Figures and Treeing in General

The effect of treeing within insulating materials is basically known for more than 240 years. Around 1779, the german physicist Georg Christoph Lichtenberg discovered, while experimenting with electricity, that wood dust on the conducting plates of his experimental setup tended to form characteristic, tree-like figures. The physics and processes behind this effect were not understood at this time, but the characteristic figures were named *Lichtenberg Figures* after their discoverer. [4]
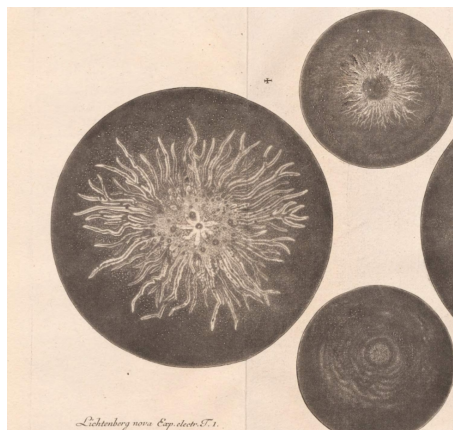

Figure 2.14: Original illustrations from Lichtenberg of his newly discovered tree-like figures on conducting plates of an electrophorus from 1779. [33]

Lichtenberg-figures like treeing in electrical insulation was already detected in the early ages of the use of electricity. Interestingly, the trees were discovered in paper-oil insulation systems as well as polymers, which means these mechanisms must be independent from the chemical composition of the insulation material. Nowadays, the term *treeing* is a summarizing name for the two major electrical pre-breakdown degradations within cables.

Over the years, treeing phenomena in insulating materials were scientifically researched and are nowadays considered one of the major causes for their failure. [31, S.69] The trees in the insulating material consist of conducting channels, which are spreading through the dielectric, and therefore weaken the insulation capability and physical properties. The existence of charge carriers like ions in water filled cavities or inclusions and their contribution to a space charge developing within the insulation plays a major role. Besides water, the space charge within the insulation as an electric field source is mainly caused by impurities, additives, fillers, cross-linking by-products, inaccuracies in manufacturing processes, thermal or radiative degradation. [8, S.30]

The main treeing effects are therefore divided into so-called **water trees** and **electrical trees**. Some sources like [7] also use the term *electrochemical trees* for a treeing effect where ion-rich water in the insulation interacts with ions in the insulation. From its nature, this effect can also be considered water treeing. An example for treeing leading to an electrical breakdown of the insulation layer is shown in figure 2.15:
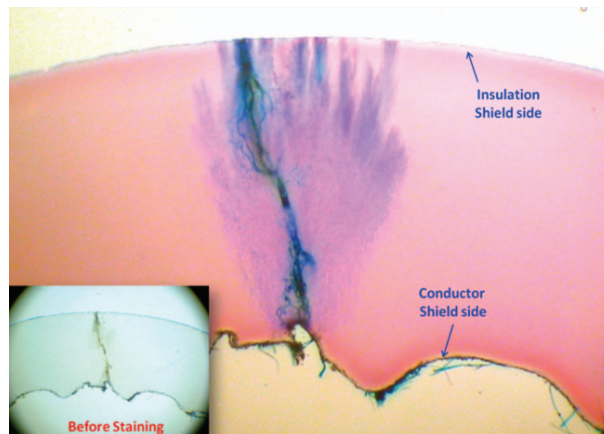

Figure 2.15: Stained (for better visibility) micrograph of an electrical tree bridging the insulation from conductor to outer shielding layer. [2]

2.3.3 Water Treeing

Especially in polymer-insulated cables, *water trees* are a main damaging factor. The exact chemical processes of water tree initiation and development are not fully understood yet [11] [31], but as the name suggests, the presence of water is a crucial factor. The initial water contamination within the cables can be originated either deeply inside the dielectric or from external moisture:

- The first category primarily results from water ingress during production of the cables. In former years of the production of extruded cables, often steam was used for curing of the insulation. Due to the increased solubility of water in the polymers at higher temperature, cables manufactured this way showed a much higher moisture content and more voids. An alternative is the so-called *dry curing* process without steam, where the moisture content is around 7 times lower. [2, S.66]

  Experimental tests have shown, that especially voids with a radius of approximately $2,5\mu m$ and about half filled with water tend to form water trees. The inner surfaces of the voids are usually oxidised or chemically modified, and in semicrystalline dielectrics the lamellae are disordered. The broad tree shape was observed due to scattering from the water in the voids. Contaminants and electrolytes are usually found in advance or at the tip of the tree. [31, S.78] These voids usually form trees in opposite directions, aligned with the electric field lines, due to their form called *bow-tie trees*.

- The second category usually happens at interfaces of different cable layers, e.g. when moisture reaches the dielectric from one side due to water ingress after a damage on the jacket. These trees originated in external moisture usually develop different, more bushy forms, so-called *vented trees*.
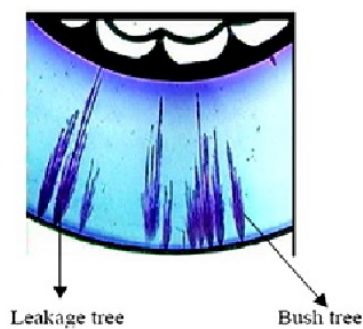

Figure 2.16
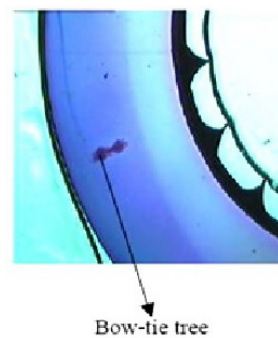Example for different vented trees in the polymer-insulation of a cable. [59]

Figure 2.17
Example of a bow-tie tree in the polymer-insulation of a cable. [59]

The development of water trees is highly dependent on the local field strength within the dielectric. Usually an electric field of at least 1 kV/mm is assumed to be necessary for water tree development, which makes this field strength an empirical threshold. Water trees have been found in cables operated under less electrical stress.[2, S.63] This shows the importance of homogenity within the dielectric as explained in the previous sections, because locally elevated field strengths can be caused by by an inhomogenous insulation as well.

Within MV-Cables, bow-tie trees are limited in their length and only reach a length of some tens of μm. Therefore, these kinds of water trees are usually not responsible for significant ageing or breakdowns of the insulation. At high temperatures, bow-tie trees grow faster because of the increased diffusion-rate of the moisture. [11, S.18]

A lot of research has been carried out to understand the initial inception and growing speed of water trees and a lot of models have been developed trying to understand and describe the mechanisms of water treeing. These are usually quite complex and - e.g. in good detail explained in [31] or [37]. Also, under normal service conditions, the growth of water trees takes years to tens of years. So experiments are usually done with accelerated growing speeds, which gives additional complication factors. A deeper describtion would be beyond the scope of this thesis.

A rough summary of the processes leading to the formation of water trees is: Due to electrochemical dissociation, organic ions are produced, which lead to oxidation and ultimately free radicals within the polymer, causing microvoids. The processes of free radicals have already been shortly explained in section 2.2.1.

It is notable, that similiar reactions also happen in liquid insulation materials, but due to the liquid character, they are fully reversible and do not cause damage to the insulation. In the solid, semicrystalline polymers, the dissociated ions reach the amorphous region and partly contribute to the oxidation reactions. [31, S.149] This general scheme of the rough processes involved is shown in [31]:
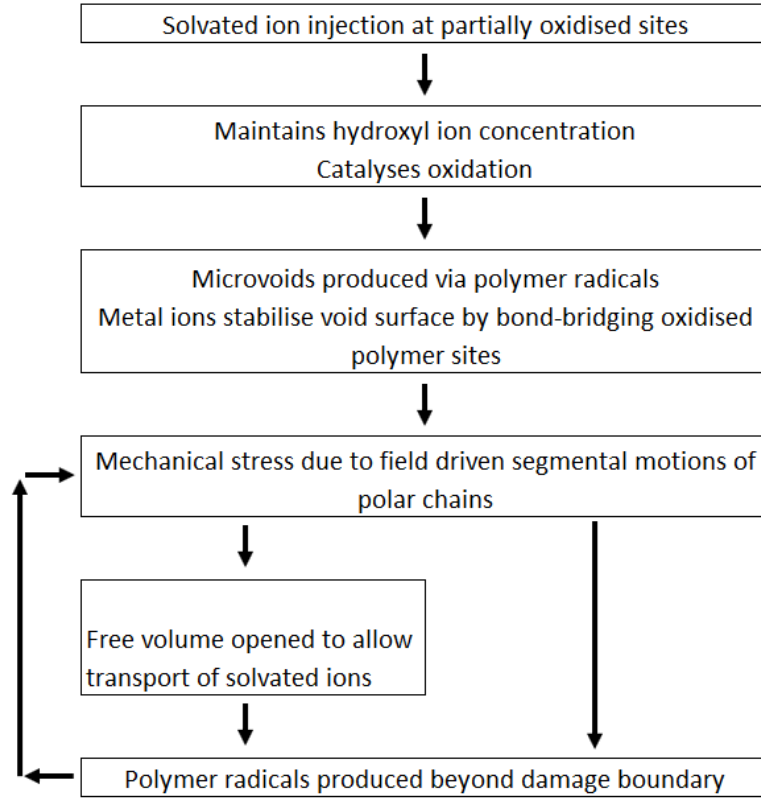
Figure 2.18: General scheme of the processes involved in water treeing. [31, S.110]

When water trees bridge the whole insulation from one conducting layer to another, the water filled microvoid-paths represent weaker dielectric paths within the insulation due to the structural changes in the microvoids. The insulating properties of the dielectric are weakened in this case, but in normal operation, the material can still be expected to withstand the voltage. The process eventually leading to breakdown in this situation and therefore the reason for cable failures are *electrical trees*, originating from the water trees. [31, S.146f]

An example for such a development of an electrical tree out of a water tree is shown in figure 2.19. The special aspects of electrical trees and the differences of the two treeing effects are explained in the next section.
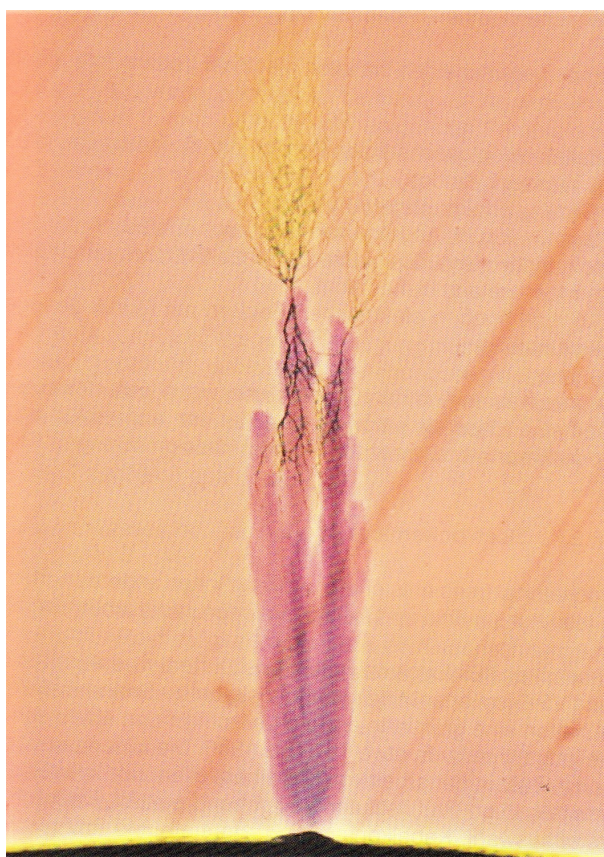
Figure 2.19: Electrical tree (the darker, more ramified structure in the upper half in the picture) originating from a water tree (the stained, blurry structure in the lower half in the picture) in XLPE-insulation[7, S.75]

2.3.4 Electrical Treeing

Electrical trees, unlike water trees, also proceed in dry conditions in the absence of water or another liquid. Basically, electrical trees are created by a sum of small discharges within the dielectric, building a connection of small voids. As a difference to water trees, these voids are not filled with moisture and usually visible to the naked eye. Electrical trees therefore form a system of hollow, non-solid or carbonized tubules resulting from material decomposition, and appear more finely ramified than the rather blurry water trees.

The formation of electrical trees depends more on high electrical stress than water trees, and therefore they occur more often in regions of metallic asperities, conducting contaminants or structural irregularities. [31, S.117][44, S.48f]

CDPVs have already repeatedly been a topic within this thesis regarding reliability and ageing of cables. The effects of electrical treeing and partial discharges, explained in the next two section are heavily influenced by them. The smallest kind of these internal inhomogenities are the mentioned free volumes within the semicrystalline structure of the polymer insulation, occuring between crystalline and uncrystallised regions with different density. According to [31], their free path lengths can go up to a few tens of nanometers at room temperature. In poorly manufactured cables voids may have almost a millimeter of diameter and are usually not detectable under the range of a few tens of nanometers. This range of a few tens of nanometers may also be seen as a rule of thumb for the differentiation between free volume and voids. [31, S.287] To get a feeling for the order of magnitude, Mayoux published experiments where a density of $10^3 - 10^7$ voids/mm^3 was counted in dry cured XLPE insulation in the 1970s and 1980s. [37, S.3] As seen in the introductory sections, a lot of cables from this time are still in operation.

Similar to water trees, the development of electrical trees shows three clearly seperable stages:

- The **inception** of the electrical tree is characterized by an inception time, which is defined as the time t_I it takes, to generate an observable tree. Experiences show, that trees of about 10 μm in length are visible, and the inception time is strongly dependent on the strength of the electric field. t_I usually goes with E^{-a} with $5 < a < \sim 20$ in comparison to $3<a<4$ for water trees. Further, t_I is proportional to the frequency of the AC stresses, in comparison to the initiation of electrical trees which is much more dependent on the field than the microvoid formation in water treeing. [31, S.120]

- The second phase of **propagation** can be divided in a first rather fast growth-stage and a slower, nearly decaying growth-stage after that. This is caused by a self-limiting the growth after the development of the first branch where the electrical discharges in this first channel are temporarily extinguished. In this stage, also the ramification into different branches takes place, out of which some can be growing and others are inactive, leading to the final tree structure. [31, S.121ff]

- In the final **runaway** stage the tree growth is again accelerated, caused by a runaway of the tip of one of the tree branches.

This development of tree growth in time is shown schematically in figure 2.20:
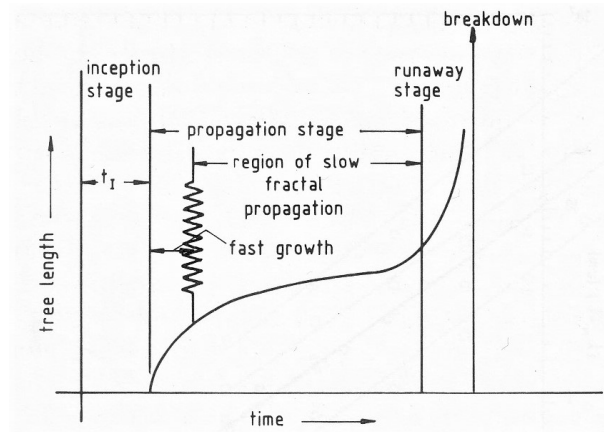
Figure 2.20: Schematic representation of the growth of electrical trees in time. [31, S.121]

Because the propagation of electrical trees basically happens via small discharges, there is a field-threshold, below which no discharges are possible. Below this threshold therefore no electrical trees can be formed. This is the most significant difference of electrical trees and water trees, which can be found at very small stresses as well (as shown in the previous section) and are more time-dependent.

The development of electrical trees out of water trees is not fully understood yet. A plausible explanation for the initial point and inception of an electrical tree would be if the water tree came nearby or approaches a conducting contaminant. Then the combination of the additional electrical stress due to polarised, water filled microcavities and the conducting contaminant could be sufficient for the development of an electrical tree. [31, S.149]

Within the AC-field, electrical trees can then be pictured as space charge accumulations within crazes or microcracks, which are cyclically injected and extracted. Low mobility cations on the sidewalls of the initiated tree cause erosion and widening of the channel and therefore lead to the classical ramified structure. These processes in course of the positive and negative cycles in AC-operation are shown in figrue 2.21:
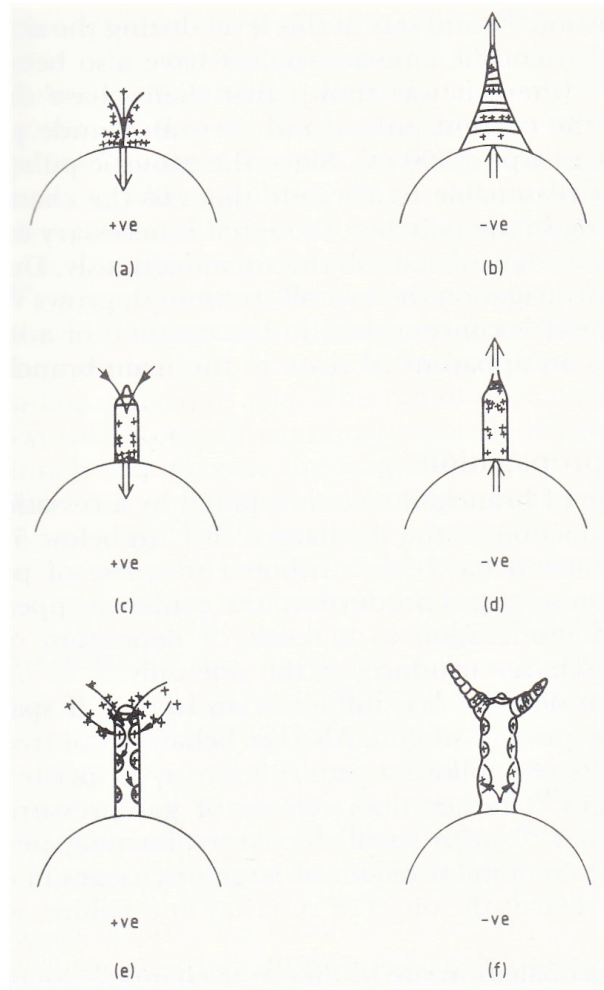
Figure 2.21: Schematic representation of the initial stages of tree formation: a) and b) are back and forward avalanches in a low density region or microcrack, c) and d) show initial gas discharges and e) and f) the sidewall erosion and ramification of the channel. [31, S.133]

Also, it must be mentioned, that not every electrical tree reaches the final stage of runaway causing an actual failure. Especially bushy type electrical trees can at some points achieve an equilibrium stage and do not progress further. In most electrical trees, the accumulation of damage in the first stages is so massive, that the insulation system becomes instable. The initiation of the runaway phase is then characterized by a cease of length-development discharges in the ramified structures, which will sum cation wall charges to the branch tips leading to runaway. The tips then work like an electrode, in the initial stage of an electrical tree.

Different processes like thermal runaway, electro-fracture or electromechanical breakdown superpose into the formation of a single leading channel over the last (<1 μm) to the other electrode. If this leader channel reaches the electrode, interestingly it does not necessarily lead to an immediate short circuit, because it is usually filled with air and the walls are not conducting. Because these channels generally only have a diameter of less than 10 μm, also gas discharges do not occur within them. The final breakdown can take up to 100 hours, and is in the end caused by wall charges and ionization of the gas in the channel. [31, S.151ff]

2.3.5 Partial Discharges

The applicable standards IEC 60505 and IEC 60270 (Partial Discharge Measurements) define Partial Discharges (PDs) as *"localized, electrical breakdown that only partially bridges the insulation between conductors and which can or cannot occur adjacent to a conductor."* [44, S.60]

Within energy cables, partial discharges are an important phenomenon because they are very good measurable, and when they occur it is always a strong sign for degradation or ageing within the insulating material. Partial discharges are not limited to solid insulation as well, they can appear in liquids or gases as well. *St.Elmo's fires* on the masts of ships during thunderstorms have been a well known phenomenon for hundreds of years, and are in fact coronal discharges through air as "insulating material". In AC-operation, the presence of PDs usually leads to drastic degradation of the dielectric due to the continuous discharges along with the AC-cycles.

In normal operation, PDs usually occur within electrical trees (as already explained in the previous section, the propagation of electrical trees is basically a series of PDs), voids, cuts, cracks, at poorly fabricated interfaces of different layers or spots of inhomogenity like fillers and contaminants in the dielectric. [30, S.251ff] Because of the already mentioned possible thermomechanical stresses due to different expansion coefficients of the different cable layers, extruded cables are especially vulnerable to voids or cavities which can lead to PDs. In paper insulated cables the cavities are usually not constant and filled with the oil- or mass-liquid, what makes PDs less of a problem for these kinds of cables. [7, S.81]

The following requirements need to be satisfied for the occurrence of partial discharges within a dielectric:

- A free electron needs to be available within the gas filled void to start an electron avalanche, and

- the field within the void needs to be higher than the inceptional field, therefore there exists a threshold value of the field.

So for cables, these requirements are fullfilled when the electric field strength is locally elevated, as e.g. caused by inhomogenities or contaminants which can lead to electrical trees. Or the dielectric strength is locally reduced, as e.g. caused by cavities, cracks or the voids of the trees. Due to this various possibilites, the mentioned threshold value for PDs can vary over wide ranges and depends on the void size and gas pressure within the void. For the largest voids filled with air at atmospheric pressure it is around approximately $3 \cdot 10^6 V/m$. [11, S.19][44, S.60ff] [31, S.57]

As already mentioned, in AC-operation PDs occur periodically with the sinusoidal voltage curve. The discharged cavities after a PD can be basically modelled as capacitances, because the "recharging" of the void is mainly capacitive. This leads to a *cavity capacitance* C_1, which can be considered discharged with every PD. The recharging afterwards happens via an assumed series partial capacitance C_2, where $C_1 >> C_2$ and a parallel capacitance C_3. This very simple model is shown in figure 2.22. There are, nevertheless, more complicated models, which take the complex physics of the electron avalanches within the cavities into better account. [54, S.382f]
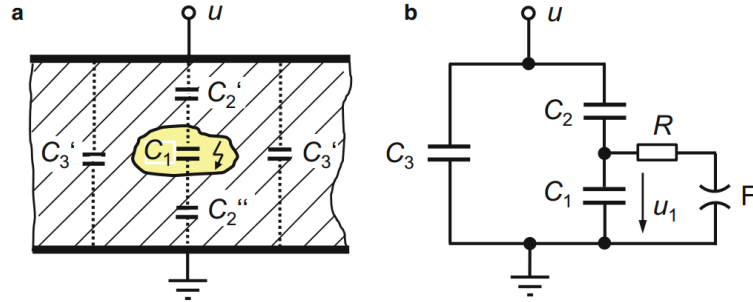

Figure 2.22: a) Scheme of a PD within a gas filled cavity in an insulation b) (simplified) equivalent circuit diagram of the PD with C_1, C_2 and C_3 as shown. [54]

Within the cavity, without a PD-ignition the *cavity voltage* U_{cav} follows the external voltage. The measured voltage U_t depends on the applied AC-test voltage $U_t(t)$ then follows the simple divison ratio rules of the capacitances:

$$U(t) = \frac{C_2}{C_1 + C_2} U_t(t) \tag{2.5}$$

If U_1 - as already explained - is higher than the ignition voltage of the breakdown U_{bd}, a discharge occurs. After the electron avalanche, the cavity voltage collapses down to a so-called *extinction voltage* U_{ex}. The capacitive recharging via C_2 then leads to a *downward displacement of voltage curve* by the voltage-difference $\Delta U = U_{bd} - U_{ex}$. Depending on the cavity voltage a sequence of discharges can occur within the sinusoidal course of the voltage to the maximum of the voltage-sinus. Subsequently, PDs typically even occur before the zero crossing of the voltage, which is illustrated in figure 2.23: [30, S.251f] [54, S.382f]
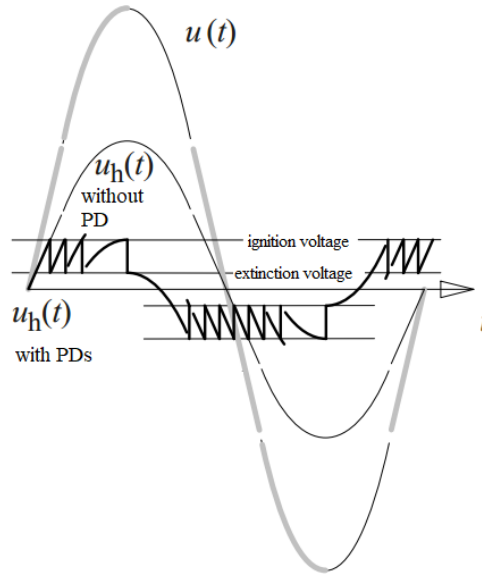

Figure 2.23: Difference in field distribution in comparison between a conducting bundle with and without an inner conducting sheath. [30, S.251]

The rise-times of these pulsed PD-sequences are in the order of a few nanoseconds, so that a pulse-frequency of 1GHz can be achieved. The measurement of these pulses, especially amounts with higher frequencies, which are less attenuated by the cables, are used for the detection and measurement of PDs in cables. PD-measurements are an integral part of diagnostics in electrical grids. Techniques for locating the discharge sites or reducing external noise have been developed and are available. [11, S.19] Techniques and practical PD-measurements are shown and discussed in chapter 3.

The formation and development of the electrical discharges is just one thing to consider regarding the condition of a cable. The second is the degradation caused

by the discharges. Regarding these damaging effects, a lot of already shown processes occur within the insulation. These involve various chemical reactions like oxidation on the void surface or diffusion of ozone and bombardment of the void surface with ions from the discharge in the gaseous cavity. The surface of the voids are also exposed to high energy photons from the gas discharge which can lead to effects shown in section 2.2.4. Finally, the high gas temperatures lead to locally elevated temperatures, heating and thermal degradation. Mechanical effects are stated unlikely, because only the mechanical shock of the discharge has too little energy.[31, S.303ff]

2.3.6 The Inverse Power Law for Electrical Ageing

In the last sections that the processes of electrical ageing, which are rather complex, multidimensional and depending on a lot of parameters and variables, have been explained. The development of models for lifetime estimation as a function of electrical stress is therefore rather complex as well.

An often used ([44, S.16f] [50, S.561] [28, S.16f] standard model is the so called inverse power law:

$$t = C \cdot U^{-n} \tag{2.6}$$

where: t is the lifetime (time to failure or time to end-point);
C is a proportionalty factor;
U is the voltage;
n is the voltage life exponent.

This model is usually plotted in a double-logarithmic scale, which then leads to a linear relation between life and voltage. As easy and clear as the model may look like, the estimation of the parameters for the individual situation represents the challenge. Usually these are developed experimentally in accelerated ageing tests as explained in [50]. Methods for the experimental estimation of these parameters are still a field of research, as shown e.g. in [67], where the parameters are gathered from accelerated step-stress tests on XLPE samples. In figure 2.24 a practical example for different inverse power law-functions is shown. Here, the experimental data was measured from different insulating materials after artificial ageing at two temperatures: 20°C room temperature (RT) and -196°C cooled with liquid nitrogen (LN_2). The difference is clearly visible, the LN_2 cooled material shows significantly better ageing behaviour, because at these low temperatures

thermal ageing effects do not occur. [39]

Paper-LN$_2$ (94)
PPLP-LN$_2$ (88)

Polymer at LN$_2$ (40)

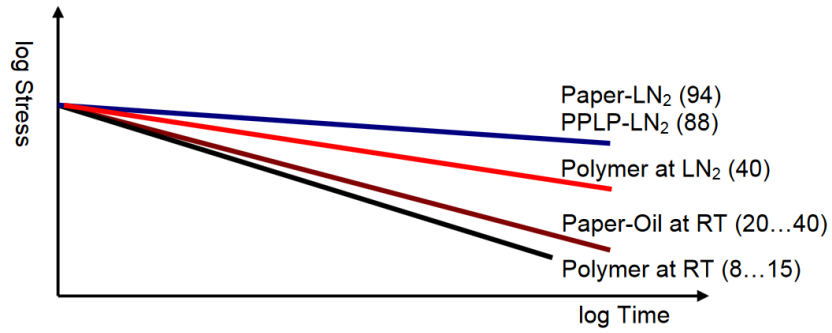Paper-Oil at RT (20...40)

Polymer at RT (8...15)

Figure 2.24: Calculated lifetime curves with experimental data for different insulating materials at room temperature (RT) and cooled with liquid nitrogen LN$_2$. [39]

3 Condition Monitoring and Diagnostics: Current Methods

In the first two chapters of this thesis the main aspects of the complex design of cables in electrical grids, the large number of stresses they are exposed to in operation, and the degradation and ageing effects that occur were explained.

In this third chapter, a few practical challenges of dealing with these ageing effects within the grid shall be shown. At first the problems, difficulties and approaches for practical lifetime estimation, assessment of the condition and failure prognosis of EIS in an electrical grid shall be shortly demonstrated. The basic problem here is in gathering the information and data from the underground cables, which are on one hand not easily accessible because they are buried underground, and on the other hand they are in operation.

The second part of this chapter is about the practical use of the two currently most used diagnostic methods: The measurement of the *dissipation factor tanδ* and the measurement of partial discharges in cables. The physics and measurement techniques behind these two are explained and advantages and disadvantages discussed using practical measurement data from diagnostic measurements done in the grid of Kärnten Netz.

3.1 Condition Assessment in Cable Grids

As already mentioned, building on the results presented in chapters 1 and 2, a few key considerations and conclusions regarding the practical problems and challenges in lifetime estimation and condition assessment of cables shall be presented first. Especially the practical relevant questions of knowledge about the status of cables within a grid after a certain time in operation or the probability of failures are not answered easily. These topics are directly derivated of the results from the first chapters and will contribute to a better understanding of the practical situation within an electric grid.

Because the focus of this thesis lies on ageing effects on cables and the physics behind them, and not on asset management strategies, the topics of this section are held rather short and superficial on purpose. Nevertheless, for these very practical issues a lot of excellent technical literature and scientific research is available which can be recommended. Examples for standard literature are [7], [15], [34], or [54], for recent research results [23], [28] or [30] and many more.

3.1.1 Multistress Ageing Models

In the last sections the main ageing mechanisms and processes within cables and especially polymeric cable insulation were presented. it was shown, that the numerous ageing mechanisms due to the different stress categories - mechanical, thermal, environmental and electrical - are rather complicated, multidimensional and interact with each other. Even though many interactions and effects are extensively researched and explained in excellent literature like [31], many processes are still not fully understood.

In practical use, none of the previously explained ageing stresses and mechanisms act seperately, but they always act in combination. Degradation of the insulation material from multiple factors combined is called *multifactor ageing* or *multistress ageing*. Needless to say, that these models are usually very complicated and extremely varying, depending on the individual situation of the insulation system. It was already shown, that single stress ageing processes can be quite complex and ambivalent, different boundary conditions have even more influence on multistress models:

- The exact properties and kind of insulation material;

- processing and construction of the cable;

- duration and frequency of each individual stress;

- effects on interfaces and boundaries;

- interdependencies regarding changes in material structure and properties:

- etc.[28, S.21]

A rather simple model for the ageing rate t' was published by Eyring in 1941, based on the already explained rate theory and similiar to the thermal Eyring model shown in equation 2.3:

$$t' = \frac{kT}{h} t'_0 exp - [\frac{\Delta G}{kT}] exp[\frac{cE}{kT}] \tag{3.1}$$

Here the electrical stress E and temperature T are combined in one model. Different other multistress models are portrayed e.g. in [50], [28] or [40].

3.1.2 Different Breakdown Mechanisms

The final stage of ageing is always a breakdown of the insulation. Models for the final electrical breakdown mechanisms in insulation material for practical use can be divided into three major categories:

1. Low level ageing or degradation models, in which the characteristics of the insulating material are continuously affected by the electric field or other stresses as shown in the last sections.

2. Deterministic models of breakdown, caused by a causal event or the specific exceeding of a critical electric field.

3. Stochastic models, in which statistical probabilities for a breakdown are calculated e.g. for a cable grid.

The final breakdown stage in the insulation is always a multistress-process as already discussed regarding electrical trees and partial discharges. The bridging of insulation with a channel always involves melting, carbonisation or vapourisation of the dielectric. Also the line between the (short time) deterministic breakdown models of possibly already aged insulation, and the (long time) degradation and ageing models is not completely clearly distinct. So partial discharges, as shown, are in fact small, localized breakdowns which lead to degradation of the insulating materials. These interconnections are shown in figure 3.1:
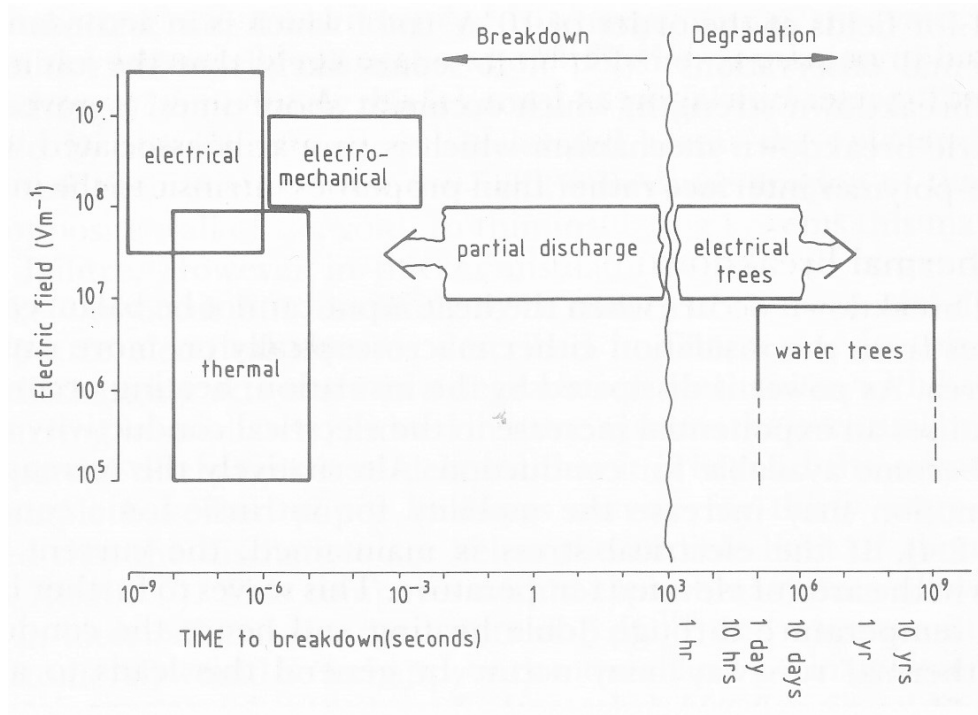
Figure 3.1: Chart of the various breakdown mechanisms plotted against electrical field and time to breakdown. The unclear boundary between deterministic breakdown mechanism and electrical ageing like treeing is shown.[31, S.63]

These complexities are well summarized in the following quote:

"Breakdown theory faces a dilemma. The relatively general models can be stated exactly with specific parameters and solutions computed in a straightforward manner. However, the results lend themselves only to order of magnitude estimates on real substances, and do not reflect the complexity of experimental data. Alternatively, one could propose a different model for every different dielectric (and possibly for different thicknesses and methods of preparation of the same dielectric) leading to complex computing that offers little insight into the physical processes involved."

(J.J. O'Dwyer, IEEE Transactions on Electrical Insulation, 1984 [31, S.199]

3.1.3 Practical Challenges and Approaches

For practical application within an energy grid, the key-results and key-problems from the previous chapter regarding cable ageing and the prevention of breakdowns can be summarized:

- Cable ageing is influenced by many different and interconnecting factors: Process quality, purity of materials regarding CDPVs and careful manufacture play a big role for the quality of the cables and therefore the risk of early failures. In operation thermal, mechanical, environmental and electrical stresses are the reason and cause for different processes, which lead to ageing and finally failure of the cable.

- For every stress, several mathematical ageing models exist. Nevertheless, these models require a lot of current information about characteristic parameters, boundary conditions and the status of the cables to work. It was shown that, from mechanical stress during the installation, humidity and quality of the soil, load patterns to operating temperatures a lot of parameters have to be considered.

- Single stress models can already be quite complicated in their use regarding the necessary parameters for the current status of a cable. Examples for multi-stress models were very shortly introduced, the issue of realistic parameters is even a lot more complicated for those.

- As mentioned, many ageing processes like water treeing take a long time developing and the progress is very slow. For laboratory tests, accelerated ageing experiments are therefore required. The extrapolation of those results towards real-life ageing can also cause complications.

So, summarizing those facts, for the exact modelling of cable ageing, a lot of influences have to be considered and a lot of parameters have to be known, which, in practical operation, most times are simply not available.

As an example for the practical handling of these uncertainties, in [6] a basic flowchart for the many influences on the condition of an EIS is shown, along with an exemplary systematic process to deal with the condition and the residual lifetime:
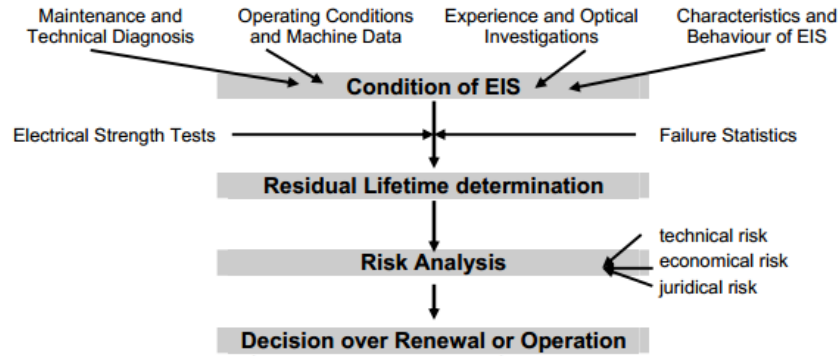
Figure 2: Assessment of condition and residual lifetime

Figure 3.2: Exemplary flowchart on the assessment of condition and residual lifetime of an EIS. [6].

So, the decision of renewal or further operation depends in practice on several other influences like technical, economical or juridical aspects and has to be done after a risk analysis, based on the data available.

According to [28, S.22ff] the three basic approaches for practical condition assessment of the condition of cables are:

- **Laboratory tests** with artificial ageing experiments and comparison to cables aged in real service.

- **Stochastic models** based on statistical probabilities of failure.

- **Forensic tests** of cables and insulation aged in service.

Different examples and results from **laboratory tests** and experiments have already been discussed in the previous sections. The idea behind them is always, to gather insights, and to understand the degradation and ageing effects and transfer those to the situation in real life grids. As already shown, especially slow ageing effects like water treeing can take years or tens of years to develop within the insulation. Many laboratory tests therefore depend heavily on accelerated ageing processes, which complicates the practical transfer to real life operation even more.

Statistical analyses are carried out using failure and operational data from grids to find predictions for the failure- and ageing-behaviour of cables. Statistical analyses are strongly dependent on a large volume of data.

Forensic tests are done on equivalent or similiar cables, due to anomalies or inexplicable failures. These examinations and tests rely on a sum of equal eqipment

parts exposed to different operation and stresses and the comparison of them. [28, S.22ff]

All together, this shows that regarding residual lifetime estimation of cables in practical use, a huge amount of incertainties has to be taken into consideration. A widely used empirical model for failure rates which is also applied to underground cables is the so-called *bathtub curve* of a failure rate depending on age. In this model, the failure rate at the beginning is high (infant mortality), due to quality problems or wrong installation. Afterwards a phase of a constant small failure rate, called the useful life. As the cable reaches the end of its estimated lifetime, the failure rate increases again in the wear-out-phase: [22]
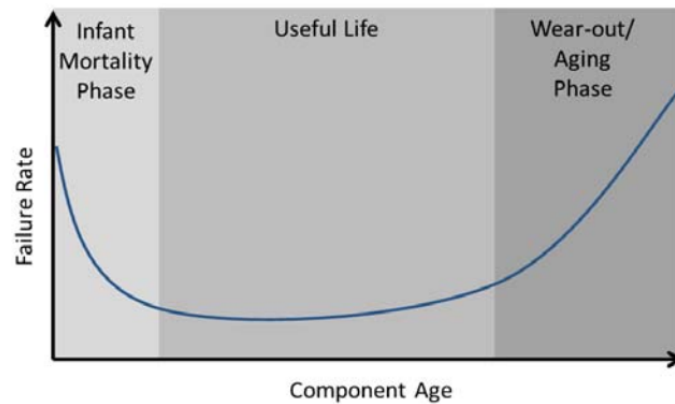

Figure 3.3: Bathtub curve of the typical failure rate for cables [22].

The large impact on failure rates due to imprecise and faulty production causing impurities and contaminations has already been discussed. This leads to a high standard regarding quality management and commissioning tests of cables prior to installation. The first peak of infant mortality can be largely avoided by these measures and proper installation. A very good current summary and overview of state of the art quality assurance and -management for MV-cables is given in [23].

The practical handling and estimation of the wear-out phase is more complicated and heavily relying on the data available from the grid. Besides from load patterns, practically no real-time data is available from the grid, so measurements need to be taken, which is called *diagnostic tests*. These are the only possibility of gathering actual data from the grid and are further explained in the next section.

3.2 Analysis of current Diagnostic Methods

In the following sections, after a short definition and explanation of the term, measurements of partial discharges and the dissipation factor $tan\delta$ as the two most widely used diagnostic techniques are shown.

The different diagnostic methods, their advantages, disadvantages, measurable properties are a wide field and the topic of many books, so is in this thesis limited to those two very basic but comprehensively used techniques. For further information regarding diagnostic techniques e.g. [30], [7] or [54] can be recommended.

3.2.1 Diagnostics in General

According to IEC 60505, diagnostic tests are defined as follows:

> "Diagnostic test - periodic or continuous application of a specified level of a diagnostic factor (diagnostic property, note from the author) to a test object to determine, whether or when the end-point criterion has been reached.". [44, S.12]

The goal of diagnostics in cable grids is therefore, to use different measurement techniques for a condition assessment of a cable, based on the measurement results. A different definition is shown in [11]: *"...to evaluate and locate degradation phenomena that will cause cable or accessory failure."* Destructive and non-destructive tests on cables, carried out on-site or in the laboratory are diagnostic tests.[11, S.15]

As the definition out of IEC 60505 shows, the crucial aspect is the diagnostic factor as the property of the cable, which is measured. The results of diagnostic tests are a basis for a decision-making process about residual lifetime, renewal or repair of a cable section as exemplary shown in figure 3.2. [28, S.26ff] [30, S.426ff]

3.2.2 Partial Discharge Analysis

The basic processes of partial discharges and the physics behind them have already been explained in section 2.3.5. Measurements of possible PDs in cables are one of the most widely used diagnostic techniques due to the fact, that the occurrence of PDs is a strong indicator for degradation within a cable. Therefore, these measurements provide vital information for cable assessment, and are considered a standard method of diagnostic for extruded insulation. [1] [7] [15] [30] [54]

3.2.2.1 Explanation of the technique

For PD measurements, not the PDs themself can be measured, but the resulting electromagnetical pulses caused by them, as already shown in figure 2.23. As shown in the simplified model in figure 2.22, the capacitance C_1 of the cavity is assumed to be much larger than the series-capacitance C_2 of the healthy part of the insulation on the PD spot. The parallel capacitance C_3 represents the healthy insulation besides the PD spot.

The scheme for an experimental setup for the measurement of PDs is shown in figure 3.4 and shall be explained in detail as follows:
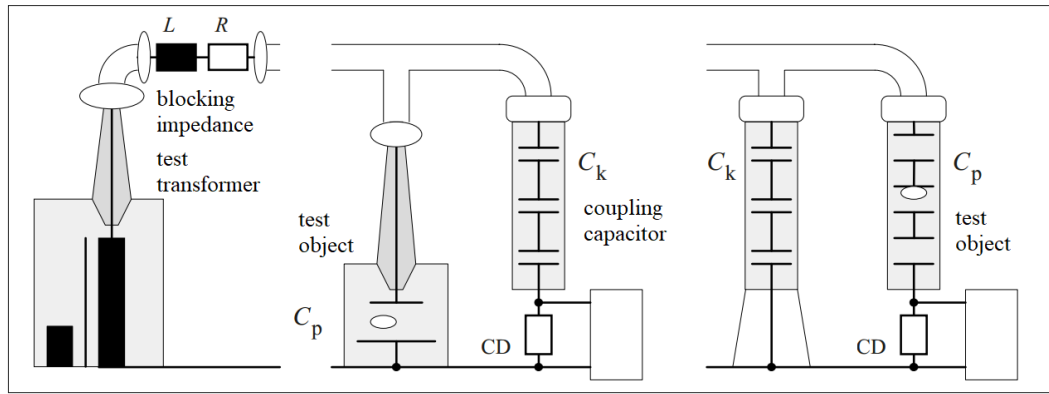

Figure 3.4: Two possible experimental setups for PD measurement (middle and right) and the voltage supply with test transformer and blocking impedance (left) [30, S.434] .

In this visualization, the test object is summarized with a total capacitance C_T. Parallel to it, a *coupling capacitor* with capacitance C_C is connected to it, and both are connected to the test-transformer via a *blocking impedance*. The blocking impedance in this circuit acts as a low-pass filter (series connection of R and L to suppress conducted interferences.

When a PD happens within the test object, as already mentioned the voltage U_1 on the cavity with C_1 drops to the level of the extinction voltage U_{ex}. Here, the charge can be calculated from the capacitance $\Delta U = \Delta q/C_1$, and is equal to the breakdown voltage $\Delta U = U_{bd}$. This small PD-charge nevertheless cannot be measured on the test object. Because of the different capacitances, the measurable value is the charge, that flows out from the coupling capacitor an recharges the whole test object, which is called *apparent charge* q_a. With the assumption, that

the resulting voltage dip can be completely compensated by the voltage source, q_a can be calculated as follows:

$$q_a = \Delta q \frac{C_2}{C_1} \tag{3.2}$$

Because C_1 is way bigger than C_2, q_a is much smaller than the real PD-charge Δq. But since neither the capacitances nor Δq per se are known, the apparent charge is the only measurable value and serves as parameter for the specification of partial discharge intensity. q_s is usually stated in the unit of Picocoulomb (pC).[30, S.434f][15, S.111f]

The PD-measurements can be done at normal 50Hz grid frequency, or in the same way as $tan\delta$-measurements with very low frequency (VLF) of 0,1Hz. At normal operational voltage U_0 a cable should be free of PDs, in cables of grids with earth fault compensation up to a voltage of 1,7 U_0. In order not to cause further ageing for the cable through the measurements, the maximum voltage applied should not exceed these $1,7U_0$. [7, S.327]

For further technical explanations of PD-measurements like exact circuit diagrams, different test-setups, calibration recommendable literature is e.g.[45] [1, S.52ff] or [54, S.381ff]

3.2.2.2 Localization of PDs

For PD-measurements in cables, a localization of the occurring PDs is possible. Necessary for a localization is on the one hand the cable length, which is known from installation, and on the other hand the pulse-velocity v within the cable. For MV-cables, v is usually around $80m/\mu s$ and is normally measured at the beginning of each diagnostic test with an echometric test. In this measurement, using a surge voltage generator, short voltage pulses are sent into the cable which are reflected at the open end of the cable. From the time-echogramm of the pulses the pulse-velocity can be calculated. The method is very similar to the time domain reflectometry-method, which is explained in detail in section 4.1 in the next chapter, therefore it is not further elaborated here.

A scheme of the principle of such a PD-localization is shown in figure 3.5:
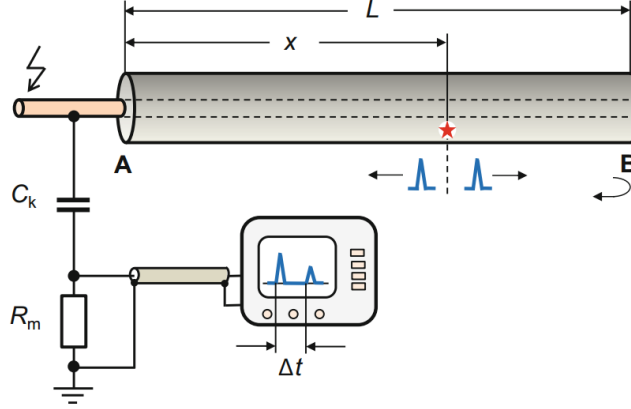
Figure 3.5: Scheme of a PD-measurement and localization principle on a cable. [54, S.419] .

When a PD occurs within the cable after a length x, the pulse propagates into both directions of the cable. The pulse toward the open cable end B is fully reflected as discussed in section 1.2.7, and can be detected as a weaker pulse (due to attenuation) with a time delay Δt to the pulse propagating towards the end A. The time delay can be calculated via:

$$\Delta t = \frac{2(L - x)}{v} \tag{3.3}$$

and therefore the length x to the PD can be calculated. [54, S.419f]

3.2.2.3 Discussion of Experimental Results

At Kärnten Netz, PD-measurements are done as regular part of a diagnostic test on a cable segment. The measurements are done with a Baur PHG 80 TD/PD VLF testing and diagnostics system. This is a multifunctional diagnostics-system, built into a cable test van with a possible VLF sine voltage up to 28/57kV. Further information about the measurement system is available in [19].

Example 1: A practical PD-measurement taken by Kärnten Netz in fall 2018 shall be considered in detail. In this case a 1541m long cable section of type AY2YHC2Y with PE-insulation from 1983 was tested. The cable consisted of three phases with 150mm^2 each. The results of the PD-measurement are shown in figure 3.2.3.2:
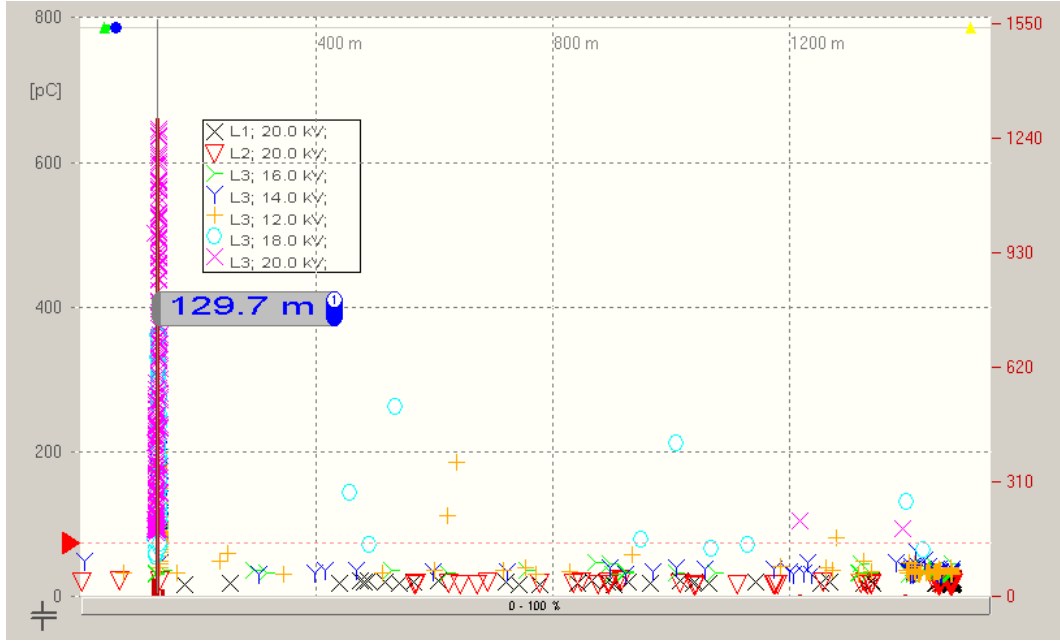
Figure 3.6: Screenshot from the Baur-Measurement Software showing a PD-measurement on a 20kV cable with severe PDs from 2018. (picture: Kärnten Netz GmbH)

Junctions are a possible source of PDs if they are not installed correctly, so the location of junctions is shown in the graphic in the top-line. A junction is located at 41m (green triangle), at 60m (blue circle) and at 1505m (yellow triangle). The scale shows measured PD q_a in [pC] depending on the cable length, the different symbols show results from different measurements taken. It is clearly visible that on the phases $L1$ and $L2$ no PDs at $U_N = 20kV$ were measured, on $L3$ severe PDs were measured at a distance of 129,7m. Because of this detection, different measurements at voltages of 12, 14, 16, 18 and 29kV were taken, which can be seen by the different symbols. It can be seen, that the PDs occur at already 12kV and have a q_a up to 700pC at 20kV. Therefore an immediate repair of this cable segment is recommended.

Usually, PD-measurements also measure the frequency of pulses, the time of their appearance compared to the sinusoidal test-voltage and external disturbances. Especially the appearance of the PDs depending on the voltage can give interesting insights and is usually stated with the phase angle ϕ of the sinusoidal voltage. The occurrence during the positive or negative half of the curve and their density form some kind of "fingerprint" for the cable, out of which with experience further information about the origin of the PD can be gathered.[15, S.116f] Two

examples for such time-charge diagrams are shown in figures 3.7 and 3.8.

Example 2: Figure 3.7 was taken in a laboratory test on phase L1 of a new 498m long NA2XS(F)2Y cable with 150mm^2 cross section and shows a few PDs of more than 900pC at 150°-165°, but besides from that the cable is in good condition:
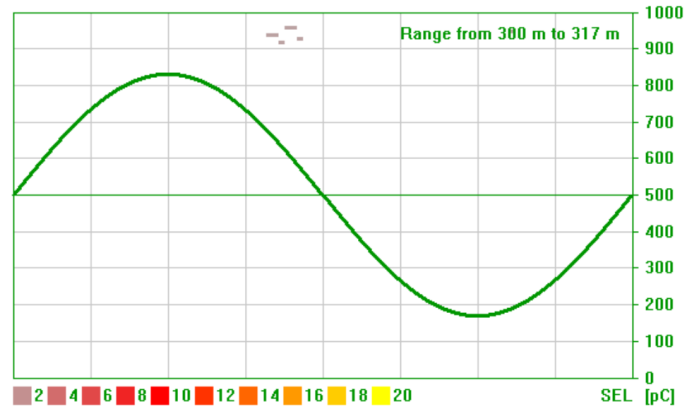

Figure 3.7: Time-charge diagram of a laboratory PD-measurement for a healthy cable. (picture: Kärnten Netz GmbH).

Example 3: As a comparison, figure 3.8 shows a PD-measurement taken on phase L2 with a 555m long A2YHC2Y cable from 1984 with 95mm^2 cross section. It shows relatively low (around 90-110pC) partial discharges at practically every phase angle of the sinus wave:
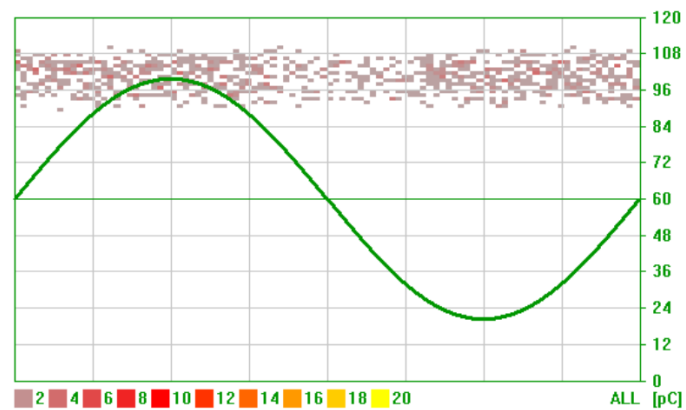

Figure 3.8: Time-charge diagram of a laboratory PD-measurement for a degraded cable. (picture: Kärnten Netz GmbH).

The PDs were localized at a length of around 370m. Because of the low q_a of the PDs, it was assumed, that they were caused by a junction. The installation data nevertheless was incomplete, so it was not possible to clarify, if there was really a junction at this location.

3.2.2.4 Advantages and Disadvantages

+ Easily practicable standard-technique with low chance of failure or false positive results if data from junctions are complete.

+ The occurrence of PDs are a clear sign of ageing and degradation within a cable.

+ PDs can be localized to allow a targeted repair.

+ Because of the wide application of the technique, lots of empirical values and experience from the measurement personell is available, from which further information can be gathered.

- For the measurement, only cable segments of hundred meters to few kilometers can be measured. The cable needs to be taken out of service and the measurements need to be taken on-site. This leads to a high requirement of time and effort and limits the possible measurements to be taken within the grid.

- The threshold for the "tolerable number" of PDs cannot be universally stated, depends on the type of the cable and many other factors. Values for "critical number" of PDs are only empirical values and based on the experience of the measuring personell.

- The measured PD activity of a cable does not determine the condition of the insulation as a whole itself, but only shows local defects.

3.2.3 Measurement of Dissipation Factor tan δ

The physics and properties of the dissipation factor $tan\delta$ have already been the topic of section 1.2.4, and its significance for the insulating behaviour of a dielectric was shown. Therefore, besides PD-measurements, field-measurements of $tan\delta$ are the second very widely used diagnostic technique.

3.2.3.1 Explanation of the technique

Historically, $tan\delta$-measurements are closely connected to the name of Harald Schering (1880-1959), a german physicist and electrical engineer. In 1919 Schering invented an electrical AC bridge-circuit for the measurement of the dissipation factor, which was later named *Schering Bridge* after him.
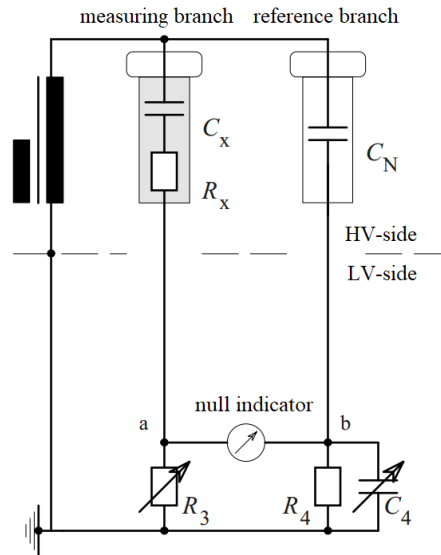

Figure 3.9: Circuit-scheme of the Schering Bridge [30, S.432] .

In the Schering Bridge, C_X is the unknown capacitance of the test object, and C_N an ideal, low loss capacitor. The capacitance C_4 and resistance R_3 are adjustable. The test object C_X is realistically stressed with high voltage, while the other parts of the bridge are at low voltage. The *null indicator* (NI) used to be a galvanometer, nowadays usually an oscilloscope with a Lissajous-figure as display is used.

When an AC-voltage $U(t)$ is applied, AC-currents flow through C_X and C_N on the "high voltage side" of the bridge. By adjusting R_3 and C_4, the points a and b are brought to the same potential, which is called *balance condition*:

$$\frac{Z_X}{Z_x} = \frac{ZN}{Z4} \tag{3.4}$$

When the balance condition is fullfilled, no current flows through the null indicator, and the Lissajous-figure on the oscilloscope shows a horizontal line. The dissipation factor then follows after a few transformations of equation 3.4. Equation 3.4 with the complex impedances written in full form looks as follows:

$$\left(R_x + \frac{1}{j\omega C_X}\right)\frac{1}{R_3} = \frac{1}{j\omega C_N}\left(\frac{1}{R_4} + j\omega C_4\right) \tag{3.5}$$

After separation into real and imaginary parts, R_X and C_X can be expressed:

$$R_X = R_3\frac{C_4}{C_N} \text{ and } C_X = C_N\frac{R_4}{R_3} \tag{3.6}$$

And the dissipation factor $tan\delta$ a serial circuit can be calculated via:

$$tan\delta = \omega C_X R_X = \omega C_4 R_4 \tag{3.7}$$

With a sophisticated arrangement of the measurement setup of the Schering bridge, the dissipation factor can therefore be read directly without calculation. And, as shown, all adjustable elements of the setup are at low voltage level. [54, S.353f] [15, S.57f]

There are different extensions and improvements of the basic Schering bridge for different measurement applications and they are described in detail e.g. in [7], [15] or [30].

Dissipation factor measurements are an important tool for condition assessment in power grids. The measurements are non-destructive and were originally used especially for paper insulated cables. When the paper insulation is poorly impregnated, the existing large cavities lead to a significantly elevated $tan\delta$. For small cavities, like in extruded cables, partial discharge measurements fit better, but elevations of $tan\delta$ in extruded cables caused e.g. by water trees can be easily detected. That is why the method is also still up to date for these cables.

Measurements of the dissipation factor with 50Hz are practically difficult to perform. This is on the one hand due to the frequency-dependency of the dissipation factor, which leads to very low $tan\delta$ values at 50Hz, as shown in table

1.1. At 0,1Hz the values are 10 times higher. On the other hand, difficulties arise from the high capacitive reactive power, which is required for a measurement at 50Hz. Therefore, $tan\delta$ measurements are usually done with 0,1Hz VLF, as already mentioned in the previous section about PD-measurements. Because the reactive power is directly proportional to the frequency, the required reactive power for a measurement with 0,1Hz is 500 times lower than at 50Hz. This also allows the use of smaller, transportable measurement-setups, usually installed in a measurement-van. [15, S.60]

Similar as for PD-measurements, no definite physical or technical threshold values for $tan\delta$ measurements exist. For practical purposes, only empirical values or deviations between the phases of a three-phase can be considered. There are different values in standards like [14] or standard literature like [7]. In practical use, $tan\delta$ is usually measured for different voltages up to U_N or 2-3U_N, to avoid damages especially on older cables, the test voltage is often limited to $U_N = \sqrt{3}U_0$. For the measurements at Kärnten Netz four states were defined: cable can be returned to service, cable with operating risk, cable with high operating risk, cable not ready to switch on. The allowed values for $tan\delta$ and $\Delta tan\delta$ between the measurements are shown in table 3.1:

state	$tan\delta$	KNG-Grading
Cable can be returned to service	<1,2	1
Cable with operating risk	1,2-2,2	2
Cable with high operating risk	2,2-6,0	3
Cable not ready to switch on	>6,0	4

Table 3.1: Limit values for $tan\delta$ measurements at 0,1Hz AC, 30min. (Kärnten Netz GmbH.)

Further information and limit values are given in the standards [14] or [46]

3.2.3.2 Discussion of Experimental Results

Three examples for real dissipation-factor tests shall be shown, which are all done on the same cables as the PD-measurements shown in section 3.2.2. At Kärnten Netz, dissipation-factor measurements are also done using the Baur PHG 80 TD/PD system with a 0,1Hz VLF sine signal.

For the tests, 8 measurements on each phase are taken for 10 seconds (1 full oscillation of the 0,1Hz sine wave) with test voltages of 5,8, 11,7, 17,2 and 19,8 kV. This is the standard measurement-procedure implemented at Kärnten Netz

and is based on experience and manufacturer specifications from Baur. Here, the dissipation factor is plotted against the voltage (in kV).

Example 1: For the measurement with the high amount of PDs shown in figure , the raw data was taken and manually evaluated, because error-margins are not shown in the Baur-Software and we wanted to calculate those manually. The results are shown in figures 3.10 and 3.11. For the manual calculations the mean value of each of the 8 measurements was taken and the error margins represent the standard deviation of the mean. The error margins are only slightly visible for L3, for L1 and L2 they are practically not visible. So a sufficient accuracy can be assumed.
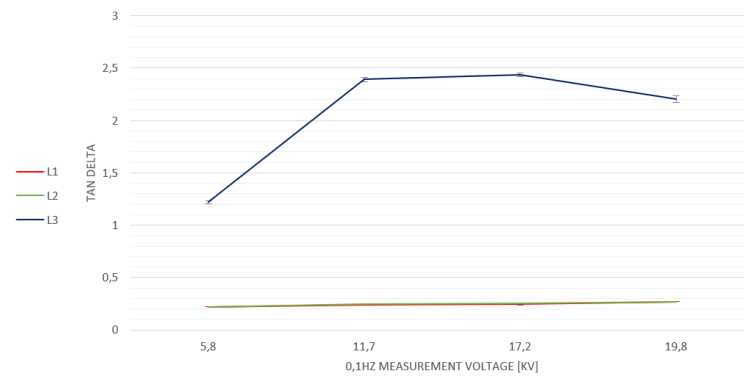

Figure 3.10: Manual calculation of the dissipation-factor measurement from figure 3.11.
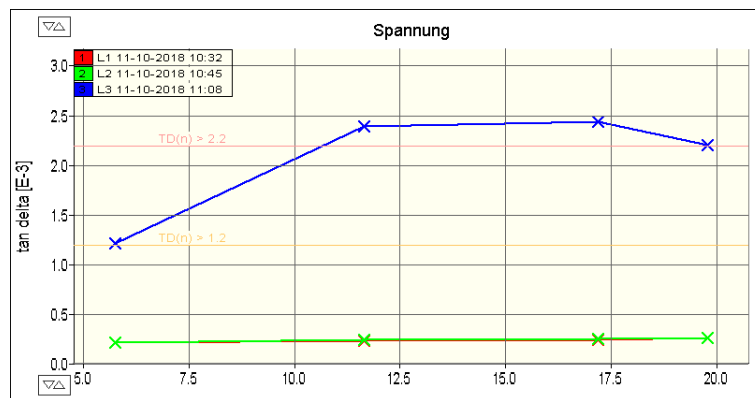

Figure 3.11: Results taken from the Baur-Software of the measurement already shown in figure 3.10

Figures 3.10 and 3.11 clearly show, that the phase L3 in this case is the probable source of the PDs. Phase L1 and L2 show constant dissipation factors of $\approx 0,25$.

Measurement experience shows, that the characteristic form of the measurements in L3 with an even declining dissipation factor at 19,8kV points to moisture within the cable, probably because of a damage of the outer jacket.

Example 2: Here it is clearly visible, that both phases of the cable are healthy with practically the same dissipation-factor, which is a little more than $0{,}3 \cdot 10^{-3}$ at U_N.
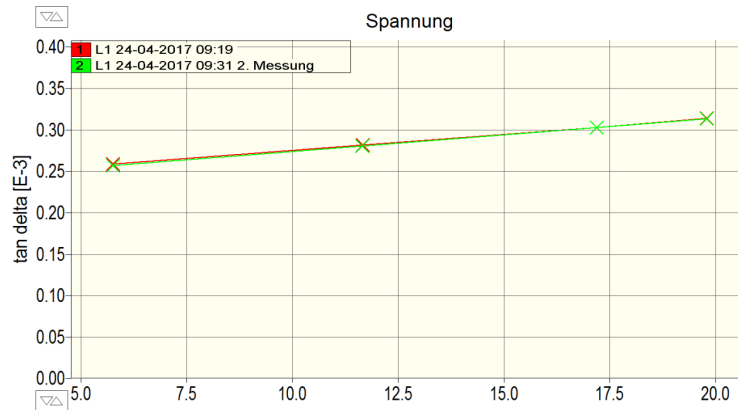

Figure 3.12: $tan\delta$-voltage diagram of a laboratory dissipation factor measurement of a healthy cable.

Example 3: For the measurement from figure 3.13. Here it is clearly visible, that the values for phase $L2$ are elevated. The dissipation factor for both phase L1 and L3 is around $0{,}5 \cdot 10^{-3}$ at U_N, for L2 it is nearly $3 \cdot 10^{-3}$ and therefore clearly unfit for service.

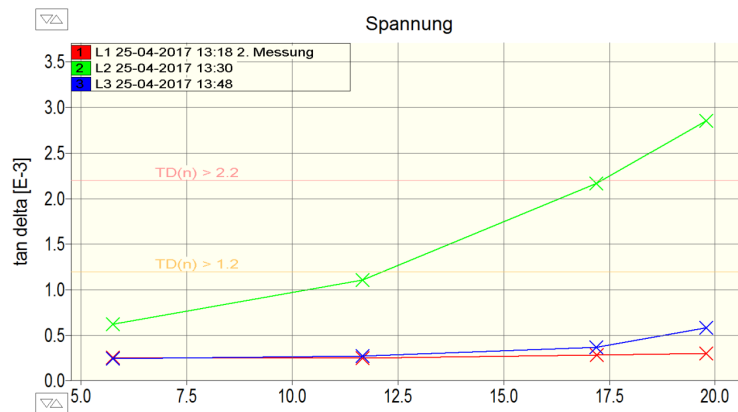**Figure 3.13:** *tanδ*-voltage diagram of a laboratory dissipation factor measurement of the degraded cable from figure 3.8.

3.2.3.3 Advantages and Disadvantages

+ The measurement of the dissipation factor is an easy practicable, low cost standard-technique with nearly 100 years of experience.

+ A lot of experience worldwide with the technique for different cable types, and a lot of empirical values.

+ A constant low dissipation factor below the empirical allowed values is a clear indicator for a healthy cable.

- Same as for PD-measurements, the cable needs to be taken out of service and measurements can only be taken on-site. For cables, an real-time or online measurement of the dissipation factor is not possible. Therefore only a very limited number of cable segments can be measured within a certain time.

- Measurements of the dissipation factor of a cable with a certain length can only evaluate the integral cable condition. The measured dissipation factor is always an average value for the whole cable.

- There is no spatial resolution of spots of higher degradation e.g. a cable segment with a high number of water trees. A localization is not possible.

- As already mentioned in section 1.2.4, the dissipation factor is temperature dependent, so a high difference in temperature can distort the results.

- If measurements with 0,1Hz are done, the results give no conclusion about the values of the dissipation factor at 50Hz.

89

3.2.4 Practical Example of an in-situ Measurement

For the illustration of the measurement-techniques shown, an example for a practical in-situ measurement is shown. The measurement was done on November the 21st 2018 in the south of carinthia. A measurement of dissipation factor and partial discharges was done on a total cable length of 1071m. The cables were of the type AY2YHC2Y, with three 95mm^2 aluminium-conductors and PE-insulation. A first segment of 191m was installed in 1983, the rest in 1988. The measurement was a routine measurement after 30 years of being in service and no faults on this cable section were known from operation. The measurement was taken at a transformer station with the already described BAUR PHG80 TD/PD measurement equipment.

Figure 3.14
Transformer station

Figure 3.15
Cable test van

For the measurements, the cable section had to be taken out of service, the measurements were done directly connected to the cables from the transformer station:

Figure 3.16
Preparation of the measurement

Figure 3.17
Preparation of the measurement

3.2.4.1 Discussion of the Results

The dissipation factor was measured with the described process, the results of the measurement are shown in figure 3.18:
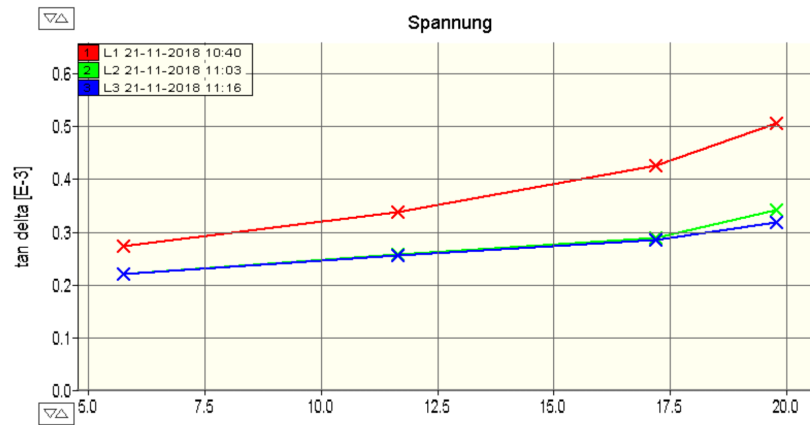

Figure 3.18: $tan\delta$-voltage diagram of the measurement from 11/21/2018.

It is clearly visible, that $tan\delta$ for the phase L1 was slightly elevated but at 19,8kV it is still not higher than 0,5. According to the scheme from table 3.1, the cable can classified into class 1 and be regarded fit for operation. The results of the PD-measurement are shown in figure 3.19:
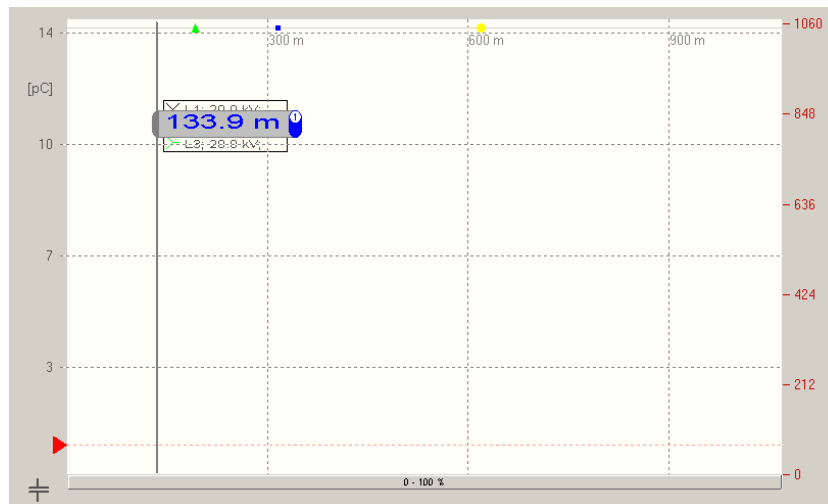

Figure 3.19: PD-diagram for the measurement from 11/21/2018.

In the upper part of the diagram, again the existing junctions are shown. Especially in comparison to figure 3.6 it is easy to see, that no PDs were measured on this cable section. The box with "133,9m" is only due to the cursor during the screenshot.

4 Outlook and possible future Developments

In the previous chapters the characteristics and challenges in the operation of MV cables, the main processes of ageing and degradation, and methods and approaches for condition assessment and diagnostic methods are shown. Measurements of partial discharges and the dissipation factor $tan\delta$ give a good insight into the ageing state and health of a cable, these measurements come with a high effort in work and time. The measurements can only be done on-site, the test-cables need to be taken out of service, and only for a single cable segment of limited length. Taking measurements on every cable of a nearly 3000km cable grid therefore takes years of time.

In the following chapter, new approaches in diagnostic technology shall be shown, which are current research topics and are dealing with exactly this problem: to gather real-time information and data regarding the condition of the cables.

Especially reflectometric methods are an interesting field of research with promising concepts and possibilities. The basic approach of these methods has already been partly discussed in chapter 3, and shall now be introduced and explained in detail. An especially interesting concept of online-monitoring via signals taken from Power Line Communication (PLC) shall be presented. This concept nevertheless is at the moment only in a stage of development and research and not marketable, but has promising qualities for future developments.

4.1 Reflectometric Diagnostics

The basics for understanding of reflectometric methods have already been explained in section 1.2.7, the diagnostic property of interest in reflectometric methods is the wave impedance Z_w.

The basic motivation in using reflectometric methods is the possibility of *spatial resolution*. The introduced $tan\delta$- and PD-measurements can only give information about local defects and an integral value of the dissipation factor. The detection

of a failure location needs to be done with different methods afterwards.

For spatial resolution of the properties within an energy cable, in a very simple model the cable is divided into n segments of equal length. This model of the transmission line composes of these n segments, each of which have the classical cable parameters per unit length capacitance C', conductance G', inductance L' and resistance R'. Due to mechanisms like the explained skin- or proximity-effect, the parameters of these segments are also frequency-dependent. The circuit diagram for the k-segment is shown in figure 4.1: [48]
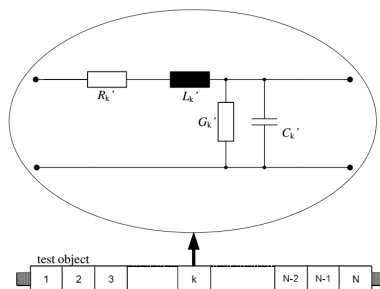

Figure 4.1: Circuit diagram for the k-segment of a cable in the transmission line model. [16, S.383]

In section 1.2.7, it was already shown, that when a wave travelling along the cable reaches a spot with a change in Z_w, a part of the wave gets reflected. The characteristical property for this effect is the already in equation 1.30 explained reflection coefficient r:

$$r = \frac{Z_{w2} - Z_{w1}}{Z_{w2} + Z_{w1}} = r \cdot e^{j\varphi} \tag{4.1}$$

The two major practical applications of these physical relations for reflectometric techniques are operated with pulsed electrical signals in the so-called *time domain reflectometry* (TDR) or with sinusoidal waves in *frequency domain reflectometry* (FDR). Both methods are used to detect cable faults via impedance discontinuities and are explained in the following sections.

4.1.1 Time Domain Reflectometry (TDR)

TDR is a very popular technique for application within cables and especially the detection of cable faults. ETxamples for and diagnostic concepts and techniques based on TDR are presented in [16], [17], [48] or [52].

The basic principle is simple: A short voltage pulse or rectangular step signal is sent into the conductor in an experimental setup shown as in figure 4.3:
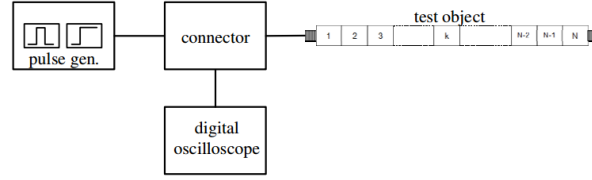

Figure 4.2: Block diagram of a TDR experimental setup. [16, S.383]

Whenever the signal encounters a change in the wave impedance Z_w, a part of it is reflected according to equation 4.1. The open end of the transmission line after the nth segment can be seen as infinite impedance $Z_{w2} \to \infty$, and therefore total reflection $r = 1$ of the signal. As already discussed in section 1.2.7, for a short circuit $r = -1$ and if the change in Z_w is between these scenarios, r is a complex number. Figures 4.2 and 4.4 show an example for a simple network topology and the responses from different reflection points B, C and D, taken from [48]:
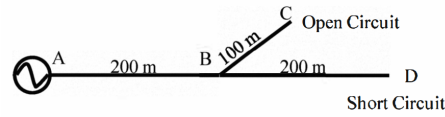

Figure 4.3: Example for a simple network topology with reflectioin points B (line branch) C (open circuit) and D (short circuit) [48, S.3]
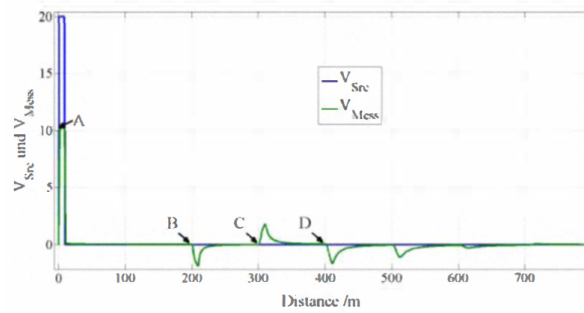

Figure 4.4: TDR results with voltage against time plotted for the reflection points. [48, S.3]

95

The distance d can easily be calculated with the frequency dependent propagation velocity v of the signal within the cable, which has to be calculated nevertheless. Notable in figure 4.4 are the smaller reflections after the main-D-reflection. These occur from the already reflected secondary waves, passing the reflection points. These secondary reflections always happen using this method, becoming of course more complex with more complicated network topologies.

These principles of TDR are quite simple and also only little equipment is necessary, the technique has disadvantages:

- Clear, large changes in impedance, as shown in figure 4.4 are clearly visible and easily detected. Especially in more complicated network topologies, smaller changes like at junctions or degradation spots are quite hard to detect.

- Especially at short cable sections, emitted and reflected waves can overlap and by that it makes the individual signals hard or impossible to detect or associate.

- Sharp square pulses are necessary for an exact time measurement between emitted and reflected signals. The emitted signals should be as narrow as possible and have an rising-pitch as high as possible, for which good equipment is necessary.

- As already mentioned, differentiating impulses of initially emitted signals and reflections can be complicated and network topology algorithms might be needed. [48, S.3]

4.1.2 Frequency Domain Reflectometry (FDR)

The approach of FDR is similiar as of TDR, but a different, sinusoidal signal is used. In FDR no sharp pulses are used, but a waveform generator which generates a sinusoidal signal with varying frequency sweep. A coupler and mixer are needed in this setup to separate the received signal from the emitted one. By that, the phase shift between emitted and reflected signal can be calculated, which is used to determine the distance to the fault spots. Afterwards, an analog-to-digital converter (ADC) as low-pass filter is used to remove the high frequency amounts. A highspeed digitizer is used to digitize the signals which are then processed on a PC via Fast-Fourier-Transform (FFT) and plotted in frequency domain. This setup is shown in figure 4.5:
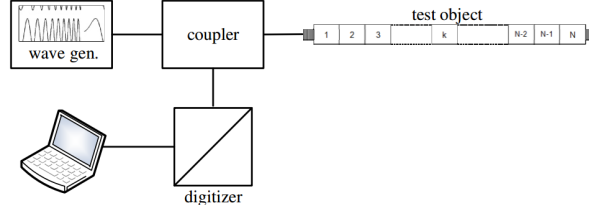
Figure 4.5: Block diagram of a FDR experimental setup. [16, S.384]

Due to this process, the resolution of FDR measurements is significantly better than those of TDR. When the sinusoidal wave reaches a change of Z_w, it gets partly reflected according to equation 4.1. Because of the round trip, the reflected wave has a phase shift of $e^{2j\beta z}$ where β is a phase constant, depending on the cable properties. When this delay is fixed, the phase shift between emitted and received signal increases with increasing frequency.

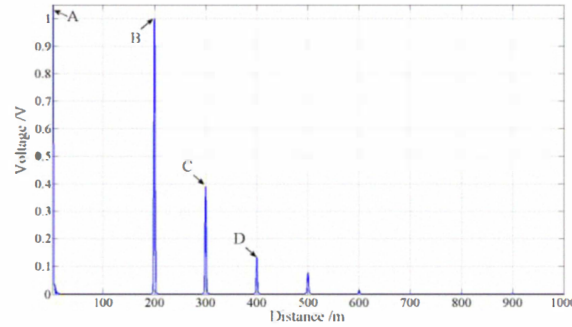For the network topology shown in figure 4.2, the FDR Fourier-transforms would look as follows:

Figure 4.6: Fourier-transforms of the FDR results plotted in voltage against distance. [48, S.5]

The peaks in the voltage-distance plot are very sharp, caused by the better sensitivity and resolution. Compared to TDR, this increase in quality is paid for with the more complex experimental setup and the expensive necessary equipment.[48, S.4f][16, S.383f]

4.1.3 Joint Time and Frequency Reflectometry (JTFDR)

JTFDR combines the previous two methods by an emitted signal in the form of a frequency sweep with a Gaussian envelope. This signal can then be interpreted as Gaussian pulse or as sinusoidal sweep. Therefore, the delay time as well as phase shift of the signals can be evaluated, combining both principles. For the setup, an Arbitrary Waveform Generator (AWG) is needed instead of a pulse generator. Apart from that the equipment is the same as for the FDR-setup:
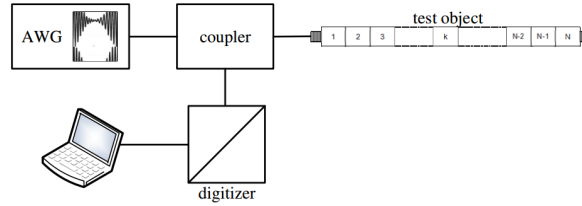

Figure 4.7: Block diagram of a JTFDR experimental setup. [16, S.384]

Regarding sensitivity and resolution, JTFDR combines the advantages of both methods. Especially the weak reflected signals can be detected better and in a sharp way like in FDR. A disadvantage in this method is the expensive AWG and high effort, also types of faults or damages cannot be differentiated, because the informationi of the amplitude of the reflected signal gets lost. Because of the high frequency bandwith of the sweep, especially the higher frequencies are strongly attenuated. This limits the application of JTFDR to detection and localization of faults in short cables. The JTFDR-cross relation for the network topology shown in figure 4.2 is plotted in figure 4.8: [48, S.3f][16, S.384]
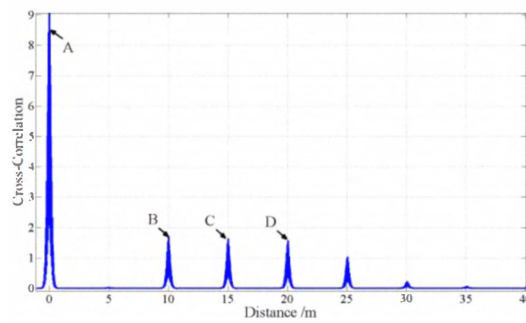

Figure 4.8: Fourier-transforms of the JTFDR results plotted in voltage against distance. [48, S.4]

4.2 The Idea of Online Condition Monitoring via PLC Signals

In the following section, a new and promising approach towards a real online condition monitoring system is introduced and the current state of research is explained. Due to the increase of decentralized energy supply and renewable energies, the so-called *Smart Grid* has become a concept of interest for the near future. *Power Line Communication*, meaning data transmission carried out over the electrical conductor via a modulated carrier signal, is one of the crucial technologies for the communication and connection of the devices within the grid. In the last few years, concepts and research for the use of these signals for condition monitoring purposes as well have been presented e.g. [3] in 2016, [32] in 2017 or [65] in 2018. The idea behind this concept, a possible technical realization, advantages and disadvantages shall be presented in the following section.

4.2.1 Power Line Communication

The basic idea and concept of PLC is already centuries old and quite simple: electric wires and cables for energy transport with 50/60Hz are used to transport modulated signals on high carrier frequencies for data transmission and communication. The existing infrastructure of energy cables and wires then fullfills the additional use of communication. In former times, this technology was used for simple applications like e.g. baby monitors in houses or already within cable grids for telephoning over long distance overhead high-voltage lines. Since the increasing use of the internet and connected electronic devices, the technology has regained the interest of research and different applications have been developed or improved. Numerous examples for the application of this technology and the implementation in industrial automization, multimedia or automotive uses are explained in detail in [35].

The developments within electrical power generation and energy distribution brought this old PLC-technology to a possible new application within the grids as well. Electrical energy grids face a lot of already mentioned challenges regarding the increase of not or poorly adjustable and predictable renewable energy sources or more flexible and difficult to plan electrical consumers like electric cars. For the resulting increased necessity of automatized communication of consumers, power generation and grid operators, PLC is a proper technology, as it uses existing cables. Within HV-overhead power lines or partly MV-underground cables, fibre optic links have been installed in many grids for data transmission. Especially for

the "last mile" to the customers in electricity grids these installations would be way to expensive.[35, S.509ff]

The European Smart Metering Alliance (ESMA) defined automatic processing, transfer, management and utilisation of metering data and 2-way data communication as two of the main features of smart metering.[47, S.4] On the one hand PLC can be an excellent technology for the smart metering, but on the other hand it generates considerable amouts of PLC data traffic, for which PLC-modems are necessary. Using modern broadband standards, the german market leading company devolo promises up to 200Mbit/s of traffic and up to 400m of possible distance between the devices. [20] An example for such a network of smart meters, powerline repeaters and headends, connected to fibre-connections, is shown in figure 4.9:
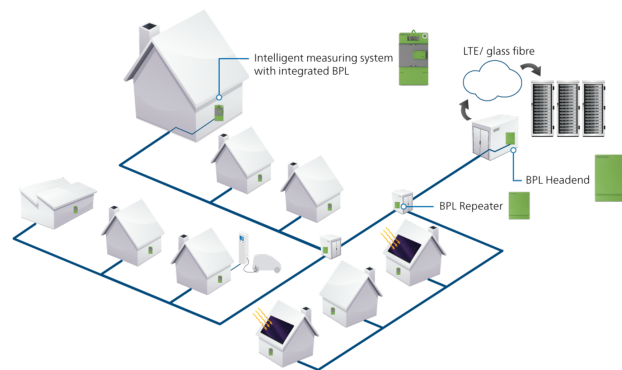

Figure 4.9: Example of a PLC-network in a community using PLC modems and smart meters. [20]

There are two basic classes of PLC for smart grids, based on their frequency bands used:

- **Narrowband (NB) PLC**, working at frequencies between 3kHz and ≈ 500kHz. The signal reach of these systems is hundreds of meters to several kilometers and the throughputs are up to hundreds of kbps.

- **Broadband (BB) PLC**, also called Broadband over Power Line (BPL) with frequency bands from 1,8MHz to 250MHz. The signal reach here covers distances from hundreds of meters to several kilometers as well and the throughputs reach from several Mbps up to hundreds of Mbps.[35, S.510]

Due to the focus on MV and LV cable grid segments, the following sections are usually focused on narrow-band protocols like G3 or PRIME. The principles an basic approach is applicable to other protocols as well.[3, S.2]

4.2.2 Basic Principle and Idea

If PLC communication between different smart meters and other active parts is implemented in a part of a grid, the basic idea now is to use this variety of signals for other means than just communication as well. The technical and physical fundamentals for this idea are described in the previous section and are based on reflectometric methods e.g. explained in good detail in [48] or [16]. The biggest disadvantage of all diagnostic measurements so far is, that the cable segments which should be measured have to be taken out of operation, which involves a consiterable effort and time. If the continuous periodic signals of a PLC data transfer within the grid could be used for reflectometric purposes - a continuous, real time measurement of the whole grid would be possible. If a network of power line modems exists, all the necessary hardware would be available, and only software solutions for the evaluation and interpretation of the signals would be needed. [3, S.1]

To use the TDR- and FRD-techniques presented in section 4.1, the periodic estimation of the system impulse(CIR) response by the modems is used. With this signal sequence, the modems obtain the CIR or channel transfer function (CTR). The diagnostic results are therefore carried out in course of the normal modem operation, practically as a "by-product".

An experimental setup for the described measurements is shown in figure 4.10:
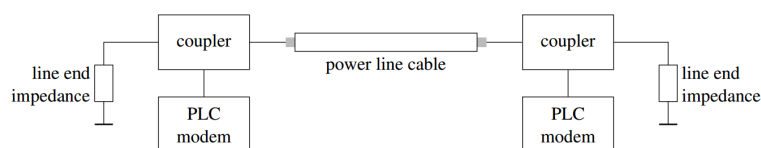

Figure 4.10: Block diagram of a PLC-aided measurement setup. [3, S.3]

Two main difficulties arise with this usage of system impulse response signals:

- Firstly, as shown in the explanation of the PLC-standards, the available bandwidth is limited due to the regulatory constraints and hardware used. Therefore, swept sine signals cannot be executed over such a broad frequency

band as it would be in classical FDR measurements. This can be compensated by using multiple measurements to increase the resolution.

- A second difficulty can arise from the line end impedances. In this case however, the cable impedances are usually very low compared to the receiver impedances, so it behaves practically like an open line end with r close to zero.[3, S.2]

In practical use, most modems use Orthogonal Frequency Division Multiplex (OFDM) as modulation scheme. In [3], for the CTF mesurement, a standard OFDM scheme without any data, just pilot signals were used and calculated in a model. The resulting measured CTF $H(f)$ can then be mathematically represented as a product (in frequency domain) or a convolution (in time domain) of a transfer function $H_{healthy}$ of the healthy cable, and a function H_{dmg} for the degradation:

$$H(f) = H_{healthy}(f) \cdot H_{dmg}(f) \tag{4.2}$$

$$h(t) = h_{healthy}(t) * h_{dmg}(t) \tag{4.3}$$

Thus, from a mathematical point of view, the degradation impulse response in time domain $h_{dmg}(t)$ from a new, healthy cable is a Dirac-δ-distribution - the neutral element of convolution. Therefore, in this case $h(t)$ is equal to $h_{healthy}(t)$. Ideally, if the modems are installed at the same time as the new cable, because of the continuous measurements the status of the new cable can be assumed as $h_{healthy}(t)$. If any change in the impulse response happens, the degradation function of the cable $h_{dmg}(t)$ can then be calculated via deconvolution.[3, S.3]

The enormous innovation of this method, if it would be used in full-coverage of a power grid, would therefore be the possibility of a current, real-time condition monitoring of the cable status. Newly arising degradations or discontinuities within the grid then would lead to a change in $h_{dmg}(t)$, and with the described reflectometric methods even the location could be assessed. Furthermore, the changes in the CTF could be identifiable long before a failure occurs. Consequently, degradations and ageing of cable segments could be detected in very early stages and appropriate measures can be taken.

Within a real grid, of course there is a considerable influence of noise on the measurements. The effect of the noise can be minimized by using multiple measurements and average of the signals. Since the noise is incorrelated and random, but the CTF is not, the signal increases with averaging for each measurement. Also the restricted bandwith due to regulatory reasons is a problem. In [3, S.3] therefore not only the narrow-band bandwidth but the maximum capable bandwith of the modem (5kHz up to 5MHz) was used. In [32] a broadband bandwidth

from 100kHz to 35MHz, in [65] from 2-30MHZ. Whether narrow band-bandwidths are sufficient for applicable results is unclear. Another considerable variable is the number of equidistant sub-carriers in OFDM N_c. The available bandwidth is divided into N_c sub-carriers and each of those set to unit amplitude.

4.2.3 Current Research Results

The research in diagnostic possibilities of PLC technology is a rather young field. As exemplaric results for the issue of this thesis the recent results of [3] are shown, where a simple single wire model is used. [32] The tests are expanded over a physical model for water trees, and [65], where a machine learning framework for a continuous monitoring system is proposed.

In [3], a proof of concept for the method was done via modelling experiments of a transmission line model, as shown in section 4.1. A model of a 1000m single cable line was simulated with a degraded part of 1m length after 150m. The resistance of the cable was set to 1Ω, and the conductance at the degraded cable part was increased by a factor of 5.

A perfect knowledge of the CTF regarding $h_{healthy}$ was assumed, as explained in the previous section with an initial $h(t) = h_{healthy}(t)$ and a known propagation velocity v.
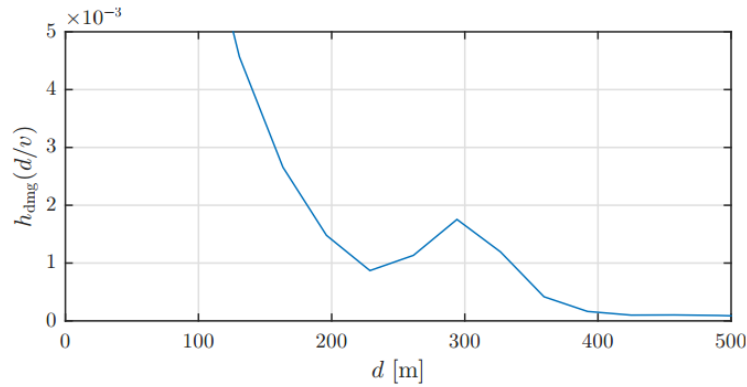

Figure 4.11: Deconvolution of $h_{dmg}(d/v)$ for the simple 1000m single line model with a degradation at 150. The disturbance in h_{dmg} at 300m (due to the reflection 2x the way) is clearly visible. [3]

Different other measurements for this simple one-line-model are published in

[3] e.g. for multiple measurements to minimize noise or other influences. Two interesting basic insights were mentionable: Firstly the usable bandwidth has a significant effect on the accuracy of the measurements, as shown in figure 4.12. Secondly, the location of the degradation and especially the distance to the end of the power line also influences the signals as shown in 4.13. Due to noise and other influences, the signal is less accurate and significant when the degradation is located close to the centre.
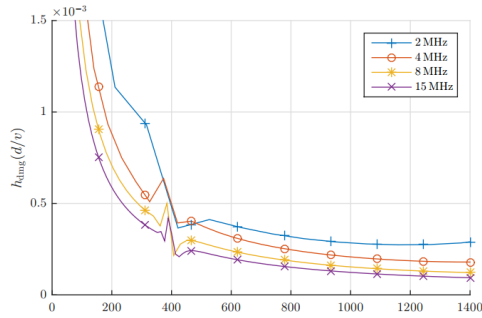

Figure 4.12
Deconvolution of h_{dmg} with a fault at 200m for different measurement bandwidths.[3]
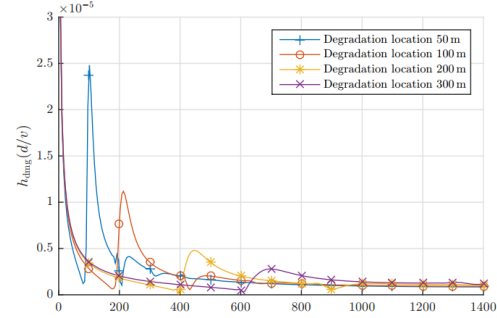

Figure 4.13
Deconvolution of h_{dmg} for the same degradation fault at different locations. [3]

The measurements shown in [3] are of course only done on an unrealistically simple model. Many influences like different cables, junctions or ambient conditions were excluded, which could cause false positives for degradation or faults.

In [32], additionally a model for water treeing effects in XLPE-insulation of MV-cables was considered, the cable was modelled as part of a network with varying load and the varying CFR responses were accomplished automatically with a support vector machine. The effect of water trees on the dielectric properties was simulated with a model of either water trees with two characteristics: Either rather small and fully embedded within the XLPE-insulation, or fully grown and bridging the insulation. In the first case, the capacitances of the PE-insulation and the water tree can be considered in series, in the second case the capacitances are in a parallel circuit. This is illustrated in figure 4.14, the parameter $0 \leq w \leq 1$ describes the severity of the water tree:
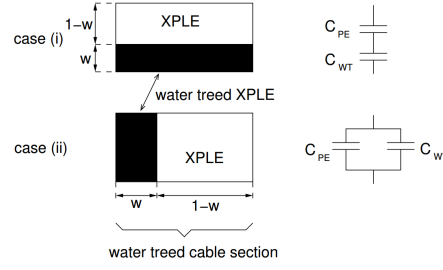
Figure 4.14: Water trees bridging the entire insulation (above) and locally contained water trees (below) and their circuit diagrams. [32]

Based on recently published models, the effective dielectric permittivity $\varepsilon_{WT,i}$ for the water treed segments are then calculated in the model as follows:

case i:

$$\varepsilon_{WT,i} = \frac{1}{\frac{w}{\varepsilon_{WT}} + \frac{1-w}{\varepsilon_{PE}}} \tag{4.4}$$

case ii:

$$\varepsilon_{WT,ii} = w\varepsilon_{WT} + (1-w)\varepsilon_{PE} \tag{4.5}$$

Where ε_{WT} is the dielectric permittivity of the water tree degraded XLPE, and ε_{PE} is the dielectric permittivity of the healthy XLPE. The calculations were done based on a three-core N2SXEY XLPE-MV cable with usual practical parameters. In simulations of a simple one-line models it was shown, that between an intact and a water treed cable a phase shift of the CFR-frequencies occurs, which increases with frequency. This effect is due to the changes in capacitance of the water treed-insulation. Furthermore tests on a more realistic network shown in figure 4.15 were done:
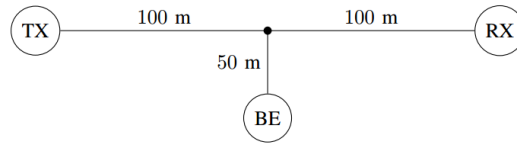

Figure 4.15: Scheme of the network used in the experiments with transmitter (TX), receiver (RX) and branch endpoint (BE). [32]

For this simple network, the four following scenarios were modelled:

1. RX and BE terminated with 50Ω, all wires intact

2. RX and BE terminated with 50 Ω, a section of 60m on side of RX is water treed

3. RX and BE terminated with 20 Ω, all wires intact

4. RX and BE terminated with 20 Ω, a section of 60m on side of RX is water treed

The resulting CFR-frequency plots also showed frequency shifts. These were nevertheless quite hardly relatable, despite 60% of the right cable branch towards RX being water treed. Therefore, the measurements were rendered with a reference function to make the shift-effects better visible.
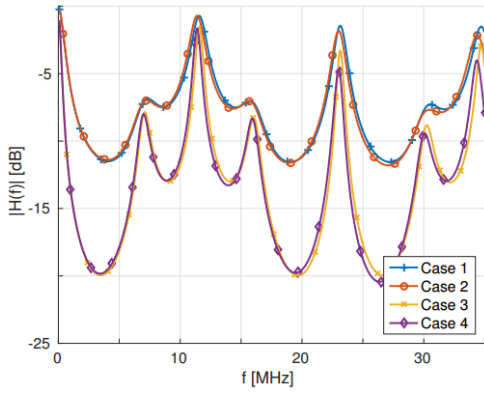

Figure 4.16

Magnitude CFR plotted against frequency for the setup in 4.15 and the four test scenarios. [32]
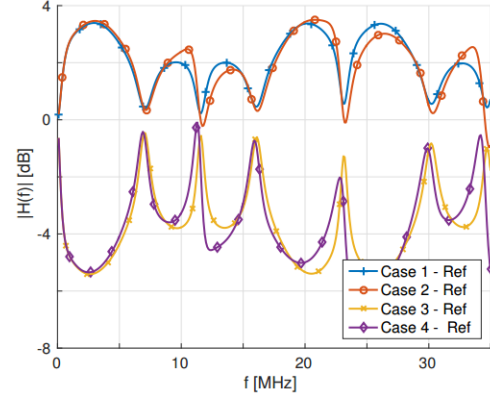
Figure 4.17

Normalized CFR plotted against frequency for the setup in 4.15 and the four test scenarios. [32]

Especially in the normalized plot the effect of the different ageing-conditions and load situations on the PLC-signals is clearly visible at the peaks. Nevertheless, already for this simple network and four clearly different scenarios, a classification or assignment of the effects is not easy. The slight shift towards lower frequencies is clearly visible for 4 in comparison to 3, but not for 2 in comparison to 1. Especially the different load conditions differ from measurements 1-2 to 3-4 clearly. The proposed method in the paper to classify these variations and differ variations due to load conditions from ageing is a support vector machine (SVM) classifying the data, which is also shown on simple examples. Nevertheless, it is also emphasized by the authors, that this binary SVM is no suitable solution for long time ageing effects, but only a first step.[32, S.4ff]

In [65], another step is described by further development of the methods and adding a machine learning (ML) based framework for automatic condition monitoring. This is also implemented only via software changes on regular PLC-modems

which can be updated as often as required via online-firmware-updates. Also, the simulations in this paper were done with water tree-affected cable segments with a model similar to the one used in [32]. For the network topology a T-network with three PLMs and distances of 500m of the PLMs to the branch point (BP). Behind the PLMs after another 500m of cable further branch extensions (BEs) are simulated. For the simulation of a realistic network, the BEs were modelled with ramdom load impedances, the same N2SXEY XLPE-MV cables as in [32] are considered. This network scheme is shown in figure 4.18:
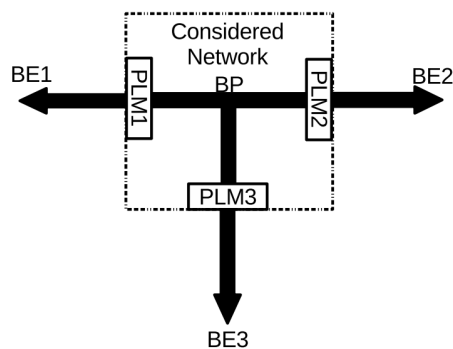
Figure 4.18: Scheme of a part of the distribution network used in [65].

The ML algorithm is then tested with different scenarios like an arbitrary degradation between two distances, which came to similiar results as in the previous presented papers. A multistep-assessment process is proposed where firstly the homogenity of the cable profile is tested. If inhomogenities are found, first the location is assessed, and then - executed by the two PLMs closest to the location - the severity and exact position is determined. Behind every process-step or ML-task, separate machines are trained. The whole process is shown in figure 4.19:

Figure 4.19: Process scheme of the ML-supported PLC-diagnostics process proposed in [65].
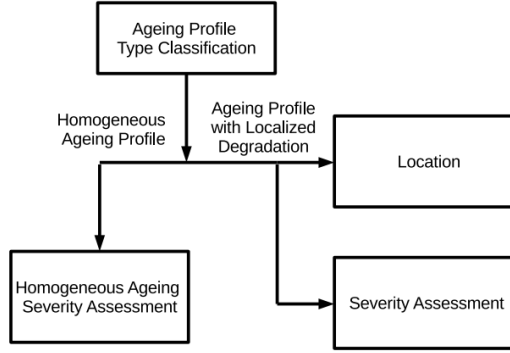
After testing the machines with simulated water tree-degradation of cables, they were tested with realworld degradation measurements taken from a PHD-thesis. These were fed into the model and the results are shown in figure 4.20:
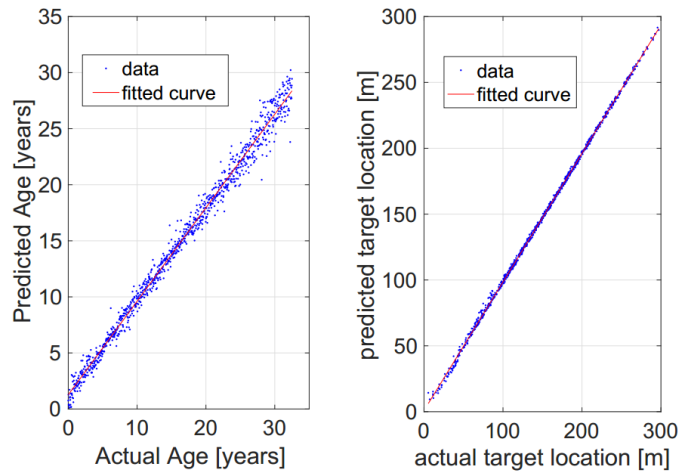
Figure 4.20: Results from the evaluation of real life water treed cable data fed into the ML-setup from [65]. The comparison of predicted and actual age of the cables (in years of degradation) is shown on the left, the location of the degradations are shown on the right.

These results show, that the proposed setup is not only capable of evaluating simulated data, but also with real-life data it shows promising results. The results of the age of the cables are not as exact as in before done simulations, the results are satisfying nevertheless. Especially the locations are very accurate with real

life data, because of the simple measurement mode of measuring peak locations within the cable.

4.2.4 Advantages and Disadvantages

+ No measurement hardware is needed, only additional software for the PLC-modems, which can be periodically updated via online-updates.

+ PLC-aided diagnostics can be done during normal operation. The cables do not need to be taken out of service for measurement. This is on the one hand an enormous reduction in efforts for diagnostic measurements and allows on the other hand a huge increase in data, which can be gathered from the grid.

+ Real-time condition monitoring can be conducted because of the constant PLC-signals within the grid. If ageing effects or degradation occurs, the affected cables can be repaired or replaced even before faults or damages happen.

- The PLC-signals have a large noise impairment, averaging over multiple measurements has to be done to gather results even for small and simple networks.

- Especially for NB-applications strictly limited bandwidth, when it is unclear if the signals can even show significant values.

- No commercial implementation at the moment, only field of research.

- At the moment the method is only modelled for rather simple network topologies. In real grids different disturbance factors such as different cable types, already aged or degrated cables etc. can cause problems.

- No field experience regarding more complex topologies.

- The degradations in the simulations, which were already carried out were always simulated very straight forward with changes in ε_r of the insulation as main characteristic. The effects of more complex degradation and ageing on real-life cables, like small mechanical damages or problems at junctions are not clear.

5 Final Discussion and Conclusion

The physics of power cables have been explained and the complex processes and effects of ageing during lifetime have been shown. For a deeper understanding of the current status of underground cables, a lot of vital information for ageing processes like temperature, humidity or local defects is simply not available in normal operation. Different models for ageing effects and lifetime estimation have been introduced, a reflection towards the situation in an actual real grid is always complicated due to these lack of information.

Diagnostics are an important tool for the condition assessment of the cables and gathering of information about their actual status. Current diagnostic methods such as the $tan\delta$-measurement of cables or measurements of partial discharges are on the one hand quite simple and proven with tens of years of experience and empirical values, they nevertheless show several serious weaknesses:

- Cable sections, on which PD- or $tan\delta$-measurements shall be done, have to be taken out of service for the measurements, which can only be done on-site. This leads to a high effort in time and limits the possible measurements taken per year. As shown, the cable grid of Kärnten Netz has nearly 3000km of cable, with these conventional methods it takes several years to do measurements to determine the status of the whole grid.

- There are no clear thresholds for dissipation-factor values or a number of tolerable PDs in a cable, only empirical values for the different cable types. A scheme consisting of four grades for $tan\delta$ values from very good to unfit for operation was created, based on these empirical limit values. A deeper analysis of the measurement results nevertheless was not possible. The measurements therefore can mainly be used for the confirmation of the absence of PDs and an integral permissible $tan\delta$-value.

- $tan\delta$ measurements can only give integral results for the measured cable sections. A localization of spots with elevated dissipation factors e.g. due to water trees is not possible. PDs can be localized, but as shown, they

can be caused by junctions as well. So a localization or register of installed junctions is necessary to interpret these results correctly.

Concluding, these weaknesses and disadvantages of possible measurements and data are getting even worse because of new developments such as renewable energy sources or electric vehicles. There are currently no solutions for a real online-monitoring of cable conditions on the market, but the demonstrated method using PLC-signals has very promising aspects. This method nevertheless is currently only a subject of research and far away from market-ready applications. For an implementation in a real grid, a lot of research needs to be done and solutions for some basic problems need to be found:

- For a practical use, PLC modems need to be installed in full coverage of the grid.

- Most of the experiments and simulations were done with the whole bandwith the modems were capable of. Especially for NB-applications, the applicability in general needs to be verified.

- Most of the experiments and simulations were done with quite simple network topologies. The effect of more complex networks and the large amount of data gathered in them is not fully clear at the moment. As shown, machine-learning applications would be needed in any case to process the data.

- Especially when the PLC-signals are installed with new cables, slow and creeping ageing compared to the new, healthy cable status can be noticed. It is unclear how much influence the installation in an existing grid with already aged or degraded sections has and how the diagnostic system can deal with these initial conditions.

Bibliography

[1] Sedat Adili. "Teilentladungen und Lebensdauerabschätzungsansätze für elektrische Betriebsmittel, mit Schwerpunkt Kabelanlagen". Master Thesis. Technische Universität Wien, 2009.

[2] Wen Shu et al. "Water Treeing in Low Voltage Cables". In: *IEEE Electrical Insulation Magazine* 29 (2013).

[3] Katrin Raab et al. Andreas Lehmann. "A Diagnostic Method for Power Line Networks by Channel Estimation of PLC Devices". In: *2016 IEEE International Conference on Smart Grid Communications (SmartGridComm)*. 2016.

[4] Arianna Borrelli. *Wiley Online Library: Haru Hamanaka, Erkenntnis und Bild. Wissenschaftsgeschichte der Lichtenbergischen Figuren um 1800, (Lichtenberg-Studien 16) Göttingen: Wallstein 2015*. Dec. 2018. URL: https://doi.org/10.1002/bewi.201601781.

[5] *CENELEC standard voltages*. Norm. May 2009.

[6] Michael Muhr Christof Sumereder. "Estimation of Residual Lifetime - Theory and Practical Problems". In: *8th Höflers Days, Portoroz*. 2005.

[7] Rolf Rüdiger Cichowski. *Kabelhandbuch, 9. Auflage*. Frankfurt am Main: EW Medien und Kongresse GmbH, 2017.

[8] Petru V. Notingher Cristina Stancu. "Computation of the Electric Field in Cable Insulation in the Presence of Water Trees and Space Charge". In: *IEEE Transactions on Industry Application* 45 (2009).

[9] Thomas W. Dakin. "Electrical Insulation Deterioration Treated as a Chemical rate Phenomenon". In: *AIEE Transactions* 67 (1948).

[10] Wolfgang Demtröder. *Experimentalphysik 2 - Elektrizität und Optik*. Berlin/Heidelberg: Springer-Verlag, 2009.

[11] John Densley. "Ageing Mechanisms and Diagnostics for Power Cables - An Overview". In: *IEEE Electrical Insulation Magazine* 17.1 (2001).

[12] Franz Schwabl Dietmar Petraschek. *Elektrodynamik*. Berlin-Heidelberg: Springer Spektrum, 2015.

[13] Bernd R. Oswald Dietrich Oeding. *Elektrische Kraftwerke und Netze*. Berlin: Springer Verlag GmbH, 2016.

[14] *DIN VDE 0276-605 - Starkstromkabel, Ergänzende Prüfverfahren.* Norm. July 2009.

[15] Fred Wiznerowicz Ekkehart Kuhnert. *Eigenschaften von Energiekabeln und deren Messung.* Berlin/Frankfurt am Main: EW Medien und Kongresse GmbH, 2012.

[16] Christian Weindl Erik Fischer. "Perspective of Spatially-Resolved diagnostic Methods for Power Cables". In: *2014 electrical Insulationi Conference, Philadelphia.* 2014.

[17] Christian Weindl Erik Fischer. *Spatially-resolved measurement and diagnostic method for power cables using interference characteristics of travelling waves.* Dec. 2018. URL: https://www.researchgate.net/publication/311470202.

[18] Giovanni Mazzanti Gian Carlo Montanari. "Ageing of polymeric insulating maaterials and insulation system design". In: *Polymer International* 51 (2002).

[19] BAUR GmbH. *PHG 80 TD/PD.* Jan. 2019. URL: https://www.baur.eu/products/2975.

[20] devolo smart grid. *Whitepaper - PLC für den Rollout. Fünf Gründe für Breitband-Powerline im intelligenten Messsystem.* Dec. 2018. URL: https://www.devolo.at/fileadmin/Web-Content/DE/Contentseiten/Smart_Grid/PLC-Technologie/Whitepaper_PLC_fuer_Rollout_0118_DE.pdf.

[21] Unnur Stella Gudmundsdottir. *Proximity effect in fast transient simulations of an underground transmission cable.* Mar. 2014. URL: https://www.sciencedirect.com/science/article/abs/pii/S0378779614001035#!.

[22] Slawomir Nwaczyk Hassan Nemati Anita Sant'Anna. "Reliability Evaluation of Underground Power Cables with Probabilistic Models". In: *DMIN'15: The 2015 International Conference on Data Mining.* 2015.

[23] Bernhard Heine. "Qualitätssicherung für Mittelspannungskabelanlagen". Master Thesis. Technische Universität Graz, 2018.

[24] http://www.polymerprocessing.com. *poly(vinyl chloride) information and properties.* Dec. 2018. URL: http://www.polymerprocessing.com/polymers/PVC.html.

[25] http://www.polymerprocessing.com. *polyethylene information and properties.* Dec. 2018. URL: http://www.polymerprocessing.com/polymers/PE.html.

[26] L. Akcelrud J.V. gulmine. "Correlations between structure and accelerated artificial ageing of XLPE". In: *European Polymer Journal* 42 (2006).

[27] Helmut Katzier. *Elektrische Kabel und Leitungen*. Bad Salgau: Leuze Verlag, 2015.

[28] Bernhard Körbler. "Zustandsbewertung von Betriebsmitteln in der elektrischen Energietechnik". PhD thesis. Technische Universität Graz, 2004.

[29] Dr. Francis Krähenbühl. *Isolationen für Mittelspannungskabel*. Oct. 2018. URL: https://www.nexans.com/Switzerland/files/MS-Technik_1.pdf.

[30] Andreas Küchler. *High Voltage Engineering*. Berlin: Springer Verlag GmbH, 2018.

[31] John Fothergill Len Dissado. *Electrical degradation and breakdown in polymers*. London: Peter Peregrinus Ltd., 1992.

[32] Lutz Lampe Lena Förstel. "Grid Diagnostics: Monitoring Cable Aging Using Power Line Transmission". In: *2017 IEEE International Symposium on Power Line Communications and its Applications 2017*. 2017.

[33] Georg Christoph Lichtenberg. *Bayerische StaatsBibliothek digial: De Nova Methodo Natvram Ac Motvm Flvidi Electrici Investigandi Commentatio Posterior*. Dec. 2018. URL: http://mdz-nbn-resolving.de/urn:nbn:de:bvb:12-bsb10058514-6.

[34] H.Wilhelm Lücking. *Energiekabeltechnik*. Braunschweig/Wiesbaden: Friedrich Vieweg und Sohn, 1981.

[35] Theo Swart Lutz Lampe Andrea Tonello. *Power Line Communications - Principles, Standards and Applications from Multimedia to Smart Grid*. Southern Gate Chichester West Sussex: John Wiley and Sons Ltd, 2016.

[36] Frank Merschel Mario Kliesch. *Starkstromkabelanlagen*. Berlin/Offenbach: VDE Verlag GmbH, 2010.

[37] Christian Mayoux. "On the degradation of insulating materials withstanding electrical stress". In: *Conference on Electrical Insulation and Dielectric Phenomena (CEIDP), annual Report* 1 (2000).

[38] Renato Melo. "Silane Crosslinked Polyethylene from Different commercial PE's: Influence of Comonomer, Catalyst Type and Evaluation of HLPB as Crosslinking Coagent". In: *Materials Research* 4 (2015).

[39] Christof Sumereder Michael Muhr Rudolf Woschitz. *Life Time Investigations at Electric Insulation Systems, Theory and Measurements*. Dec. 2018. URL: https://online.tugraz.at/tug_online/voe_main2.getvolltext?pCurrPk=8084.

[40] Selma Awadallah Muhammad Buhari Victor Levi. "Modelling of Ageing Distribution Cable for Replacement Planning". In: *IEEE Transactions on Poyer Systems* 31 (2016).

[41] NKT. *Mittelspannungskabel von NKT*. Nov. 2018. URL: `https://www.nkt.de/mittelspannungskabel`.

[42] Wilhelm Oburger. *Die Isolierstoffe der Elektrotechnik*. Wien: Springer-Verlag, 1957.

[43] Harry Orton. "History of Underground Power Cables". In: *IEEE Electrical Insulation Magazine* 29.4 (2013).

[44] *ÖVE/ÖNORM EN 60505 - Evaluation and qualification of electrical insulation systems*. Norm. June 2012.

[45] *ÖVE/ÖNORM EN 60505 - Hochspannungs-Prüftechnik - Teilentladungsmessungen*. Norm. Dec. 2016.

[46] *ÖVE/ÖNORM EN 62631-2-1 - Dielektrische und resistive Eigenschaften fester Elektroisolierstoffe; Teil 2-1: Relative Permittivität und Verlustfaktor - Technische Frequenzen (0,1-10MHz) - Wechselspannungsverfahren*. Norm. Jan. 2019.

[47] Nigel Orchard et. al Pekka Koponen Luis diaz Saco. *Definition of Smart Metering and Applications and Identification of Benefits - Technical Report*. Dec. 2018. URL: `https://www.researchgate.net/publication/235709839_Definition_of_Smart_Metering_and_Applications_and_Identification_of_Benefits`.

[48] Olfa Kanoun Quinghai Shi Uwe Troeltzsch. "Detection and Localization of Cable Faults by Time and Frequency Domain Measurements". In: *7th International Multi-Conference on Systems, Signals and Devices*. 2010.

[49] W.Panosch et al. R. Woschitz. "Qualitätsuntersuchungen an VPE-isolierten Kabeln mittels Stoßspannungsprüfung". In: *Elektrotechnik und Informationstechnik* (2005).

[50] B. Bernstein R.J. Densley R. Bartnikas. "Multiple Stress Aging of Solid-Dielectric Extruded Dry-Cured Insulation Systems for Power Transmission Cables". In: *IEEE Transactions on Power Delivery* 9.1 (1994).

[51] Günther Hilgarth René Flosdorff. *Elektrische Energieverteilung*. Wiesbaden: B.G. Teubner Verlag, 2005.

[52] Gavita Mugala Robert Eriksson Ruslan Papazyan. "Localization of Insulation Degradation in Medium Voltage Distribution cables". In: *First International Conference on industrial and Information Systems*. 2006.

[53] B. Krasteva S.Fakirov. "On the Glass Transition Temperature of Polyethylene as Revealed by Microhardness Measurements". In: *Journal of Macromolecular Science, Part B* 39 (2000).

[54] Klaus Schon. *Hochspannungsmesstechnik - Grundlagen - Messgeräte - Messverfahren.* Wiesbaden: Springer Vieweg, 2016.

[55] Oskar Nuyken Sebastian Koltzenburg Michael Maskos. *Polymere: Synthese, Eigenschaften und Anwendungen.* Berlin-Heidelberg: Springer-Spektrum, 2014.

[56] Michael Sepe. *MATERIALS: The Mystery of Physical Aging: Part 1.* Dec. 2018. URL: https://www.ptonline.com/columns/the-mystery-of-physical-aging-part-1.

[57] shz.de. *Bagger verursacht stundenlangen Blackout.* Dec. 2018. URL: https://www.shz.de/lokales/sylter-rundschau/bagger-verursacht-stundenlangen-blackout-id16303351.html.

[58] Siemens. *November 1913 – First section of Rhineland Cable between Berlin and Magdeburg put into service.* Dec. 2018. URL: https://www.siemens.com/history/pool/newsarchiv/newsmeldungen/20131104_bild_2_458px.jpg.

[59] Terézia Skorsepová. *The growth of water trees in XLPE cable's insulation.* Dec. 2018. URL: http://www.posterus.sk/?p=16307.

[60] Leendert Cornelis Elisa Struik. "Physical aging in amorphous polymers and other materials". PhD thesis. Technische Hogeschool van Delft, 1977.

[61] Leendert Cornelis Elisa Struik. "Physical Aging in Plastics and Other Glassy Materials". In: *Polymer Engineering and Science* 17 (1977).

[62] Paul A. Tipler. *Physik für Wissenschaftler und Ingenieure.* Berlin/Heidelberg: Springer-Verlag, 2015.

[63] claus Wrana. *Polymerphysik.* Berlin-Heidelberg: Springer-Spektrum, 2014.

[64] Slimane Bouzabia Yacine Mecheri Ahmed Boubakeur. "Effect of thermal Ageing on the Properties of XLPE as an Insulating Material for HV Cables". In: *Conference Paper - International Insulation Conference.* 2013.

[65] Lutz Lampe et. al Yinjia Huo Gautham Prasad. *Cable Diagnostics with Power Line Modems for Smart Grid Monitoring.* Dec. 2018. URL: https://www.researchgate.net/publication/326852419_Cable_Diagnostics_with_Power_Line_Modems_for_Smart_Grid_Monitoring.

[66] Ephemeral New York. *Lower Manhattan criss-crossed by wires.* Dec. 2018. URL: https://ephemeralnewyork.files.wordpress.com/2009/12/broadwayandcortlandst.jpg?w=450&h=362.

[67] Kai Wu Zepeng Lu. "A new method of estimating the inverse power law ageing parameter of XLPE based on step-stress tests". In: *Annual Report Conference on Electrical Insulation and Dielectric Phenomena* (2013).